A STUDY OF THE NATURE OF THE PHOTOCHROMIC MECHANISM IN VARIOUS SODALITES

by

RICHARD MARTIN CHARNAH B. Sc., A.R.C.S.

A Thesis submitted
for the Degree of Doctor of Philosophy
in the University of London.

September 1973

Department of Electrical Engineering
IMPERIAL COLLEGE
University of London

Abstract

The major inorganic photochromic materials are reviewed, and in particular sodalite in greater detail.

The growth of sodalites by hydrothermal and fluxed-melt techniques and by a low temperature aqueous medium method from kaolinite is dealt with, and the production of a novel material with more convenient activation properties than hitherto is described.

Using chiefly epr measurements and spectra reconstructions the electron centres previously suggested as the source of the photochromic activity are eliminated and a new model developed, though others are also considered possible. Other effects in sodalites are explained using configuration co-ordinate diagrams, and suggestions are made concerning non-photochromic sodalites.

To my wife, Haze

Acknowledgements

I would like to thank Dr D W G Ballentyne for his encouragement and supervision during this work. I am also grateful to Dr E A D White for advice on crystal growth, to Professor J C Anderson for his interest and support and to Dr J F Gibson for providing unhindered access to the Varian epr spectrometer and with whom I had many illuminating discussions.

May I also thank my colleagues and friends of the materials section for their advice and criticism and for the environment they created, and the technical staff of the electrical engineering department, especially Mr P Robinson whose guidance on hardware saved much time.

The financial support of the Science Research Council has also been gratefully appreciated.

Finally may I thank my wife, Haze, for typing this thesis and for her invaluable support.

CONTENTS

		page
	Abstract	ii
CHAPTER 1	PHOTOCHROMIC MATERIALS	
1.1	Introduction	1
1.2	Photochromic materials	2
1.2.1	Silver halide glasses	2
1.2.2	Rare earth doped glasses	4
1.2.3	Alkali halides	4
1.2.4	Silver halide doped magnesium fluoride	6
1.2.5	Calcium fluoride	6
1.2.6	Alkaline earth titanates and rutile	9
1.2.7	Apatites	10
1.3	Applications of photochromic materials	13
1.3.1	Factors important for applications	13
1.3.2	Storage display tubes	16
1.3.3	Projection systems	19
1.3.4	Hard copy systems	19
1.3.5	Radiation sensitive optical components	19
1.3.6	Information storage elements	20
1.3.7	Non-destructive inspection of defects in structures	25

		page
1.3.8	Conditions of materials in the various applications	26
1.3.9	Summary of uses	27
1.4	Sodalite	30
1.4.1	Structure	30
1.4.2	Early investigations of the photochromism	31
1.4.3	Sulphur and iron as activators	35
1.4.4	Recent studies	36
1.5	Objectives of the present work	38
1.6	Future areas for study	39
CHAPTER 2	PRODUCTION AND ACTIVATION OF SODALITE	
2.1	Introduction	41
2.2	Hydrothermal growth	42
2.2.1	Bolt-on-head delta-ring autoclave system	49
2.2.2	Tuttle-type autoclave system	53
2.2.3	Sealing of gold capsules	60
2.2.4	Materials used	63
2.2.5	Hydrothermal preparation of microcrystalline sodalite	64
2.3	Fluxed melt growth	65
2.3.1	Introduction	65
2.3.2	Pre-melt procedure	67

		page
2.3.3	Controlled cooling growth	68
2.3.4	Precipitation from flux	68
2.3.5	Wire-seeded temperature gradient growth	70
2.3.6	Extraction of products	70
2.4	Low temperature hydrothermal synthesis of sodalite from kaolinite	71
2.4.1	Introduction	71
2.4.2	Experimental procedure	73
2.5	Activation studies	75
2.5.1	Introduction and apparatus	75
2.5.2	Procedure	76
2.5.3	Effects of activation studies on photochromism - 'HT10'	78
2.6	Summary	81
CHAPTER 3	STRUCTURAL INVESTIGATIONS ON SODALITE	
3.1	X-ray powder diffraction	82
3.2	Infra-red spectrometry	85
3.3	Results of structural studies	85
CHAPTER 4	ELECTRON PARAMAGNETIC RESONANCE (EPR)	
4.1	Introduction	99

		page
4.1.1	Paramagnetism and the resonance phenomenon	99
4.2.1	Magnetic energy levels and the g-factor	102
4.2.2	The Hamiltonian approach	105
4.2.3	The spin Hamiltonian	109
4.2.4	Fine structure: zero field splitting	111
4.2.5	Nuclear hyperfine splitting	117
4.2.6	Line shape and relaxation	124
4.3	Equipment and procedure	128
4.3.1	Basic features of epr spectrometers	128
4.3.2	Experimental equipment	132
4.4	Epr results	134
4.4.1	Introduction	134
4.4.2	The coloured state	136
4.4.3	Pre-radiation state	136
4.4.4	Ferromagnetic impurities	140
4.4.5	Variable temperature studies	143
4.4.6	Perchlorate sodalites	145
4.4.7	Other sodalite materials	150
4.5	Discussion: epr	152
CHAPTER 5	PHOTOCHROMIC ACTIVITY IN SODALITES	
5.1	Introduction	157

		page
5.2	Computer simulation of epr powder spectra	159
5.2.1	SHAPE 5	159
5.2.2	SPINGT½	161
5.3	The source of the electron	163
5.3.1	Antistructure disorder model	163
5.3.2	Models involving other centres	168
5.3.3	Oxygen containing centres	172
5.3.4	Reconstruction of the epr powder spectrum of the photoactive centre	178
5.4	Oxygen in other media	181
5.5	Oxygen in sodalite	185
5.5.1	Formation of oxygen centres	187
5.5.2	Non-photochromic sodalites	192
5.6	Photochromism energetics - configuration co-ordinate diagrams	194
5.7	New photochromic materials	196
5.8	Conclusions	197
	References	199
APPENDIX I	Program SHAPE 5	203-208
	Program SPINGT½	209-215

Total number of figures (including 5 plates) = 68

1 PHOTOCHROMIC MATERIALS

1.1 Introduction

Photochromism is a process by which a material undergoes a reversible colour change (ie a shift in energy of the optical absorption band), on the application of one frequency of electromagnetic radiation, the process being reversed by electromagnetic radiation of a different frequency. The reverse process can also in certain cases be brought about thermally. In the case of chloro-sodalite, the fundamental absorption band in the ultra-violet region (around 2500Å) disappears and a new band (around 5350Å) appears in the green, if the material is irradiated in the fundamental absorption edge, whilst the reverse process occurs on irradiation with green light or on heating to 300-400°C. The process is not equivalent to a photographic process which is non-reversible and shows gain. Cathodochromism is similar to photochromism but the initial shift of the absorption band is induced by an electron beam.

1.2 Photochromic Materials

Both organic and inorganic photochromic materials exist. The photochromic mechanisms in organic compounds, eg the spiropyrans, involve electron rearrangements around or between molecules and will not be dealt with here where there will be a concentration on inorganic materials, and in particular on sodalite, in a later section.

1.2.1 Silver halide glasses

These glasses consist of silver halide crystallites distributed in a homogeneous glass matrix, the photochromic colouring being due to the separation of silver and halogen species (Megla 1966). The halide species are prevented from diffusing away by the glass matrix and the reverse process can occur when the exciting radiation is removed, being accelerated by heat or long wavelength visible light. This reverse process differentiates them from photographic emulsions where the silver and halide entities separate under the action of light and the halide diffuses away through the emulsion, leaving behind the silver as a latent image.

Clear, opal or translucent glasses can be made, the latter two being due to light scattering, according as the crystallite diameter is 50-300Å, 300 to less than 2000Å, or greater than 2000Å. With crystallites smaller than 50Å, the composite is not photochromic. A typical useful glass in this class would be one with 4×10^{15} crystallites cm^{-3} of diameter 50-100Å at intervals of 500-1000Å and has a resolution of 2100 fringe cycles mm^{-1}. Colouring wavelength varies from 3500Å for silver chloride/glass to 6000Å for one using silver iodide. Bleaching occurs in the range 5500-6500Å. These glasses, therefore, have the desirable property of colouring with ultraviolet radiation and bleaching with red, but also of absorbing green light in the coloured state, whilst not being bleached by it.

Whilst silver halide glasses can have high transparency in the coloured state and apparently show no fatigue on repeated reversal, they give less change in optical density for a given thickness and irradiation intensity than some other photochromic materials, thus for a change in optical density (OD) of 0.1 in samples 0.2cm thick, 3-15mJcm^{-2} are required (Megla 1966).

1.2.2 Rare earth doped glasses

Europium (II) and cerium (II) present in a concentration of about 100ppm in glass of composition $Na_2O.\ 2.5SiO_2$ activate it so that irradiation in a band centred on 3325Å produces an absorption band at 5700Å which is the bleaching wavelength (Cohen and Smith 1962; Muller and Milberg 1968). This effect exhibits fatigue but can be restored by irradiation at 2537Å. This type of photochromism can be explained in terms of photo-oxidation and photo-reduction of Eu(II) or Ce(II).

The visible absorption band is produced in many glasses by 2537Å radiation if the concentrations of impurities such as titanium and iron are kept extremely low, for colouration in longer wavelength UV, however, the rare-earth activators are necessary.

1.2.3 Alkali halides

Photochromism is induced in some alkali halide crystals by the presence of U-centres - hydride ions (H^-) occupying a halide ion site in the crystal lattice. U-centres can be formed by heating the crystal in alkali metal vapour followed by hydrogen,

or by growing the crystal from a melt doped with the alkali metal hydride. Irradiation in the UV absorption band ionizes the H^- ion, the hydrogen atom diffuses away and the electron is captured on a halide ion vacancy, forming an F-centre which has its optical absorption in the visible region. F-band irradiation at temperatures between 200K and ambient retraces the steps, bleaching the colouration (efficiency varies with temperature).

In work on information storage in potassium iodide single crystals (Bessent and Runciman 1966), UV irradiation in the β-band was used to form F-centres. $10 Jcm^{-2}$ (equivalent to $1mW.\mu m^{-2}$ for 10^{-4} sec) produced an optical density of 0.1 at room temperature and a tenth of this at 250K. The process is therefore rather inefficient and the colouration fades slightly over a period of days, but optical densities over 4.0 can be obtained in crystals 0.5mm thick. The wavelength of the light used limits the resolution which is about $2\mu m$ here.

1.2.4 Silver halide doped magnesium fluoride

Evaporated MgF_2 thin films containing co-evaporated silver halide, darken on exposure to ultra-violet radiation (Band et al 1973). The mode of action is similar to that of the silver halide glasses in section 1.2.1; however, the containment of the outward diffusing halide species is not as yet efficient; the films therefore show rapid fatigue. Work in this field is still in progress.

1.2.5 Calcium fluoride

Naturally occurring fluorite exhibits a variety of colours due to rare earth impurities. Early in the nineteenth century, miners in the north of England found that this colouration could be bleached by heating the crystals and reproduced by exposure to sunlight, and it was later found that reversible photocolouration occurs especially in calcium fluoride doped with divalent lanthanum, gadolinium, cerium and terbium (Staebler and Kiss 1969). The mechanism of the colouration is a charge transfer process between either:

1 two species of rare earth impurities, or

2 a rare earth and a colour centre that involves an impurity (Faughnan et al 1971)

An example of the latter is CaF_2:La produced by heating La(III) doped CaF_2 in calcium vapour which reduces the rare earth to the divalent state (Kiss and Yocom 1964), producing La^{2+}:F-centre complexes. UV radiation removes an electron from this centre and it is then trapped by a La^{3+} ion in a cubic site (Duncan et al 1970). The optical absorption is due both to the cubic La^{2+} centre and the ionized La^{2+}:F-centre complex. The efficiency of this process is about 10%.

In double doped fluorite, eg CaF_2:Eu,Sm (Welber 1965), charge transfer between the rare earth ions proceeds via the conduction band and can be represented by equation 1.1 and figure 1.1

$$Eu^{2+} + Sm^{3+} \underset{h\nu(Sm)}{\overset{h\nu(Eu)}{\rightleftharpoons}} Sm^{2+} + Eu^{3+} \qquad 1.1$$

This process has only been observed at 4K.

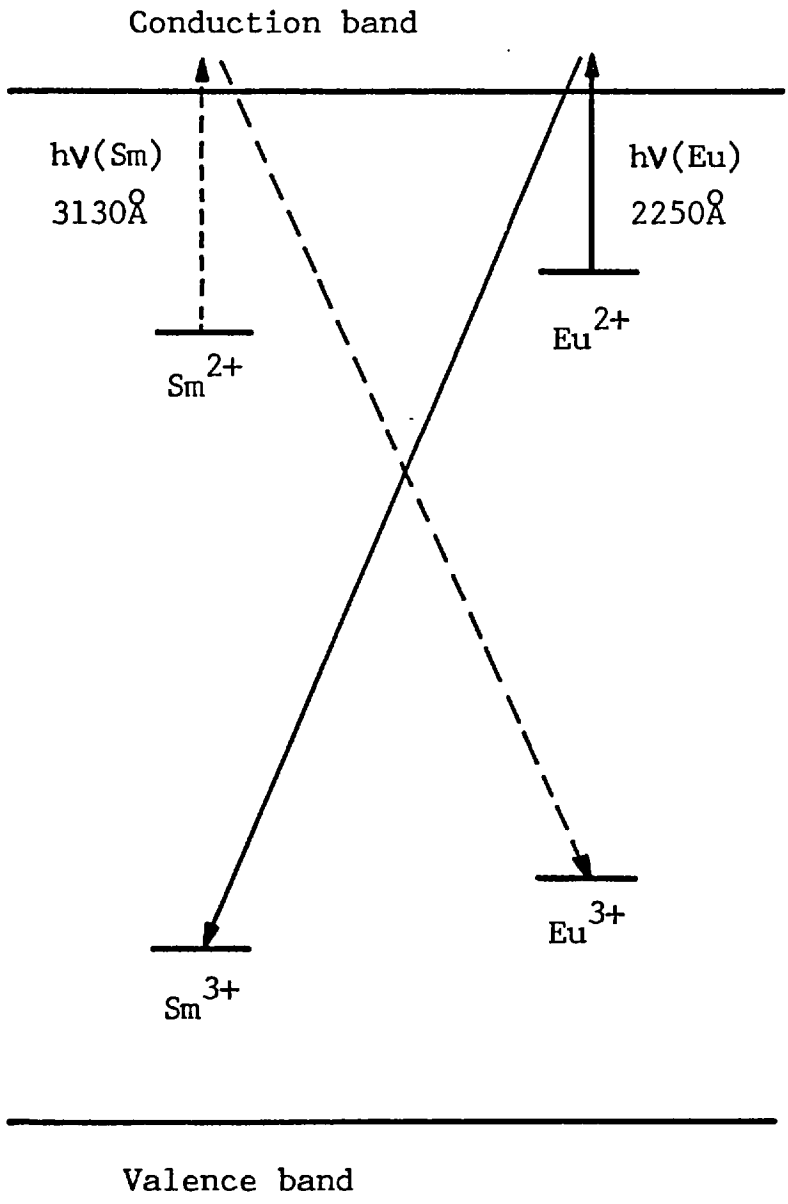


Figure 1.1

Photochromic charge transfer processes in CaF_2:Eu,Sm

1.2.6 Alkaline earth titanates and rutile

Calcium, strontium and barium titanates, though not magnesium titanate which has different crystal structure, can show photochromism. MacNevin and Ogle (1954) explained the effect in terms of the crystal structure and the presence of impurities viz Fe^{3+}, Zn^{2+}, V^{5+} and Sb^{5+}. In general they suggested the impurity should have a valence other than 4 and an ionic radius close to that of Ti^{4+} for the material to be photochromic.

As before, charge transfer processes are responsible for activity in $SrTiO_3$ when doped with iron or nickel and molybdenum. The colouring and bleaching steps are (Faughnan and Kiss 1968, 1969):

$$\underbrace{Fe^{3+} + Mo^{6+}}_{\text{little or no absorption in the visible region}} \underset{h\nu'(\text{visible}) \text{ or heat}}{\overset{h\nu(\text{near UV + blue})}{\rightleftharpoons}}$$

$$\underbrace{Fe^{4+}}_{\text{absorption in blue-green}} + \underbrace{Mo^{5+}}_{\text{absorption in red-green}} \qquad 1.2$$

Very broad absorption in visible region

A similar transfer occurs for molybdenum with Ni^{2+} (giving Ni^{3+}), Cr and Co. It is probable that iron, at least, occupies titanium sites in the lattice (Kiss 1969).

Single doping and chemical reduction techniques have been used to confirm these processes but it has not been possible to discriminate between an electron and a hole transfer.

Titanates have been used for thick holograms (Bosomworth and Geritsen 1968) and in cathodochromic screens. When used in the erase mode, 1mm thick crystals require $50mJcm^{-2}$ of visible light to induce a change in optical density of 0.2.

1.2.7 Apatites

Irradiation of calcium fluoro- or chloro-phosphates ($Ca_5(PO_4)_3F$ and $Ca_5(PO_4)_3Cl$ respectively) with X-rays, 1850Å ultra-violet radiation or an electron beam produces colour centres with photochromic properties (Swank 1964). These centres are not produced by additive colouration (calcium or lithium

vapour), or by application of a high electric field via point contacts at elevated temperatures ($10^4 Vcm^{-1}$, 600°C).

On irradiation, fluroapatite turns green then gradually turns blue at room temperature. The original colouration is due to the formation of 3 centres - A, B and C. The A centres degrade slowly at room temperature but almost instantaneously at 100°C and all three can be bleached out in ½hr at 125°C. At least 50 reversals are possible without fatigue, but subsequently fatigue does occur and limits the use of the material. The centres can be interconverted by UV irradiation: irradiation in the A band diminishes it and increases the other two and vice-versa.

The three centres have been tentatively identified in $Ca_5(PO_4)_3F$ as follows:

1 the A centre is an electron trapped in a fluorine vacancy, ie analogous to the F-centre

2 the B centre is two, adjacent, associated A-centres ie the dimer of A, analogous to an M-centre in alkali halides

3 the C centre is probably an A-centre/fluorine vacancy composite, equivalent to an ionized B centre though the identification is not definite

The main 'anticentres' to the three centres described are O^- in F^- sites (Segall et al 1962).

Chloroapatite has a slightly different structure from its fluoro analogue, the halide ion being displaced along the c-axis. However, Swank (1964) has identified centres corresponding to the A and B centres above and a new one designated X.

In photochromic apatites, the maximum colour centre concentration has been measured as $10^{18} cm^{-3}$, comparable with other active materials. Its main disadvantages seem to be fatigue and the short wavelengths necessary for its initial colouration. It seems likely, however, that it will be used as a cathodochromic material, and its highly polar absorption characteristics may find novel application.

1.3 Applications of Photochromic Materials

1.3.1 Factors important for applications

1 Sensitivity

Sensitivity can be defined as the optical density change per unit of absorbed light energy. Photochromic, unlike photographic, materials do not show gain and production of one, or exceptionally two, centres per absorbed photon represents an upper limit. The energy required to colour an ideal photochromic can be calculated using Smakula's equation below

$$Nf = (0.87 \times 10^{17}) \frac{n}{(n^2 + 2)^2} \text{ kmax } W_{\frac{1}{2}} \qquad 1.3$$

f = oscillator strength

N = number of colour centres cm^{-3}

n = refractive index of the medium

kmax = peak absorption coefficient in cm^{-1}

$W_{\frac{1}{2}}$ = full width of the absorption band in ev at half maximum

From this, for a typical optical absorption band half-width (0.4ev), to obtain an optical density change of unity requires about $5 \times 10^{-3} Jcm^{-2}$. CaF_2

and $SrTiO_3$ require about 30 times this energy which would imply say f = 0.3 and an efficiency of about 0.1;10% efficiency is fairly typical.

2 Speed of colouring and bleaching

Three transition rates are important:

a) electronic transitions from centre to centre, probably via the conduction band. This time should be of the order of 10^{-9} sec but in practice is largely determined by the trapping time. For example, in $SrTiO_3$ doped with transition metals this time has been determined as less than 10^{-7} sec using a Q-switched ruby laser (Amodei in Faughnan et al 1971)

b) limitations due to lack of sensitivity, ie insufficient light intensity. Variations between a few seconds for irradiation with a 500W high pressure mercury lamp to 0.1 sec for a 1W argon laser where the absorption bands are matched to the laser

c) thermal decay of the switched state can cause its stable period to vary from months to 10^{-3} sec

3 Resolution

Apart from two phase systems like silver halide doped glasses, the resolution element is the size of the atomic impurity centre. However, the practical limit is the diffraction limit of the colouring light as shown in the production of 3-D holograms in photochromic materials (Bosomworth and Geritsen 1968; Amodei and Bosomworth 1969).

The absorption coefficient also has an effect, eg for a material whose maximum absorption coefficient change gives an optical density change of 3.5×10^{-3} m^{-1} at the measuring wavelength, then for a change in OD of 0.5 requires a 150 μm thickness, a much larger element than the diffraction limit.

4 Resistance to fatigue

Some organic films have higher absorption coefficients than many inorganics; however, they suffer more severely from fatigue. Most inorganic photochromics show no fatigue after 10^6 colouring - bleaching cycles.

Applications commonly involve both photo and

cathodochromic properties either together or separately.

1.3.2 Storage display tubes

The first tubes of this type used potassium chloride in place of phosphor in a fairly conventional CRT assembly and was known as a skiatron. In recent years it has been developed further (Kazan and Knoll 1968), and produces a dark line on a white background. Several other designs have been developed using settled powder screens of transition metal doped titanates, sodalites and others. Colouring of the screen, ie writing-in, is usually achieved by an electron beam either by scanning the screen sequentially (Gorog 1970) or by random scan addressing (Hughes and Hankins 1972). Additional information can be written-in manually with UV radiation using a light pen.

Erasure of the image can be performed in a number of ways:

1 optically by an electronic flash - a fast method which is non-selective and 'ergonomically unsuitable' for direct viewing. Also, the

storage property of the material is lost and a residual colouration builds up which requires bleaching thermally or by laser (Tubbs and Wright 1971)

2 thermally by incorporation into the screen of a transparent resistance heating element (Fyler 1964), giving complete bleaching which is non-selective and relatively slow, erasure taking of the order of seconds. The time taken to cool must also be considered

3 thermally, using the electron beam to selectively heat any sites requiring erasure (Hughes and Hankins 1972)

The information can also be displayed in a number of ways, viz:

4 as a dark trace on a white background

5 as a white, ie bleached, trace on a coloured screen

6 as a white trace on a coloured screen with the rear surface of the screen coated with a phosphor which is repeatedly scanned by an electron beam

causing it to glow through the bleached material.

(4) and (5) show better with high ambient light level.

For cathodochromic uses, resolution is dependent on the electron beam diameter.

According to Hughes and Hankins (1972) an ideal display terminal would combine the advantages of other display systems, viz:

1) non-cycled display, free from flicker
2) random-scan deflection
3) high storage density and resolution
4) large viewing area of high brightness
5) selective erasure capability
6) standard type CRT
7) indefinite storage
8) grey level capability
9) relatively low cost

Cathodochromic CRTs closely approach these criteria using sodalite as the active material, and compare favourably with other types of screen for cost and writing speeds (Phillips and Kiss 1968; Taylor et al 1970).

1.3.3 Projection systems

In these systems, the screen of one of the tubes in section 1.3.2 or a moving continuous band is in effect used as the 'transparency' or object of a projecting system. The system can be used for colour projection by varying the colour of the projection light, eg by filters.

1.3.4 Hard copy systems

Photochromic powder coated on to a suitable backing, eg standard size paper or plates, can be 'printed' on either by contact printing from the faceplate of a CRT or focussing an image on it using a suitable optical system.

1.3.5 Radiation sensitive optical components

Photochromic glasses and plastics have been fabricated into lenses for spectacles having optical clarity at low light levels but which darken in a few seconds in bright sunlight. The bleaching process occurs in the order of minutes. Glasses of this type are 'Photogrey' and Corning 'Bestlite'.

Devices of this kind have been suggested as possible progenitors of anti-nuclear-burst eye projection hardware. Stringent requirements for these have been listed by Britten (1964); however, no currently known material fulfils these qualities.

Photochromic glass is used in the automotive industry (Rover 3500) and architecturally under the trade name 'Sundym' for windscreens and windows. Here, the limitations of the glass, eg the thickness required to obtain a given optical density change, speed of change etc, are not tested too severely, whilst advantage is taken of special properties of the glass such as the capacity to be produced in large areas and to be formed into arbitrary shapes.

1.3.6 Information storage elements

Magnetic core memories storing up to 10^7 bits of binary information can be duplicated in storage capacity by a $1cm^3$ photochromic plate or film with $3\mu m \times 3\mu m$ resolution elements; within the capability of diffraction limited laser optics. Similar storage densities are also obtainable using thick film holograms (Bosomworth and Geritsen 1968) (figure 1.2).

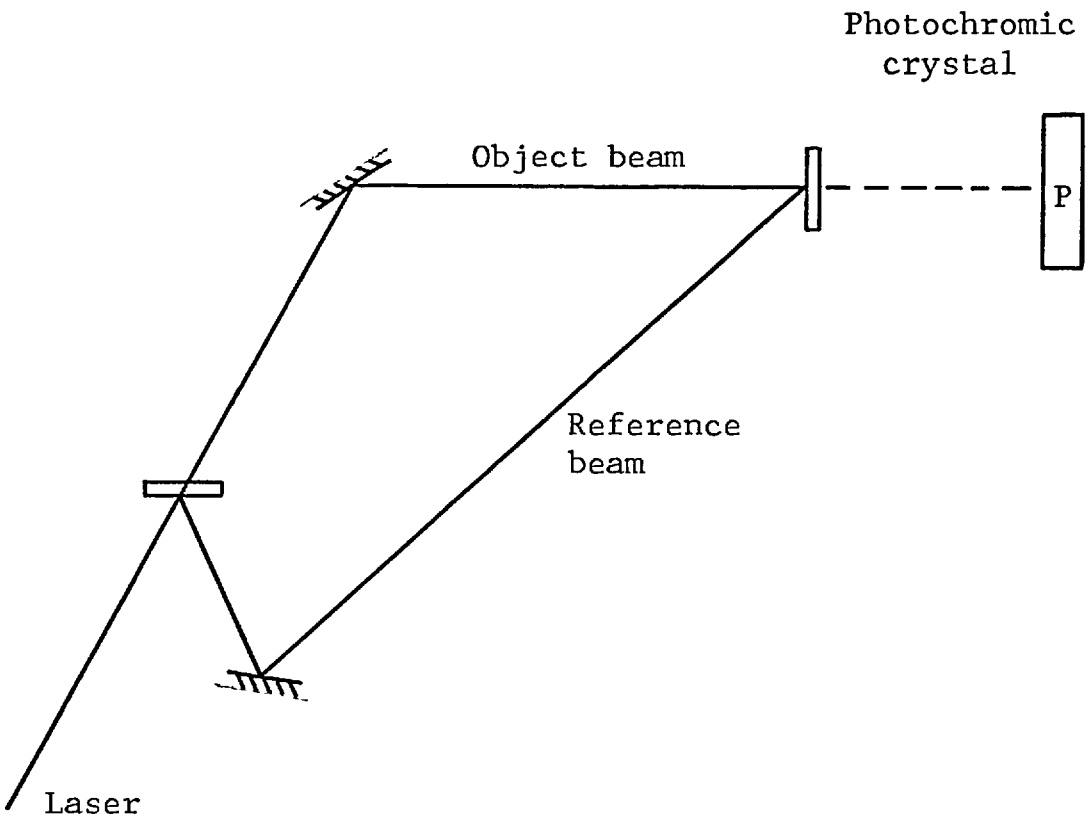


Figure 1.2

Thick film hologram production

Also Megla (1966) has shown that Corning glasses are capable of recording 2100 fringe cycles mm^{-1} or 4.4×10^{8} bits cm^{-2}.

How the photochromic single crystal would fit in with existing memory systems is not clear. Thermal decay makes it impermanent, requiring updating. High speed applications would also be ruled out by power requirements for switching limiting the response time.

Van Heerden (1963) has discussed this method of information storage in semitransparent materials where the image is formed as interface patterns of two plane parallel waves. Writing-in is accomplished by bleaching the pre-coloured crystal and read-out by light diffracted at the non-uniform absorptions in the crystal. Multiple images are stored using different wavelengths or angles of incidence. The process is limited by successive images bleaching further colour centres.

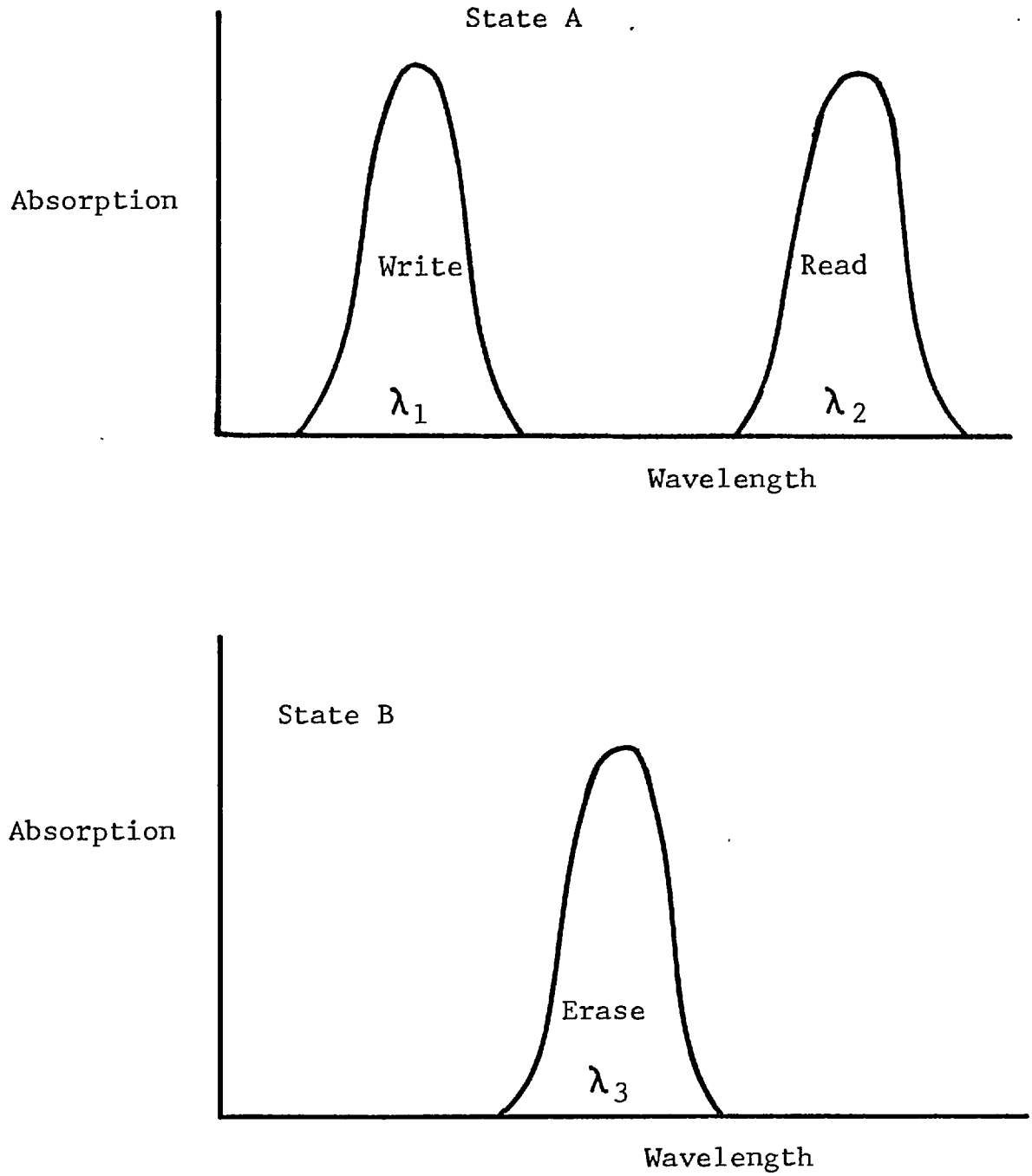


Figure 1.3

Optical requirements for a photochromic memory

Kiss (1969) stated the required optical characteristics of a photochromic material for information storage as shown in figure 1.3. In state A there are two absorption bands. Radiation in λ_2 does not affect the state but its absorption shows its existence or otherwise and is, therefore, the read wavelength. Light in λ_1, however, changes the state of the material to state B (no absorption at λ_2), whilst irradiation in λ_3 sends the material to state A, erasing the memory. $CaF_2:Sm^{2+}$, Eu^{3+} has characteristics approaching this ideal.

F aggregate centres can also be used to provide non-destructive read-out (Carson 1965). Here, Carson irradiated potassium chloride crystals doped with H^-, with ultra-violet to form F-centres. Information is stored as M and R centres (Compton and Rabin 1964) produced by F-band light, the non-destructive read-out being in the R_2-band, and erasure is by irradiation in the U-band, producing hydrogen atoms and molecules which diffuse to the complex centres destroying them, probably by the mechanisms

$$H_2 + M \longrightarrow 2U \qquad 1.4$$

$$H_2 + R \longrightarrow 2U + F \qquad 1.5$$

Low intensity reading beams must usually be used in photochromic stores. Intensities comparable to the erase light intensity most often produce some bleaching because of the coincidence of the two wavelengths in question which commonly produces a limit on the number of cycles possible.

1.3.7 Non-destructive inspection of defects in structures

A coating of temperature sensitive photochromic material which changes colour on exposure to light but becomes colourless on moderate heating, can be used for this purpose, for example in glass fibre and other composites. A coating of spiropyran dye in vinyl butyral resin is applied to the structure and UV irradiated for about 4 sec when it changes from white (if pigmented) or colourless, to bright violet. When the sensitized coating is developed by gentle heating, defects in bonding or porosity in the structure show up as sharply delineated areas of white against a violet background. The image persists for several hours at room temperature.

Slow conduction of heat away from the coated surface (indicative of poor bonding etc) causes a heat build up or warming of the area, gradually bleaching the coating. Reverse side heating produces a reverse colour effect (Allinikov 1970).

1.3.8 Conditions of materials in the various applications

For holograms and optical memory systems it is necessary to use single crystal photochromic materials, although it may be possible to use powders for a 'memory'.

Photochromic powders are more suitable for display screens, projection and moving band systems and 'hard copy' generators. It is possible to obtain contrast ratios of over three to one with these materials, where contrast ratio is the ratio of the optical density of coloured state to the optical density of bleached state. Apart from relative ease of production of material and systems using powders, they have other advantages for these functions. Because of the shape and size of the particles there is a light trapping effect, especially with materials

of high refractive index, which enhances the contrast ratio. Light striking the powder is also more likely to be absorbed than that striking a single crystal of comparable thickness, since internal reflections occur in the powder. In addition, shorter wavelength UV radiation sometimes used to colour the material, penetrates thin powders, whereas it would be absorbed near the surface of a single crystal slice.

The coating material for structure defect study and the silver halide doped glasses are similar in that they are inhomogeneous dispersions in a matrix. The rare earth doped glasses are homogeneous supercooled liquid solutions.

1.3.9 Summary of uses

Table 1.1 shows the main applications of photochromic materials.

TABLE 1.1

application	materials
Storage display tubes Projection systems Hard copy systems	Sodalites, CaF_2:RE, $Sr(Ca)TiO_3$:TM, powders
Radiation sensitive optics	Silver halide doped glasses and MgF_2 films and other photochromic glasses
Information storage	Sodalites, CaF_2:RE, $Sr(Ca)TiO_3$:TM, single crystals (possibly powders)
Non-destructive defect study	Photochromic materials in resin

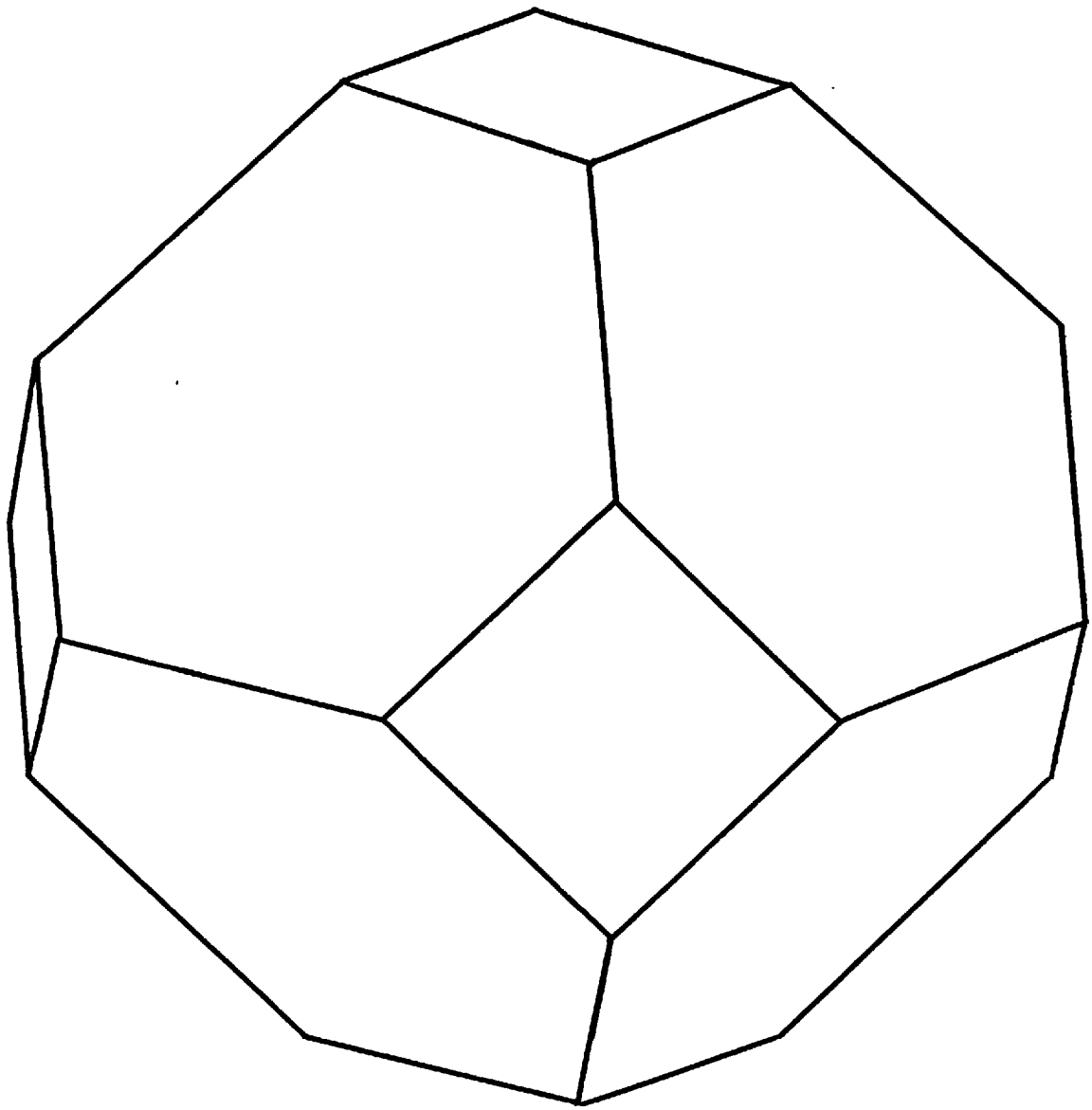


Figure 1.4

The Cubo-octahedron of the sodalite structure

1.4 Sodalite

1.4.1 Structure

Sodalite is the name for a group of materials of the same type as zeolites, ultramarines and lazurite which are composed of a spacefilling aluminosilicate framework. Sodalites can occur in colourless, blue, green or white forms and may be photochromic, in which case it is called hackmanite.

The archetype for the sodalites, chlorosodalite, has the ideal formula $6(NaAlSiO_4).2NaCl$ and is of crystal class $\bar{4}3m$. In its aluminosilicate framework, the silicon and aluminium atoms alternate with a bridging oxygen atom between each Si-Al pair; one structural unit contains six four-membered rings (2 x Si + 2 x Al), and eight six-membered rings (3 x Si + 3 x Al), which are respectively the cube and octahedral faces of a cubo-octahedron (figure 1.4). This unit has common octahedral faces with eight other units, the hexagonal channel between them having a free diameter of 6Å. The sodium and chlorine atoms are arranged symmetrically as (Cl + 4Na) units with

the chlorine at the centre of the cubo-octahedral lattice cage and the sodium ions tetrahedrally placed around it, about halfway between the chlorine ion and the centre of the hexagonal channels. The lattice constant is 8.87Å, the O-Na distance 2.36Å and the Cl-Na distance 2.70Å.

1.4.2 Early investigations of the photochromism

Reversible discolouration of alkali halides was observed late last century by Goldstein (1896) but this observation is antedated by a report by Allan in his 'Manual of Mineralogy' 1834 about hackmanite: 'Its colour is green unless freshly fractured, when it presents a brilliant pink tinge, but this on exposure to light goes off in a few hours". Contemporary mineralogists regarded this observation as poorly founded and ignored it until it was confirmed in 1901.

Lee (1936) found that hackmanite could be coloured by 2250-4800Å radiation and bleached by 4800-7500Å light. The first synthesis of a photochromic sodalite was accomplished by Medved (1954) who sintered a stoichiometric mixture of alumina, silica,

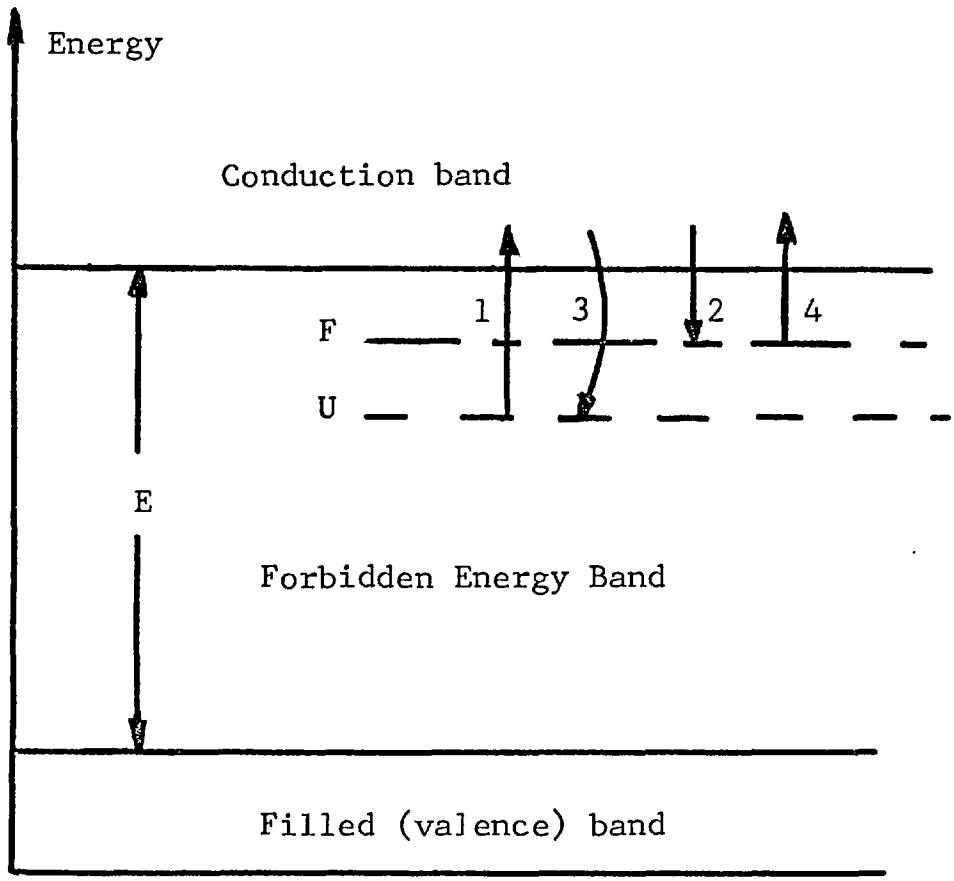


Figure 1.5

Band Structure of Photochromic Sodalite

- Medved Model

sodium hydroxide and sodium chloride giving

$$6NaOH + 3Al_2O_3 + 6SiO_2 + 2NaCl \longrightarrow$$

$$Na_6Al_6Si_6O_{24}.2NaCl + 3H_2O \qquad 1.6$$

This reaction had to be performed below 1060°C to form the sodalite by solid state reaction. Attempts to lower the reaction temperature using fluxes such as LiF and $NaWO_4$ failed. Thermal and ultra-violet studies showed that the colour centres of natural hackmanite were not being duplicated, nor were they introduced by addition of various amounts of groups I, II, IV, V, transition or rare earth metals or sulphur.

Medved explained the photochromism in terms of the band theory of solids (figure 1.5), with two impurity type levels. The levels marked F were assigned to lattice imperfections such as cracks, strains, missing ions etc, which could trap electrons forming F-type centres whilst those marked U, considered responsible for UV sensitivity, arose from the presence of substitutional or interstitial impurities in the lattice. Transition 1 represents the absorption of UV radiation to give a conduction band electron

which can return to the U level (3) or go to the F level (2), the latter being responsible for the observed salmon-orange fluorescence under UV. Absorption of visible light (4) combined with process 3 gave rise to optical bleaching of the material.

Since Medved had to activate his sodalites by firing in a hydrogen atmosphere or a carbon crucible with limited access to air, he thought that H^- or C^- ions in halide ion sites gave rise to the U-centres. An F-centre is formed when the hydrogen (or carbon) atom diffuses away from its extra electron, under the influence of UV radiation leaving a vacancy whilst the reverse diffusion process can be induced by visible light. This colouring process may be plausible for H^- centres, but is less likely for the more bulky C^-; this bleaching process is not probable for either species. Also, a tendency for hydrogen atoms to pair up into molecules must be expected which would decrease even further the degree of bleaching.

Kirk (1954 and 1955) argued that sulphur is necessary for sodalite to be (a) photochromic and (b) luminescent, and which of these processes dominates depends on the

form of sulphur added and thermal history of the material. He showed that many natural sodalites contain sulphur and that the yellow or orange-yellow luminescence of scapolite ($Na_3(AlSi_3O_8)_3.NaCl$) and sodalites are due to the presence of sodium polysulphide (compare Bershov et al 1969). However, the work of Radler (1962, 1963) on inorganic photochromic materials for information storage indicated that while sulphur containing salts of sodium aided photochromic effects, they were not necessary, since when they were left out of the starting materials, photochromic sodalite still resulted.

1.4.3 Sulphur and iron as activators

In addition to Kirk, Williams et al (1969) also found sulphur to be a necessary ingredient of sodalite for good photochromism and identified the electron donor in the process as S_2^{2-} from stoichiometry and epr measurements. Hodgson et al (1967) had previously assumed the active centre to be sulphur but their epr data was insufficient to decide what type of sulphur species. Phillips (1970) found a correlation between the extent of iron doping

and photochromism and that sulphur had little positive effect. It is interesting that Williams et al (1969) also noted an effect on the activity of their materials of trace amounts of transition metals, but did not give detailed results.

1.4.4 Recent studies

Hodgson et al (1967) made a positive identification of the 'F-centres' of Medved when they obtained the epr spectrum of sodalite in its coloured state and found a signal of 13 lines with equal spacing centred on $g = 2.002 \pm 0.001$ in the correct ratios for 1 electron interacting with four nuclei of spin $\frac{3}{2}$. In sodalite these nuclei can only be the four sodium nuclei. These centres are analgous to F-centres in alkali halides being a single electron trapped in a chlorine vacancy at the centre of the tetrahedron. The problem of accounting for the photochromism now becomes one of elucidating the source of the trapped electron.

Though sulphur and iron had been shown to be present in photochromic material, and to assist the activity, they had not been shown to be the source of the

F-centre electron. Using high purity techniques and optical spectra Ballentyne and Bye (1970) showed that these impurities are not necessary for photochromic activity but ions containing S, Se and Te and possibly others can take part in the process. Two general mechanisms were suggested, intrinsic and extrinsic processes. Hydrothermally grown sodalite is not photochromic but only shows activity after heating at 900°C in a reducing (hydrogen) or inert (argon) atmosphere; for the activation step Ballentyne and Bye suggested 1.7

$$2OH^-_{Cl} \xrightarrow{kT} 2V_{Cl} + O^{2-} + H_2O \qquad 1.7a$$

$$O^{2-} + V_{Cl} \longrightarrow O^{2-}_{Cl} \qquad 1.7b$$

The photochromic reactions are then shown in 1.8

$$O^{2-}_{Cl} + V_{Cl} \underset{h\nu(F)\ \text{bleaching}}{\overset{\text{colouring}\ h\nu(O^{2-})}{\rightleftharpoons}} O^-_{Cl} + \underset{\text{f-centre}}{e_{Cl}} \qquad 1.8$$

These reactions would be the same for intrinsic and extrinsic activity but for the latter the impurity anions, of charge greater than unity, will have created greater numbers of chlorine vacancies for charge compensation, therefore making the photochromic

action easier and more intense. The O^- ion suggested as formed in the coloured state should be observed by epr spectroscopy.

1.5 Objectives of the present work

Sections 1.4.2 to 1.4.4 illustrate the different mechanisms postulated for the photochromic process in sodalite. Elucidation of the mechanism involved is desirable from two standpoints; firstly electron transfer reactions in solids are of interest because of the basic physics involved and secondly a knowledge of the processes occurring can help to find other photochromic materials and treat them to produce properties required for given applications. Technologically, sodalite powders are more important than single crystals and it was therefore decided to confine these studies to them. The main techniques used in this investigation are:

1 the growth of a variety of sodalites by different methods and in different media whilst changing the dopants

2 activation studies

3 electron paramagnetic resonance (epr) studies

In addition to these main techniques other supplementary techniques are introduced as necessary; for example, infra-red spectroscopy and computer construction of epr spectra. The general aim is to discover the electron donor in the photochromic process and produce new technologically useful materials.

1.6 Future areas for study

Future work should include a search for new photochromic materials (particularly the technologically more important powders and glasses), which will colour more efficiently, have greater contrast ratio, and fade more slowly or to a negligible extent.

Research into applications of sodalites might be most fruitful if it was channelled into those areas which best use their unique properties, ie relatively long write and more particularly erase times, slight fade, low cost of production etc. An application of this type would be the production in the home of 'hard'

copies of news and weather situations, particularly of a local nature, in the manner of a local newspaper; existing television technology could cope with a system of this type. Write and erase times here are non-critical since updating need not be frequent, say every 15 or 30 minutes and sodalite cathodochromic tubes have already been produced with write/thermal erase cycle times of about eight seconds.

2 PRODUCTION AND ACTIVATION OF SODALITE

2.1 Introduction

Although photochromic sodalite occurs naturally (as hackmanite), for quantitative measurements synthetic material has more consistent properties. Photochromic sodalite was first synthesized by Medved (1954) and Kirk (1954), who sintered together silica, alumina, sodium chloride, sodium hydroxide or carbonate respectively and sodium sulphate and/or sulphide. Williams et al (1969) prepared similar materials by treating zeolite-X, pretreated with sodium chloride, with SO_2 or H_2S, and Carr et al (1968) has grown sodalite from high pH gels. However, in this work hydrothermal synthesis was mainly used along with flux melt synthesis and the treatment of kaolinite with sodium hydroxide in the presence of other sodium salts.

Hydrothermal growth was the method most used as it produced sodalite of the required crystal size and shape for our applications. This method has the

disadvantage that the material is not photochromic as grown but requires activating by one of several methods discussed below.

2.2 Hydrothermal growth

The solubility of most materials in a solvent is increased if the temperature is raised. The increase in solubility is not limited by the boiling point of the solvent or its critical point, providing the system is enclosed since solutes, including solids, are soluble in gases (Morey 1957), and for water considerably above its critical density no discontinuity occurs in solvent properties at the critical point.

This observation forms the basis of the method of hydrothermal synthesis; solid feed materials can be transported through water or a water based medium from a position where thermodynamic conditions favour solution to one where deposition is favoured. The main criteria for growth of this type are the stability of the solid phase under the conditions used, and a solubility of this

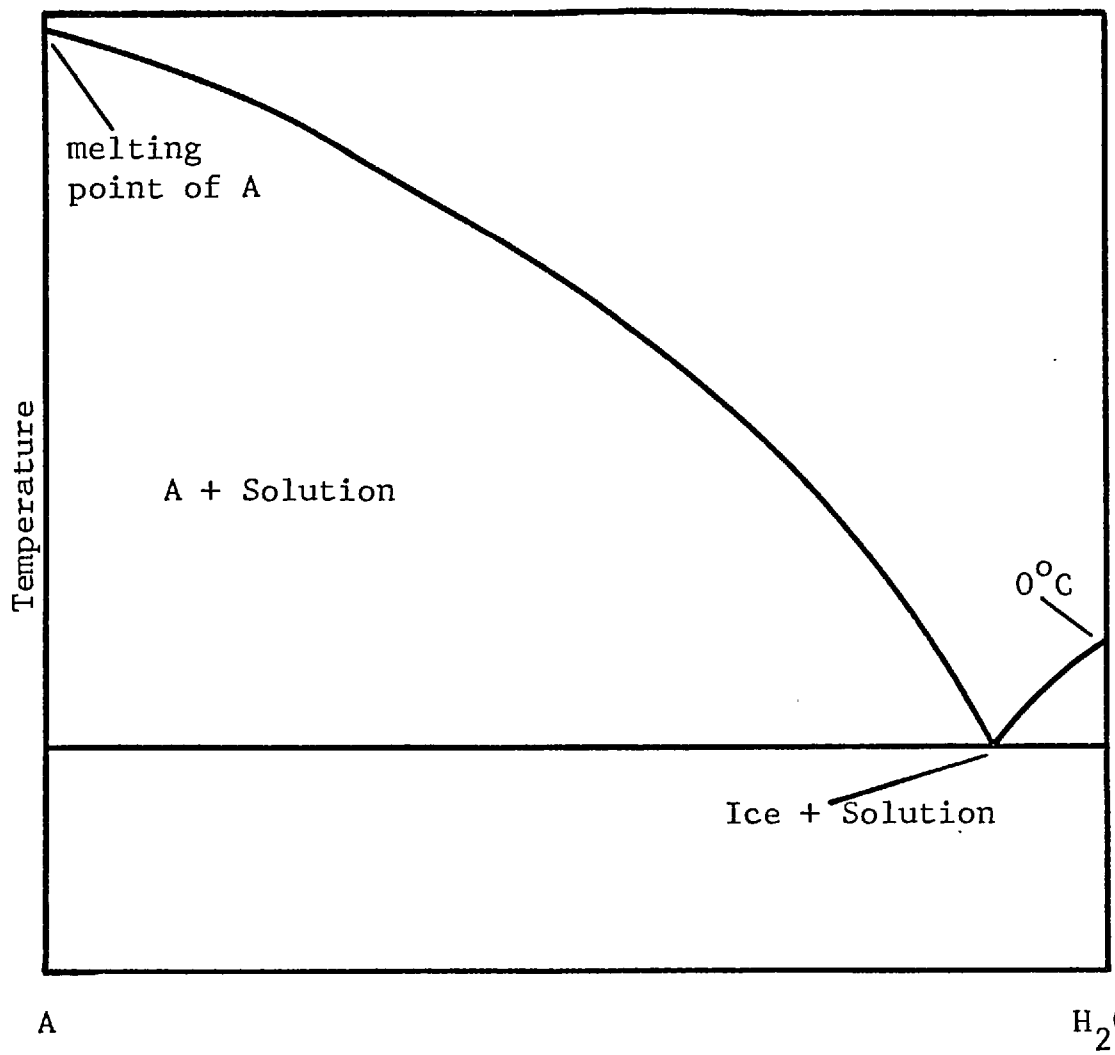


Figure 2.1

Binary phase diagram between a typical refractory material and water

phase in the solvent of at least 1% (Laudise and Nielson 1961). Hydrothermal synthesis can also be understood if it is seen as water depressing the melting point of a refractory material so that it can be crystallised at a lower temperature (fig 2.1). Usually a 'mineraliser' is added to the water to increase the solubility of the solute which is not usually high for the refractory materials commonly grown by this technique. It is probable that the mechanism of reaction of these mineralisers is the formation of complex ions of the compounds in the feedstock (Laudise and Kolb 1969).

This method has been used notably for α-quartz crystals (Laudise and Ballman 1961) for crystal oscillators, but also for sapphire (Marais 1968), zinc oxide, zinc sulphide, yttrium iron garnet (YIG) and yttrium gallium garnet (YGG) (Laudise et al 1961); for these materials the mineralisers used are alkali metal hydroxides and carbonates.

Acidic Media such as hydrohalic acids, especially HI, have also been used as mineralisers, mainly

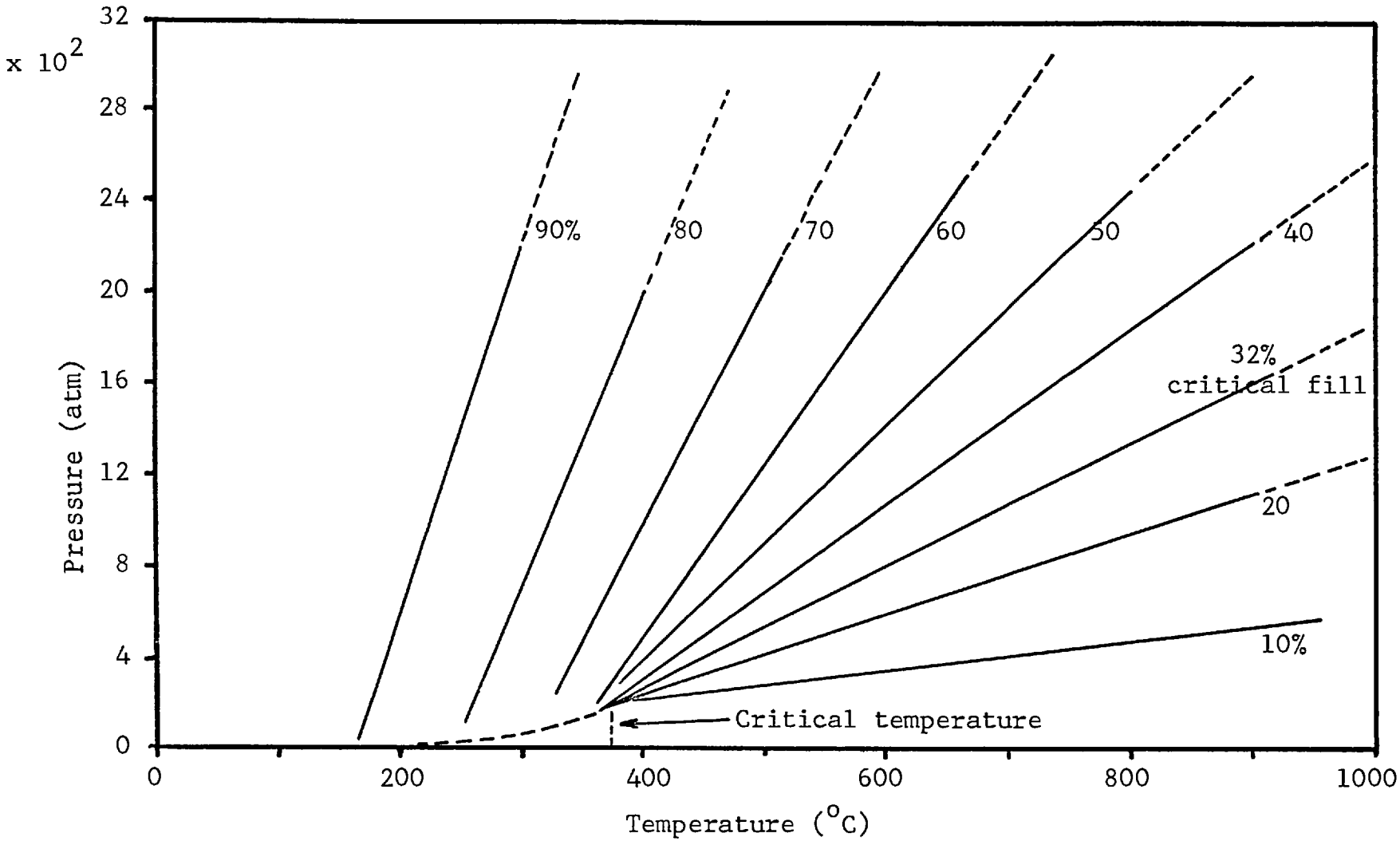


Figure 2.2

Pressure-temperature relationships for water at various densities

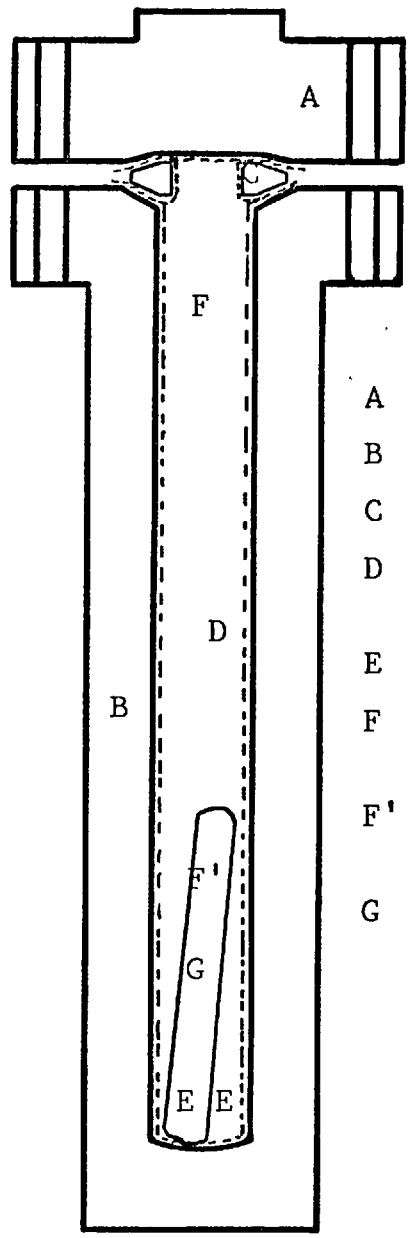
for growth of crystals of metals, chalcogenides and halides (Rabenau and Rau 1969).

Hydrothermal growth also occurs in nature, many naturally occurring minerals being formed by this process. In the laboratory, however, the method has the advantage that it is possible to dope the crystals grown fairly uniformly and, by using noble metal containers, it is possible to grow extremely pure crystals.

In the laboratory, the process is usually carried out in a sealed pressure vessel, an autoclave, and, since above 100^{o}C the pressure of water, at densities high enough to make its solvent power appreciable, increases rapidly (fig 2.2), the autoclave is built to withstand the pressures involved (typically 1000-2000 atmospheres). In this study two different autoclave systems were employed for producing polycrystalline sodalite:

i bolt-on-head, modified delta-ring sealed, type (Butcher and White 1964), and

ii cone-in-cone, Tuttle type (Luth and Tuttle 1963).



A Head with boltholes
B Body of autoclave
C Delta-ring seal
D Platinum lining (where used)
E Dissolving zone
F Crystallising zone (main body)
F' Crystallising zone (capsule)
G Gold capsule

Figure 2.3

Bolt-on-head autoclave

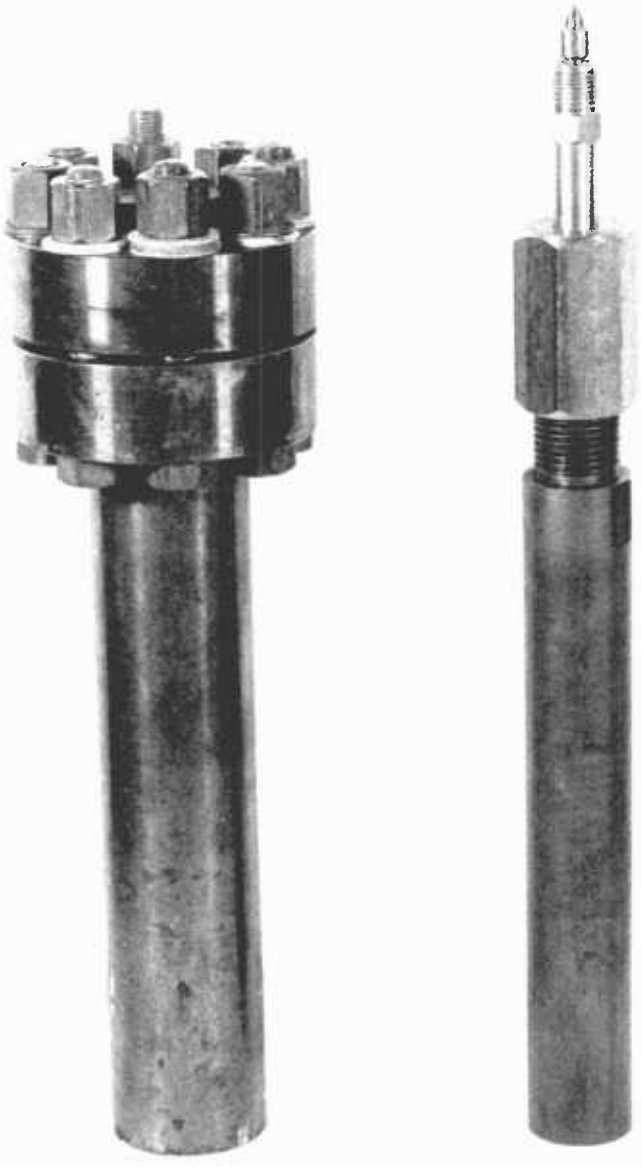


Figure 2.4

Autoclaves: Bolt-on-head (left),

Tuttle type (right)

This second type of autoclave was used with and without external pumping, in its 'normal' single ended form, and in a double ended modification.

2.2.1 Bolt-on-head delta-ring autoclave system

Autoclaves of the type described by Bye (1970) and Butcher and White (1964) constructed of Nimonic 80A alloy or EN58G stainless steel were used (figures 2.3 and 2.4). These vessels had an internal volume of about 90ml. Some were lined with platinum whilst in other cases, gold tubes about 1cm diameter and 10cm long were used to contain the charge; to prevent the capsules from exploding from the pressure generated by the charge at the temperature of the run, the pressure in the rest of the autoclave was kept the same as that in the capsule, for all temperatures, by filling it to an equal fraction of its free volume as the capsule with water. Sealing of the gold tubes is discussed in section 2.2.4 below.

Conditions of growth used were in the ranges 400-1000 atmospheres (6-15 kpsi) and 300-500^{o}C for 36-120 hours.

In a sealed system the pressure is determined by the initial fraction or degree of fill, which in turn was determined by interpolation from pressure-volume-temperature relationships for water (Holser and Kennedy 1959) giving, for example, the necessary degree of fill for a pressure of 1000 atmospheres at 400°C as 61.2% or 55.1ml for the 90ml autoclaves. At 61.2% fill the ultimate density of the water will be 0.612 since it will completely fill the autoclave both above the critical temperature (374.2°C), when it is gaseous, and some way below it, when it is liquid. (In fact if the degree of fill is such that the ultimate density would be above the critical density (0.326) then the liquid expands until it fills the autoclave at some temperature below critical, where it turns to gas. If the degree of fill is below 32.6%, the autoclave 'boils dry' below 374.2°C, ie fills with water vapour. For a fill of exactly 32.6%, the liquid meniscus remains stationary and disappears exactly at the critical temperature.)

Where noble metal capsules were used, the degree of fill inside them and the autoclave was the same,

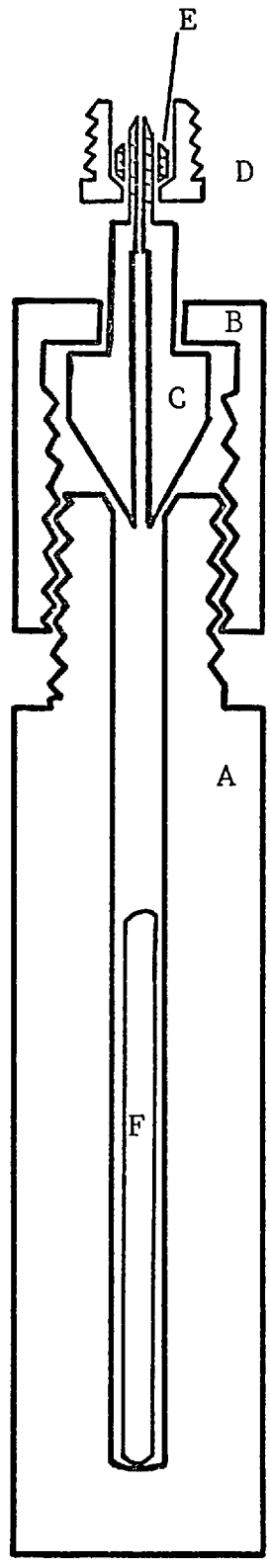
any slight discrepancy being compensated by minor expansion or collapse of the capsule.

The autoclaves were heated in two different types of furnaces:

a) a horizontal tube of sintered alumina, heated by 'Crusilite' rods, and thermally insulated with 'Fibrefrax' blanket (Carborundum Co Ltd). In this furnace the autoclave was supported at about 10^{o} to the horizontal

b) an assembly of refractory bricks with an enclosed cavity in which the autoclave stood vertically, radiatively heated by 'Crusilite' rods (Morganite Electroheat Co Ltd)

The temperature in both types of furnace was controlled by Eurotherm PID/SCR phase-angle fired controllers using Pt/Pt-13% Rh thermocouples. The furnaces were open ended thus producing a temperature gradient along the length of the furnace tube. The autoclave was positioned so that the growth region was at a lower temperature than the charge (around $25C^{o}$).



A Autoclave body

B Header nut

C Cone seal

D Gland nut

E Collar

F Growth capsule

Figure 2.5

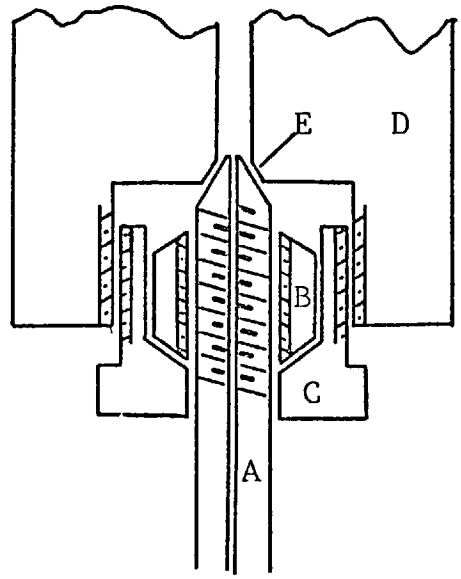
Tuttle type autoclave

The autoclaves themselves had eight bolts holding on the lid and these were tightened gradually in pairs to 40 or 45 ft lbs with a torque wrench.

2.2.2 Tuttle type autoclave system

Autoclaves similar to those described by Luth and Tuttle (1963) were constructed of Nimonic 80A alloy (figures 2.4 and 2.5), with stainless steel EN58E or EN58J (≡ SS316 or SS321) cones and mild steel EN2A header nuts. These were externally pumped with water to produce the required pressure by a Pressure Products Industries gas-hydro pump type APPS-30, which could produce a maximum pressure of 30kpsi (2000 atmospheres). The gas used to drive the pump was compressed cylinder nitrogen or air, and the water conduit was ¼ inch high-pressure tubing of SS316 stainless steel as were the junctions and 'T'-blocks etc, which were standard Pressure Products Industries equipment and used gland nut and collar, cone-in-cone connectors (figure 2.6a).

The autoclaves were suspended vertically by their pressure leads from a frame, and heated by furnaces which ran on vertical rails. The furnaces consisted



LH thread

RH thread

A pressure tubing

B collar

C gland nut

D seating (T-block etc)

E cone-in-cone seal

Figure 2.6a

HP connections

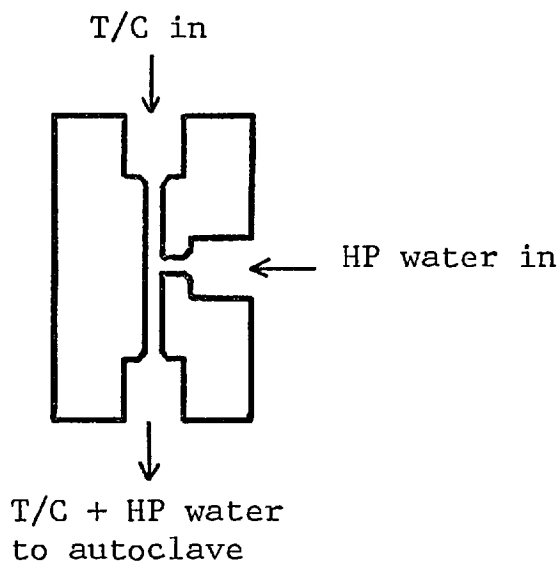
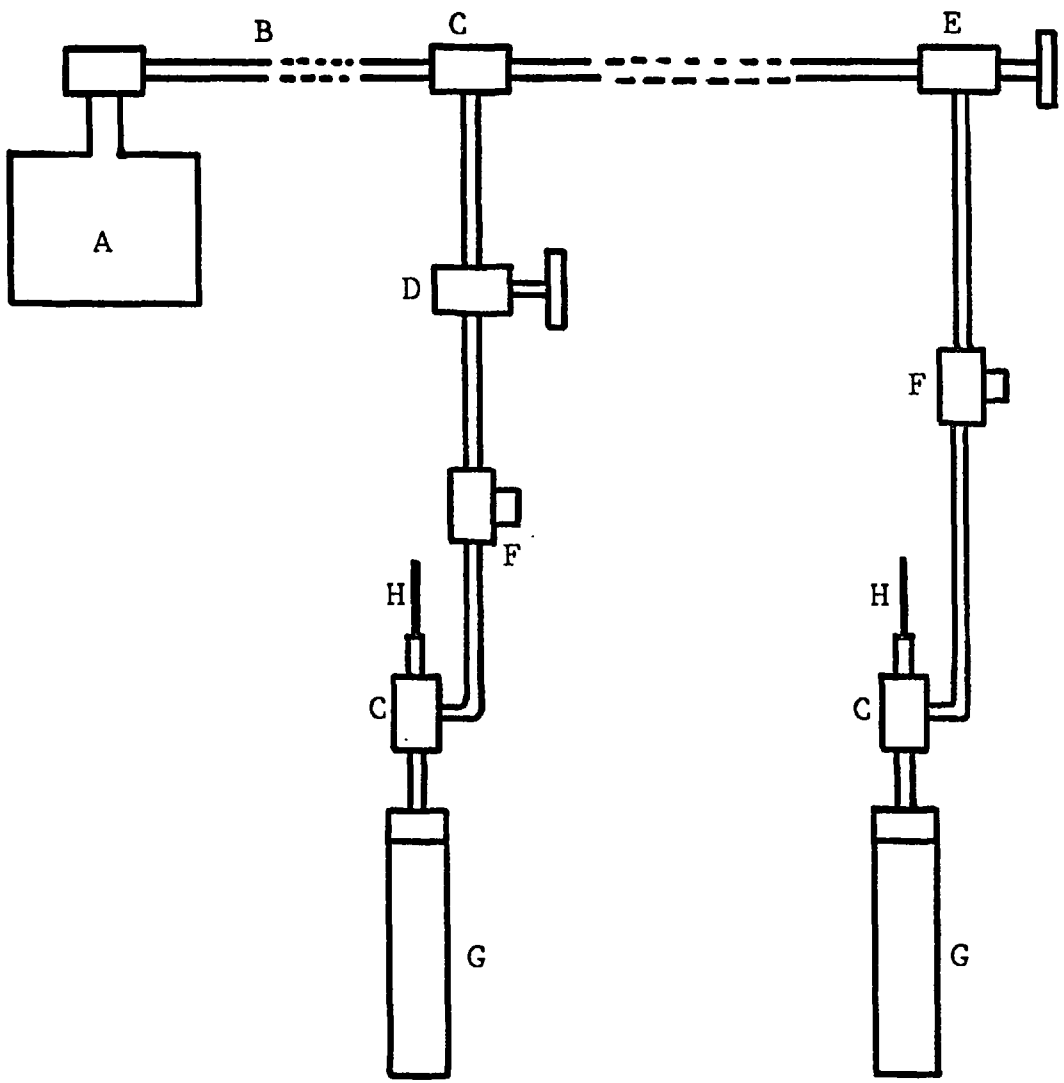


Figure 2.6b

Tee block immediately before autoclave

of aluminous porcelain tubes (ID = 45mm, OD = 55mm from Thermal Syndicate Ltd) with windings of Kanthal A1, insulated by Fibrefrax Lo-con blanket with aluminium and duralumin bodies, controlled by Eurotherm PID/SCR rapid cycling temperature controllers, via chromel-alumel thermocouples situated between the autoclave body and the furnace wall. Temperatures inside the autoclave could be monitored by metal (inconel) clad, MgO insulated chromel-alumel thermocouples (Pyrotenax Ltd), braised into a short length of pressure tubing, coned and left-hand threaded on one end, in similar fashion to that used for the pressure lead (figure 2.6a). This could then be inserted through one port of a 'T'-block, whilst the other two are used for water under pressure from the pump, and water to the autoclave respectively (figure 2.6b). A similar arrangement could be used for two temperature sensors (down one port), or for temperature and pressure sensors, for detailed observations on conditions within the growth zone.

The furnaces had two zones, one near the bottom where the temperature was nearly constant over



A Pump
B Pressure tubing
C Tee blocks
D 2 way straight valves
E 2 way angle valves
F Pressure fuses
G Autoclaves (up to 4)
H Thermocouples

Figure 2.7

Pumped autoclave system (diagramatic)

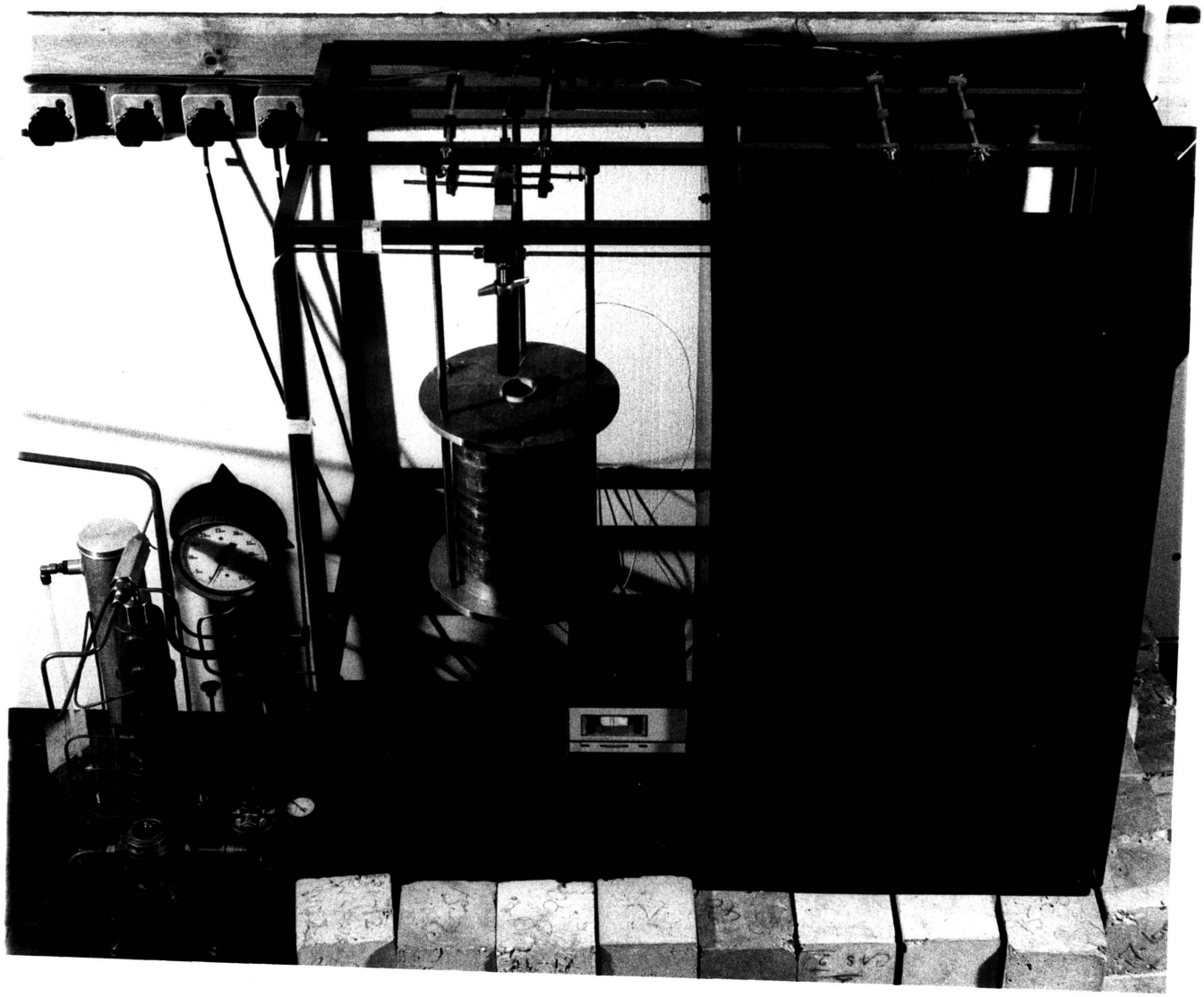


Figure 2.8

Pumped hydrothermal system

several centimetres and another just above this, where the temperature gradient, although varying slightly with temperature setting, gave about 30C° drop in 15cm. Thus isothermal or temperature gradient conditions could be used.

A schematic diagram and photograph of the equipment are shown in figures 2.7 and 2.8.

In view of the danger of using this equipment, certain safety precautions were taken. On the frame which supports the furnaces, temperature controllers, autoclaves and pressure leads were hung soft mild-steel sheets by steel hooks. Normally these sheets stand on 6 inch cubes of concrete so that their hooks are just clear of the frame and they lean against it. Should high pressure superheated water or high speed metal strike these safety screens, first the sheet would be dislodged from the concrete blocks and its weight transferred to the frame via the hooks, then any residual momentum can be expended in deforming the (relatively) soft sheet and swinging it outwards on its hooks. In this position the screen deflects any shrapnel etc downwards and

to safety.

In the photograph the equipment is shown with one sheet removed to display the autoclave assembly. The equipment can operate at pressures in excess of 15,000 psi (1000 bars) and temperatures up to 600°C. Some autoclaves were also made in modified form, the closed end being finished in identical fashion to the pumped end, except that the cone used to seal it was blank, without a water inlet hole. This type of autoclave was more convenient to use since the growth mixture was contained in sealed 6mm OD high purity gold tubes which closely fitted the autoclave, and removing these was facilitated by having an open ended cavity.

In use, the gold capsule was filled to produce the pressure required at the growth temperature and pressure compensation is provided by the pump. The method of use was as follows:

i final pressure of the run pumped into the autoclave while cold as a test for leaks etc

ii pressure brought back to atmospheric

iii furnace controller set to about 100°C and a corresponding pressure pumped in

iv when the system attains equilibrium after (iii), pressure and temperature are increased in approximately 100C° steps (and the corresponding pressure also) and equilibrium attained, until the required P and T are obtained.

In some runs, blank cones were used at both ends (or one only for the single ended autoclaves) and pressure balance was controlled by degree of fill of the vessel.

2.2.4 Sealing of gold capsules

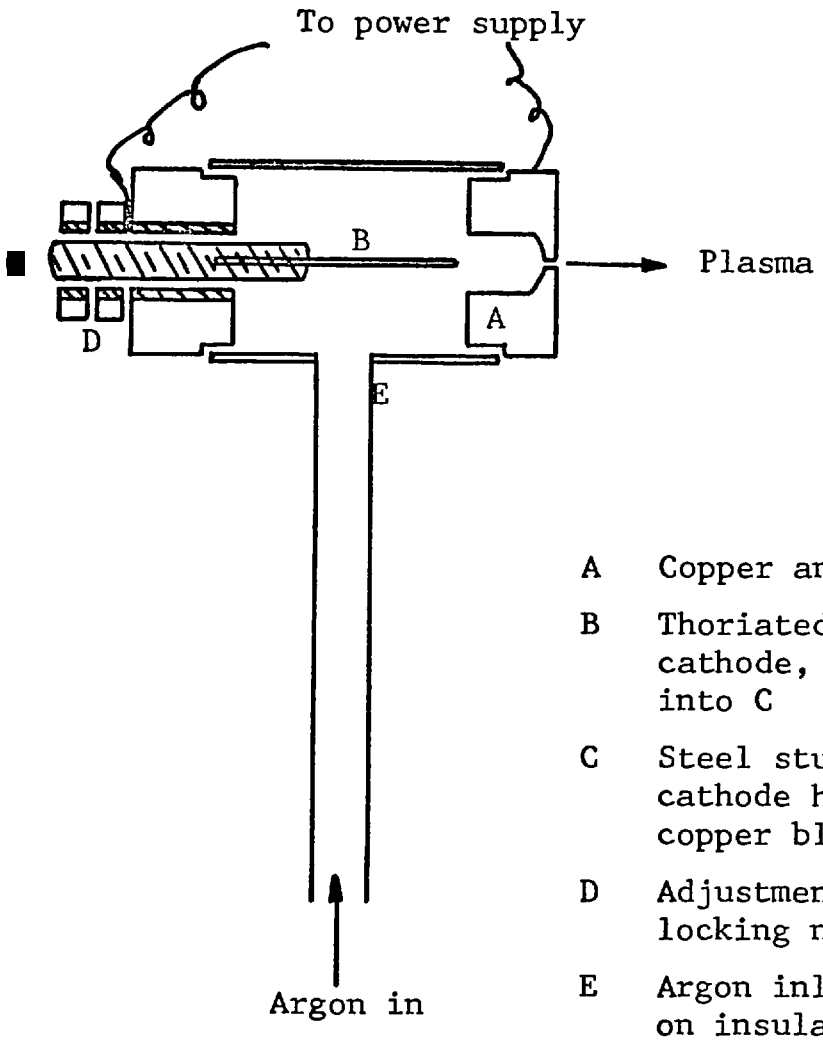
When the bolt on head autoclaves were used, no problems were encountered with the growth capsules since the internal diameter of the vessels was about 1 inch giving a large clearance between the gold tube and the autoclave. For this growth method, therefore, the capsules were sealed by folding followed by cold pressure welding.

The Tuttle type autoclaves were more difficult to use since the gold tube was chosen to have as large



Figure 2.9

Folding and pressure welding of gold capsules.
Left to right - flattened; folded; curved,
refolded and pressure welded



A Copper anode

B Thoriated tungsten cathode, push fit into C

C Steel studding cathode holder in copper block

D Adjustment and locking nuts

E Argon inlet/handle on insulating body

Figure 2.10

Argon arc plasma gun

a diameter as possible to fit inside the autoclave. Folding and pressure welding was possible only if the flattened ends were folded and curved about an axis parallel to the longitudinal axis of the capsule (figure 2.9). Other methods were therefore tried, ie arc and argon arc welding and arc plasma welding. For the first two methods the gold tube was made the positive electrode and a thoriated-tungsten rod set in a copper block the cathode. A miniature argon arc plasma gun was constructed using a similar arrangement for the cathode, with the addition of a copper anode and argon lead (figure 2.10).

Finally, however, folding and cold welding was mainly used, though much care was needed to avoid rupturing the thin wall of the tube.

2.2.4 Materials used

All solid materials were 'Analar' grade or better. 'Analar' materials were from Hopkin and Williams Ltd and 6N SiO_2 from Koch-light Laboratories Ltd.

Other materials used were:

D_2O	99.7 at %D	Koch-light Laboratories
40% NaOD in D_2O	98 at %D	Koch-light Laboratories
Argon	4N5	British Oxygen Ltd
Oxygen		British Oxygen Ltd

2.2.5 Hydrothermal preparation of microcrystalline sodalite

All apparatus which came into contact with the charge components, including the gold capsule, were ultrasonically cleaned in 'Teepol' solution and distilled water, then acetone and water rinsed and oven dried.

The basic charge consisted of the proportions shown below:

	weight proportion	relative number of millimoles
SiO_2	0.420g	6.990
Al_2O_3	0.392g	3.845
NaCl	0.344g	5.787
NaOH	0.611g	14.906
H_2O	2.6ml	144.444

The exact proportion of H_2O depended on the degree of fill required. Additives such as sulphate, phosphate and perchlorate were added to the charge as the sodium salts, typically at a molar concentration of 5% of the water concentration of NaCl, where doped sodalites were required. The mixture was then placed in a gold capsule, sealed, and placed in an autoclave (with appropriate degree of fill if a sealed system was being used), and transferred to an appropriate furnace which was gradually brought to the growth conditions, as described above.

On completion of the run and cooling to room temperature the gold tubes were opened and their contents filtered on a Buchner funnel, washed with distilled water, followed by 'Analar' acetone and air dried (except for deuterated sodalites which were quickly oven dried).

2.3 Fluxed melt growth

2.3.1 Introduction

Flux growth uses a 'flux' which is a low melting point (say 400-800^{o}C) solvent to dissolve the feed

materials, conditions being arranged so that these deposit from the solution as a stable phase. There are two important methods:

a) by dissolution then gradual evaporation of the solvent, making the solution supersaturated

b) gradual solution of the components of a material, which react in solution forming the compound which can then precipitate out as the solution becomes supersaturated.

The latter is often performed with a temperature gradient between feed and growth site or slow cooling of the mixture.

Reviews of fluxed growth have been compiled by Laudise (1963) and by White (1965).

In this particular case sodalite was formed by slow cooling in a flux of sodium carbonate/sodium vanadate (White 1970). Although this method was used for most runs, several other methods were also tried; for example, precipitation from a flux and wire seeded, temperature gradient growth were also used but only

the slow cooling produced photochromic sodalites. In each case, a premelt procedure was followed. The materials used were of Analar grade and the standard charge consisted of:

	relative weights (g)	relative number of moles
Na_2CO_3	25.60	0.242
V_2O_5	13.64	0.075
Al_2O_3	3.40	0.033
SiO_2	5.00	0.083
NaCl	10.00	0.171

To this 'standard' formula various dopants were added, eg transition metal oxides; sulphate ions, molybdate ions or phosphate ions as sodium salts in varying quantities. Crushed synthetic white sapphire was used in some runs in place of powdered Al_2O_3 whilst crushed fused quartz was sometimes used in place of powdered silica. Also NaCl could be replaced by other sodium halides.

2.3.2 Pre-melt procedure

The constituents of the charge without the sodium

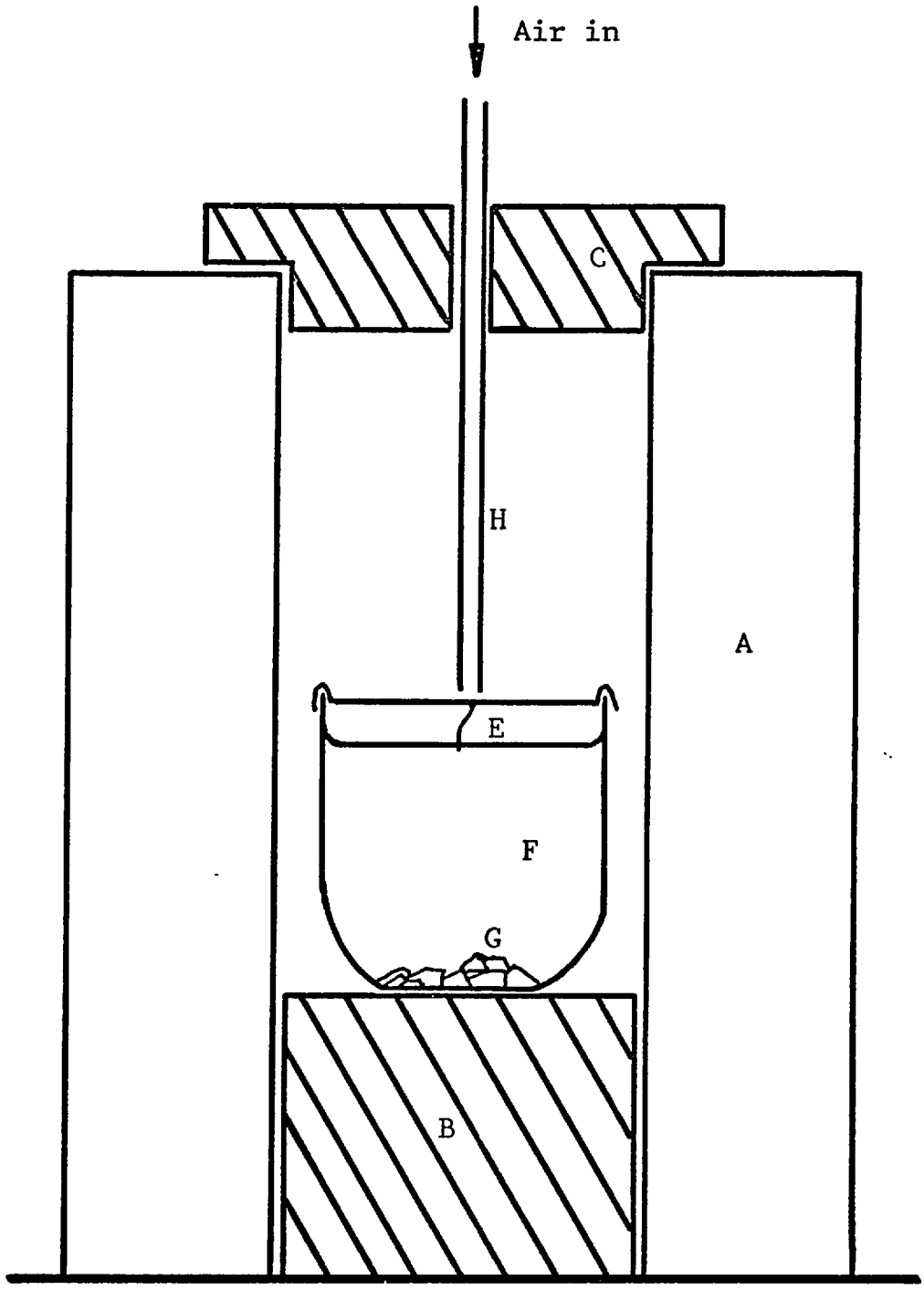
chloride were thoroughly mixed dry in a roller mixer. The resultant powder was then placed a little at a time into a platinum crucible heated by a resistively heated, vertical, tube furnace to about 800°C, the rate of addition being determined by the effervescence due to reaction of the Na_2CO_3 and V_2O_5. Platinum was used to avoid contamination from corrosion by the liquid. When the melt ceased effervescing (about 3 hrs), the mixture was allowed to cool.

2.3.3 Controlled cooling growth

Sodium chloride, omitted previously to avoid loss by evaporation, was added to the product of the premelt and a platinum lid was crimped on to the crucible. The crucible was placed in a furnace at 980°C and cooled at two or three degrees per hour to 650°C. The crucible was then allowed to cool naturally to room temperature.

2.3.4 Precipitation from flux

The procedure was as above but the temperature of the growth furnace was held at about 980°C for



A	Vertical tube furnace	E	Pt seeding wire
B	Fireclay block	F	Growth liquid
C	Fireclay lid	G	Feed solids
D	Pt crucible with crimped on lid	H	Alumina air tube

Figure 2.11

Wire-seeded flux-melt growth furnace

about 10 hours, then allowed to cool naturally.

2.3.5 Wire-seeded temperature gradient growth

For this method, the same charge as the other methods was used but the crucible lid had welded to its inner surface a platinum wire, arranged so that its tip dipped just below the surface of the molten mixture. The furnace (figure 2.11) was maintained at a temperature of 900^{o}C and air was blown on to the end of the platinum wire in order to seed sodalite crystals. After eight days the furnace was turned off and the crucible was cooled to room temperature.

2.3.6 Extraction of products

After each run, microscopic examination showed the products to be sodalite crystals embedded in the flux. Since the latter is soluble in hot water, and the unreacted materials all have a lower density than sodalite, the sodalite crystals can be recovered by settling them out in hot water. X-ray powder diffraction confirmed the only material present is sodalite except for very small amounts of unreacted silica and alumina.

2.4 Low temperature hydrothermal synthesis of sodalite from kaolinite

2.4.1 Introduction

Kaolinite is a china clay mineral with a typical analysis as shown in table 2:1

Table 2:1

	%
SiO_2	46.6
Al_2O_3	38.3
Fe_2O_3	0.49
TiO_2	0.05
CaO	0.2
MgO	0.2
K_2O	0.68
Na_2O	0.07
loss on ignition	13.43
(moisture content	1.0 ± 0.5)

When this material is heated with sodium hydroxide solution, sodalite or the related cancrinite is formed, depending on the conditions. The presence of a variety of salts affects which of these products

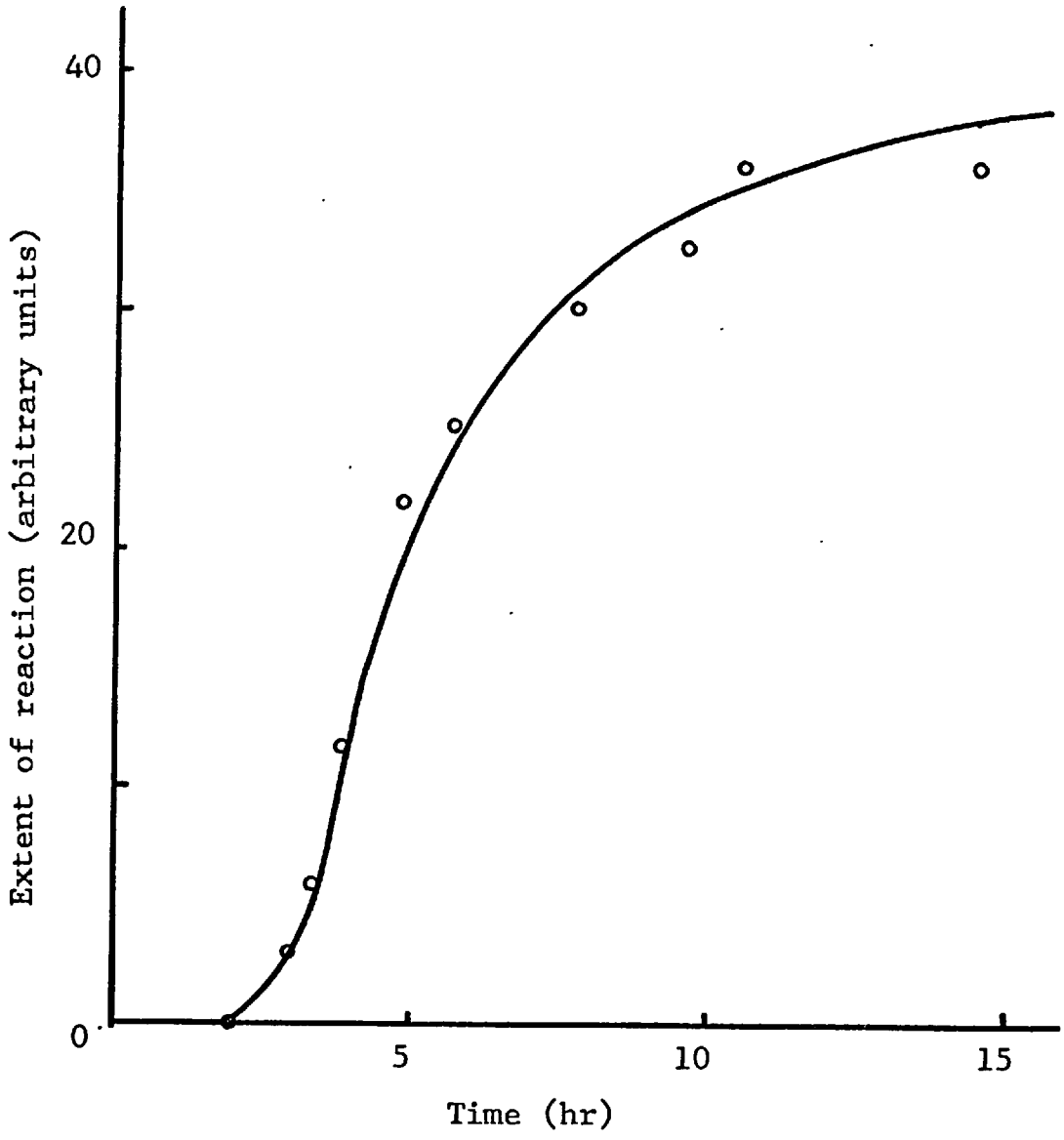


Figure 2.12

Kinetics of formation of $NaClO_4$: sodalite

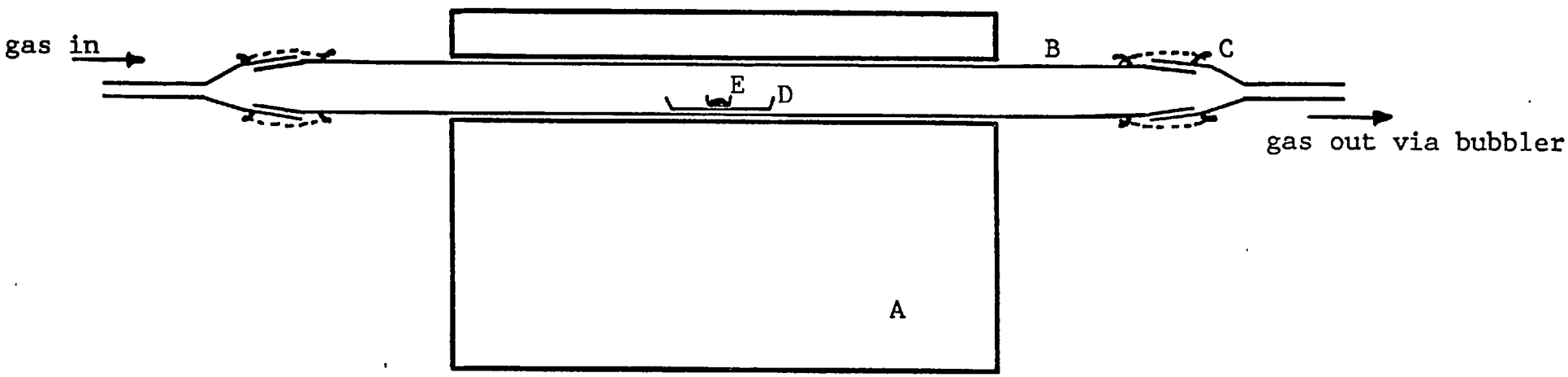
is formed and also its chemical composition, since they can enter the crystal lattice of either (see Barrer, Cole and Sticher 1968, Barrer and Cole 1970, Cole and Villiger 1970).

The kinetics of the reaction are shown in figure 2.12. Barrer and Cole (1970) weighed the oxygen released during thermal analysis of the reaction mixture at various stages in the formation of perchlorate sodalite, ie with ClO_4^- replacing Cl^- in chlorosodalite.

From X-ray diffraction studies Barrer and Cole (1970) showed that the kaolinite was attacked and partly rendered amorphous in the first 2 hr whilst sodalite begins to appear after 4 hr. After this induction period a period of rapid growth ensues, followed by slowing down of growth on exhaustion of the nutrients.

2.4.2 Experimental procedure

The most successful synthesis of sodalite by this method used the reactants in the proportions:



A Tube furnace

B Silica tube

C Ground silica/pyrex cone-in-cone seal + retaining springs

D Alumina boat

E Gold container + sample

Figure 2.13

Activation Furnace

2g kaolinite (English Clays Lovering Pochin and Co), 200ml 4M sodium hydroxide solution and 10g of the chosen sodium salt. They were refluxed (about 105°C) and stirred in a polypropylene lined flask for 12-60hr. The product was filtered whilst hot, washed with distilled water and air dried.

2.5 Activation studies

2.5.1 Introduction and apparatus

Sodalites grown at high temperatures, eg by sintering and flux melt, if they are photochromic at all, are active as grown. However, the materials grown by hydrothermal methods are not, and require activating by heating in a reducing or inert atmosphere at 600-1050°C.

The apparatus used is shown in figure 2.13. It is a horizontal tube furnace (Gallenkamp FS212), through the tube of which passes a 32-33mm silica tube (Thermal Sindicate Ltd, Vitreosil). The tube is terminated by ground, silica cones and gas is led in and out via ground pyrex 'Quickfit' sockets. The silica-pyrex joint is adequate since these parts of

the tube never become hot. The exhaust gas bubbles through 2 Dreschel bottles, the second containing silicone oil to measure the flow rate.

2.5.2 Procedure

Powdered hydrothermal sodalite was placed in a gold foil container in a sintered alumina boat. After removing the exhaust end pyrex socket, this assembly was slid into the centre of the tube which had been previously flushed with the required gas, at usually 900^{o}C, with a silica rod against the flow of gas. The socket was replaced.

On completion of the activation, typically 30 min, the downstream end socket was again removed, and the boat slid further along, through the hot zone. Simultaneously the silica tube was slid in the same direction, taking the boat well out of the hot zone. (The flow of gas is such that the sample is always surrounded by it). The socket was replaced and the sample cooled in the flow of gas. In addition experiments were performed using oxygen and also where the tube was left open ended, effectively,

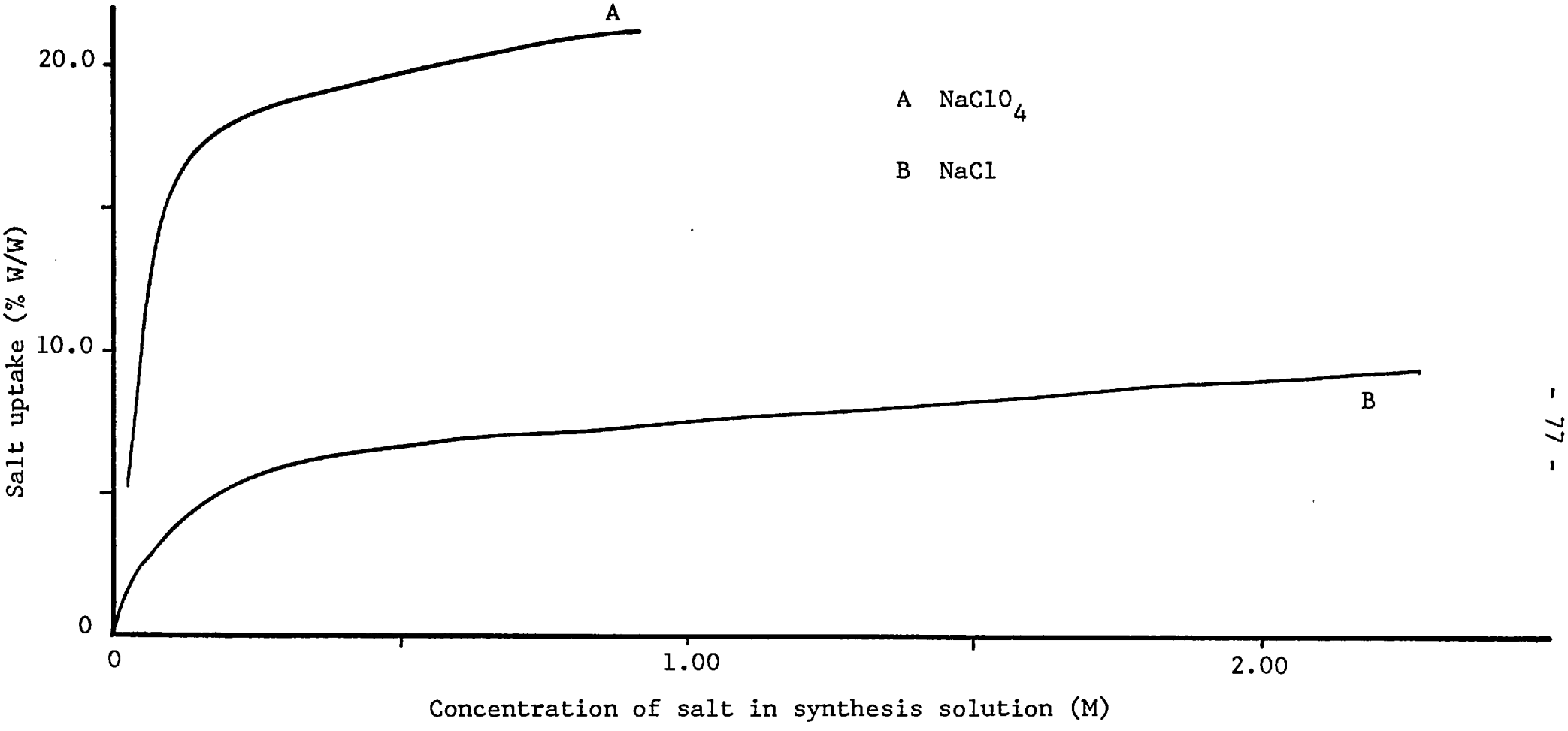


Figure 2.14

Salt inclusion isotherms in sodalite (from kaolinite)

therefore, heating the sample in air. When cool, the sample was tested for photochromism with an unfiltered Hanovia 'Chromatolite' UV lamp (15w).

2.5.3 Effects of activation studies on photochromism - 'HT10'

The optimum conditions for most sodalites were found to be 900°C for 30 minutes in an atmosphere of argon. One type of material grown, designated HT10, was produced from a hydrothermal growth mixture containing sodium perchlorate at a concentration of 5 molar% that of sodium chloride. Because of the differences in the salt inclusion isotherms of NaCl and $NaClO_4$ in sodalite, however, the product would not be doped to the same extent. These isotherms are shown in figure 2.14 and Table 2.2 shows the theoretical maxima of NaX content for the formula $Na_6Al_6Si_6O_{24}.2NaX$.

Table 2.2

included species determined as Na salt	theoretical maximum weight %
NaCl	12.0
NaBr	19.5
$NaClO_3$	20.0
$NaClO_4$	22.3
(H_2O	14.5)

The concentrations of NaCl and $NaClO_4$ in this case are 1.2M and 0.6M respectively and assuming the salt take up is under thermodynamic control, reference to figure 2.14 then table 2.2 gives that 0.65 of the Cl sites are filled by Cl and 0.515 by ClO_4. The result of normalisation of these fractions gives the fraction of sites filled by Cl^- = 0.558 and ClO_4^- = 0.442.

Similar results are obtained for calculations with chlorate ions in the system instead of perchlorate. These figures illustrate the competition between the chloride and perchlorate radicals and shows the strong selectivity of sodalite for perchlorate (and chlorate) over chloride and other halides. Also some of the Cl sites will be occupied by OH^- ions and water molecules.

An effort was made to determine the proportions of Cl, ClO_4 and H_2O or OH in the structure by differential thermal analysis (DTA). In this, water and hydroxyl groups leaving the lattice would cause absorption of heat but decomposition of perchlorate groups would be exothermic. The departure of the former could be seen in the DTA trace but perchlorate decomposition could

not be seen, even up to 1045°C.

Direct measurement of the distribution of groups in the lattice was not very successful by this method, but the proportions calculated seem reasonable since HTlO is unlike both sodalite: Cl and sodalite: ClO_4 in properties, eg its epr spectrum (chapter 4) and activation. The distribution of groups is reconsidered in chapter 3.

The optimum activation heating time for chlorosodalite at 900°C is about 30 minutes; longer times reduce the intensity of the photochromic response considerably. Exposure of the material to air whilst above 450°C also reduces and eventually destroys the photochromism. For the materials in which both Cl^- and ClO_4^- are present, viz HTlO, the time of activation is not particularly critical from 16 to 120 minutes and activity is still shown after 4 hr at 900°C. Furthermore, the activity is little affected by activation in air or oxygen. This represents a considerable advance as outlined below.

2.6 Summary

The general procedure for growth and activation of sodalites has been discussed. A novel hydrothermal sodalite material has been described which can be activated not only in inert atmospheres but also in air or even oxygen. This is significant technologically as the main use of sodalite is in cathodo- or photochromic screens when it is applied by settling out from suspension. The crystallites need to be of uniform size and fairly regular in size (for rolling and settling), and they are obtained in this form from hydrothermal synthesis. From flux melt growth and sintering the product is irregularly shaped and of highly variable size. The material HTIO also holds advantages industrially over other sodalite materials as it can be activated more cheaply.

3 STRUCTURAL INVESTIGATIONS ON SODALITE

Two techniques were used for investigations into the structure of sodalite, namely, X-ray powder diffraction and infra-red spectrometry.

3.1 X-ray powder diffraction

The microcrystalline products from each method of growth, as grown and heat treated where appropriate, were identified by Debye-Scherrer X-radiographs. The diffraction pattern shown in figure 3.1 was taken on a 5.7cm diameter (180mm circumference) camera. In all cases the sample used was a finely ground powder suspended in gum tragacanth. The X-ray equipment used was a Philips PW1009/30, with a copper target and nickel filter, run at 40kv and 20mA. The film was Kodak 'Kodyrex' KD59T.

The line positions were as expected for sodalite with a lattice constant of 8.87Å, this constant value dependent on the dopants used, eg chloride sodalite has a lattice constant (ao) of 8.870Å whilst for bromide sodalite ao = 8.941Å and for iodide sodalite ao = 9.016Å.

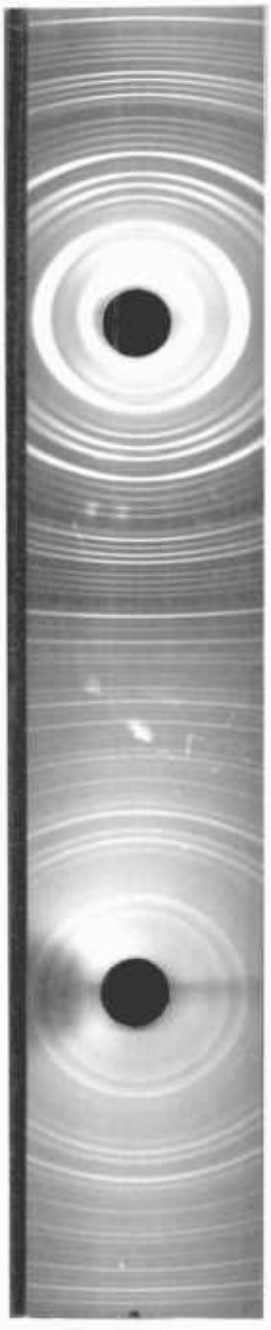


Figure 3.1

X-ray powder diffraction pattern of a typical sodalite

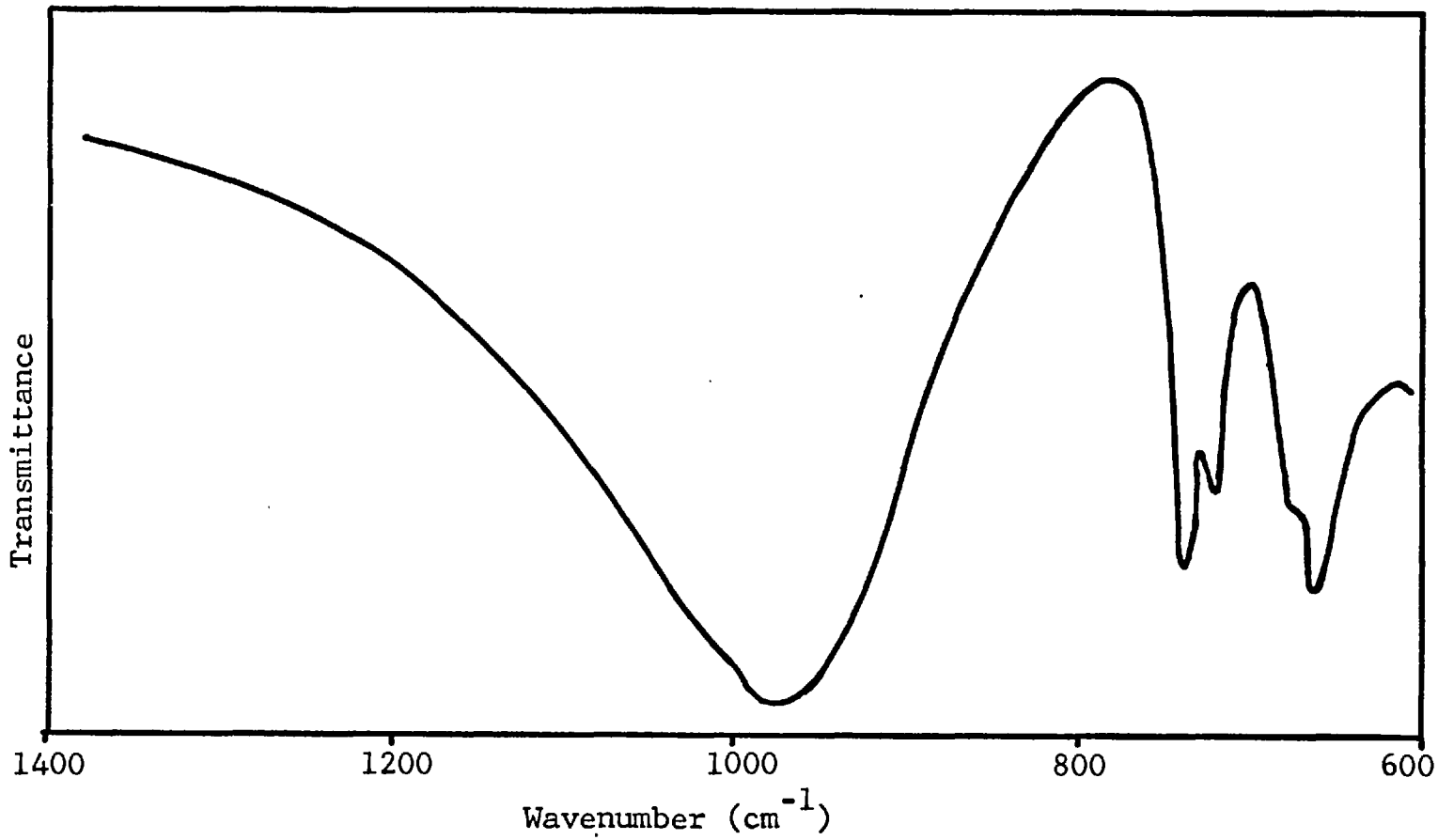


Figure 3.2

Infra-red spectrum of chlorosodalite in the region of 1000cm^{-1}

The sodalites grown from kaolinite gave more diffuse lines than those given by materials obtained by growth using other methods, indicating that they were less perfectly crystalline, which may explain their lack of photochromic activity.

3.2 Infra-red spectrometry

Measurements were made using a Perkin-Elmer 457 infra-red grating spectrometer in the transmission mode, scanning between 250 and 4000cm^{-1} (40-2.0 μm). The samples were made up as 'Nujol' (liquid paraffin) and hexachlorobutadiene (HCB) mulls between sodium chloride plates. Spectra were recorded on as-grown and heat treated materials.

3.3 Results of structural studies

The infra-red spectra of all the sodalites grown, which had been identified by X-ray diffraction, showed the expected absorption peaks in the region of 1000cm^{-1} common to all aluminosilicates and due probably to the stretching modes of SiO_4 and AlO_4 tetrahedra (figure 3.2) (Milkey 1960). The absorption bands in the 600-800cm^{-1} region are characteristic of the sodalite

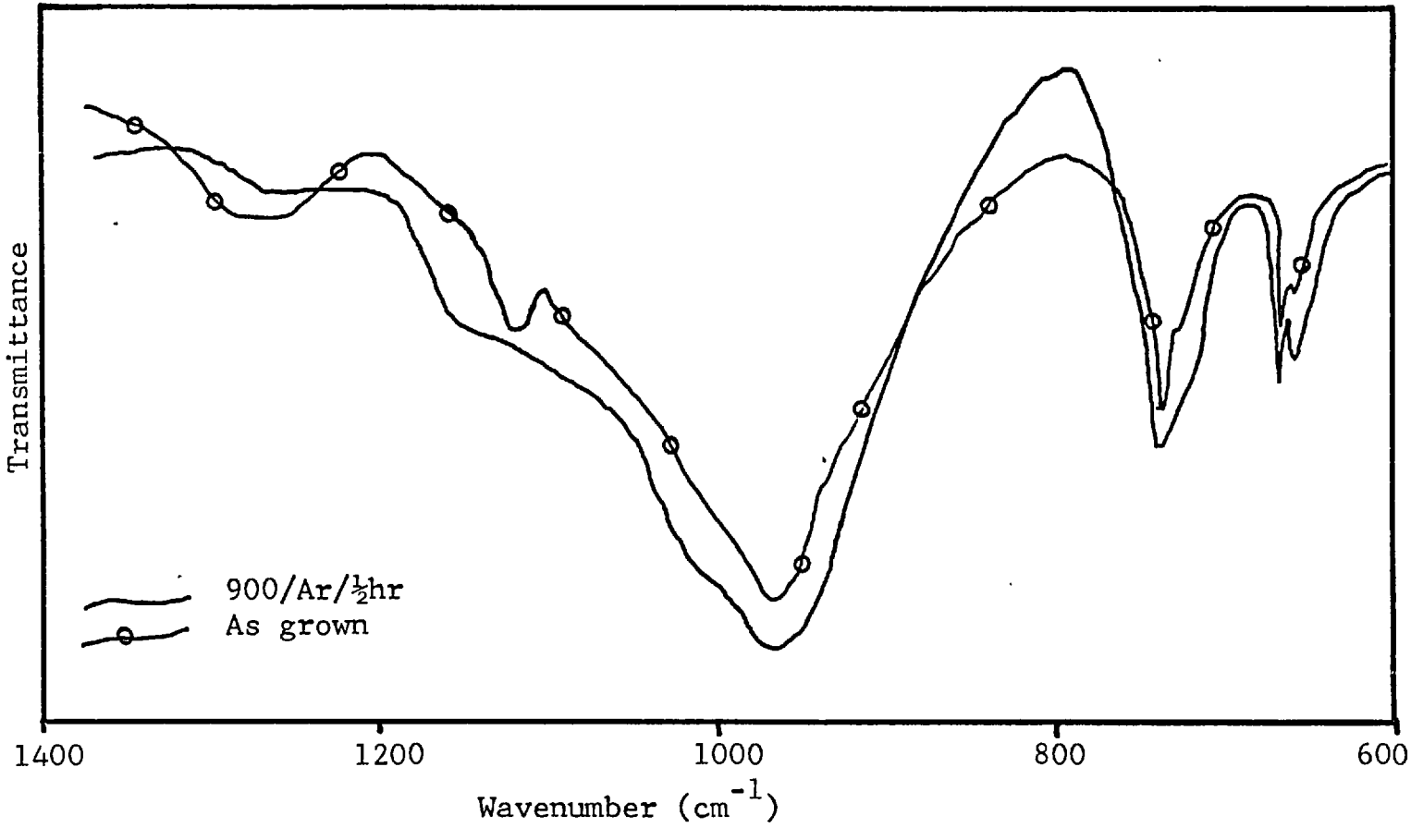


Figure 3.3

Infra-red spectra of HTlO in the region of 1000cm^{-1}

lattice and are due to bending modes in the lattice. However, the similarity of these infra-red spectra to others from naturally occurring minerals of the feldspar group precludes them from being used to determine whether the material is sodalite.

Since none of the sodalites prepared were totally hydroxy-sodalites (even from hydrothermal synthesis), heating them causes no collapse of the structural unit, the halide or other substituent (perchlorate etc) stabilizes the lattice (Taylor et al 1971). This fact is illustrated in figure 3.3 which shows the low energy end of the IR spectra of the material HT10 before and after heating to 900^{o}C in argon for 30 minutes.

There is a cut-off at 500 - 600cm^{-1} due to the IR absorption band edge of the sodium chloride plates supporting the mull. Most of the spectra shown have had the absorption bands of Nujol and HCB removed, but the spectra of these mulling agents are shown in figures 3.4 and 3.5.

The higher energy infra-red absorption spectra of the hydrothermal sodalites in the 1600-4000cm^{-1} range

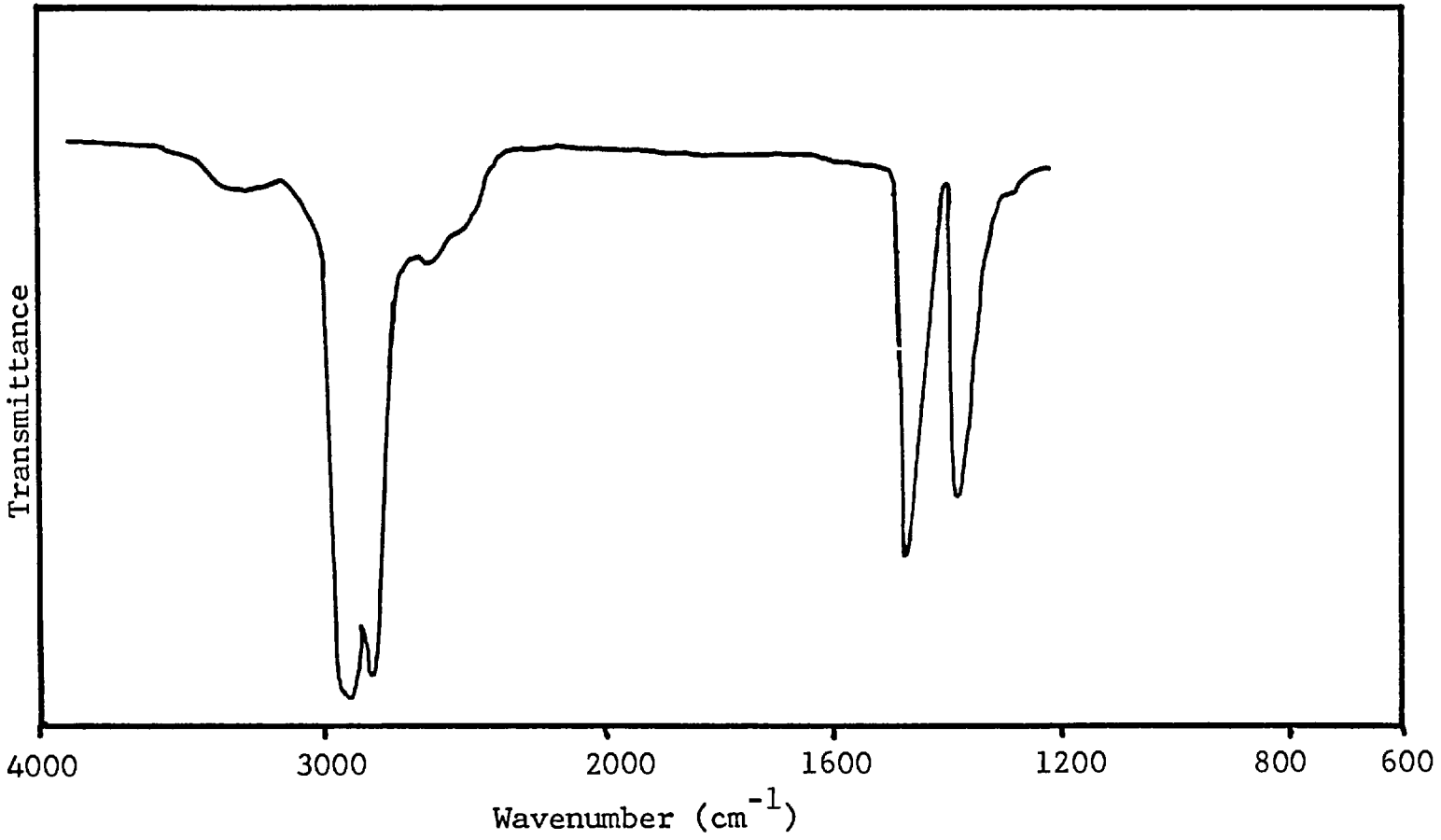


Figure 3.4

Infra-red spectrum of Nujol

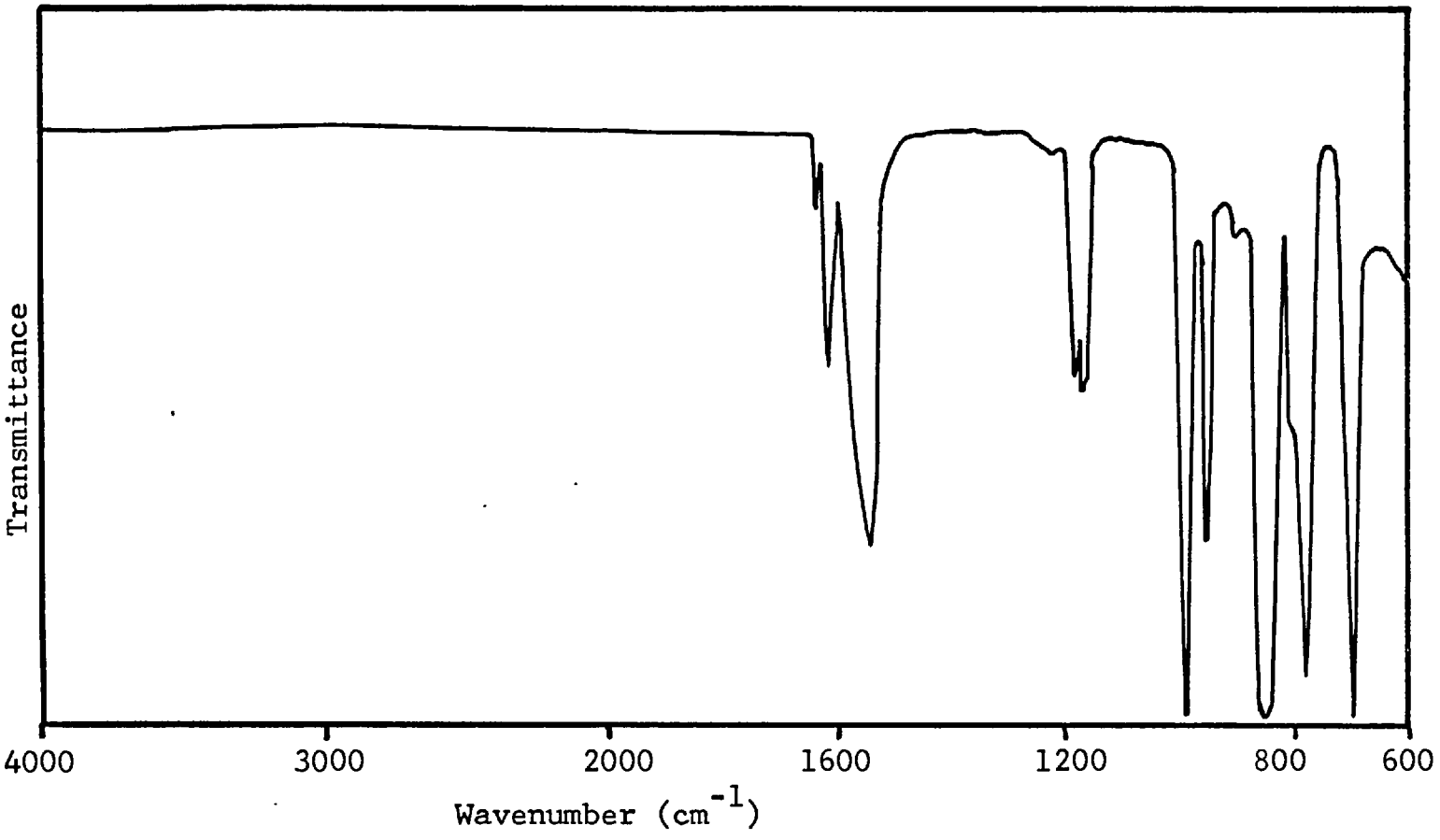


Figure 3.5

Infra-red spectrum of hexachlorobutadiene

showed a broad band centred on 3450cm^{-1} due to the water molecules in the lattice. No absorption bands were observed from hydroxy groups. This observation was contrary to expectations and to the findings of Taylor et al (1971) who found OH bands at 3400cm^{-1} and 3635cm^{-1} and ascribed them respectively to surface adsorbed water molecules and hydroxyl groups located within the sodalite cages.

It was possible using infra-red spectroscopy to follow changes not only in the intrinsic sodalite structure, but also to observe the effects of substituents. Thus for HT10 in which some of the chloride in the formula $Na_6Al_6Si_6O_{24}$ NaCl is replaced by perchlorate (see below), one of the vibration modes of the ClO_4^- group can be identified at 1119cm^{-1} and appears as a peak superimposed on the stretching peak of the aluminosilicate lattice (figure 3.6). ClO_4^- also shows other peaks at 928, 459 and 625cm^{-1} (Nakamoto 1970), but these were not seen in my materials, probably because their oscillator strength is lower. This peak at 1119cm^{-1} also occurs strongly in the 100% perchlorate material (HT11) and the

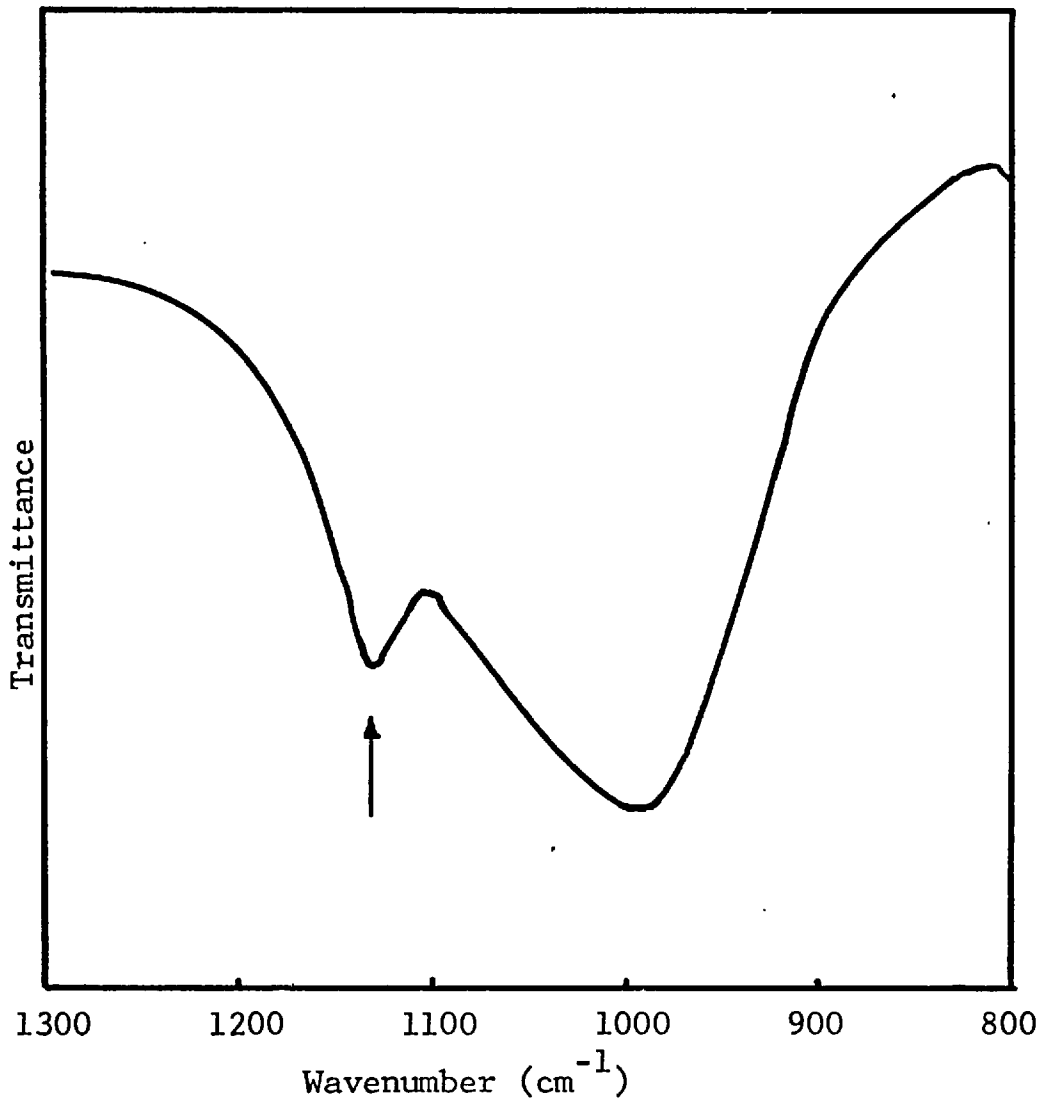


Figure 3.6

ClO_4^- (in HTlO) stretching peak

- marked with arrow

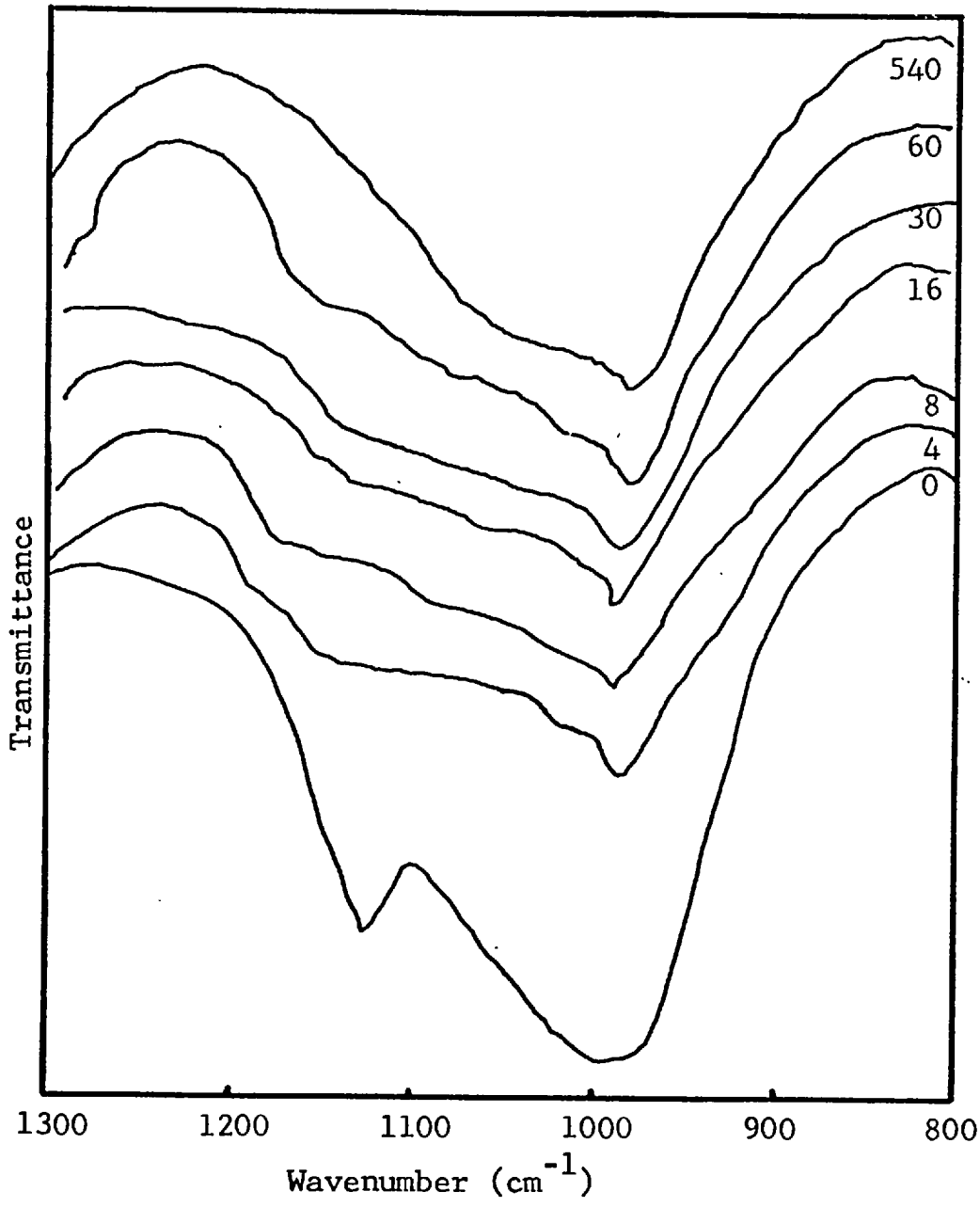


Figure 3.7

Fade of ClO_4^- IR peak on heating HT11 at 900°C in argon for the number of minutes shown

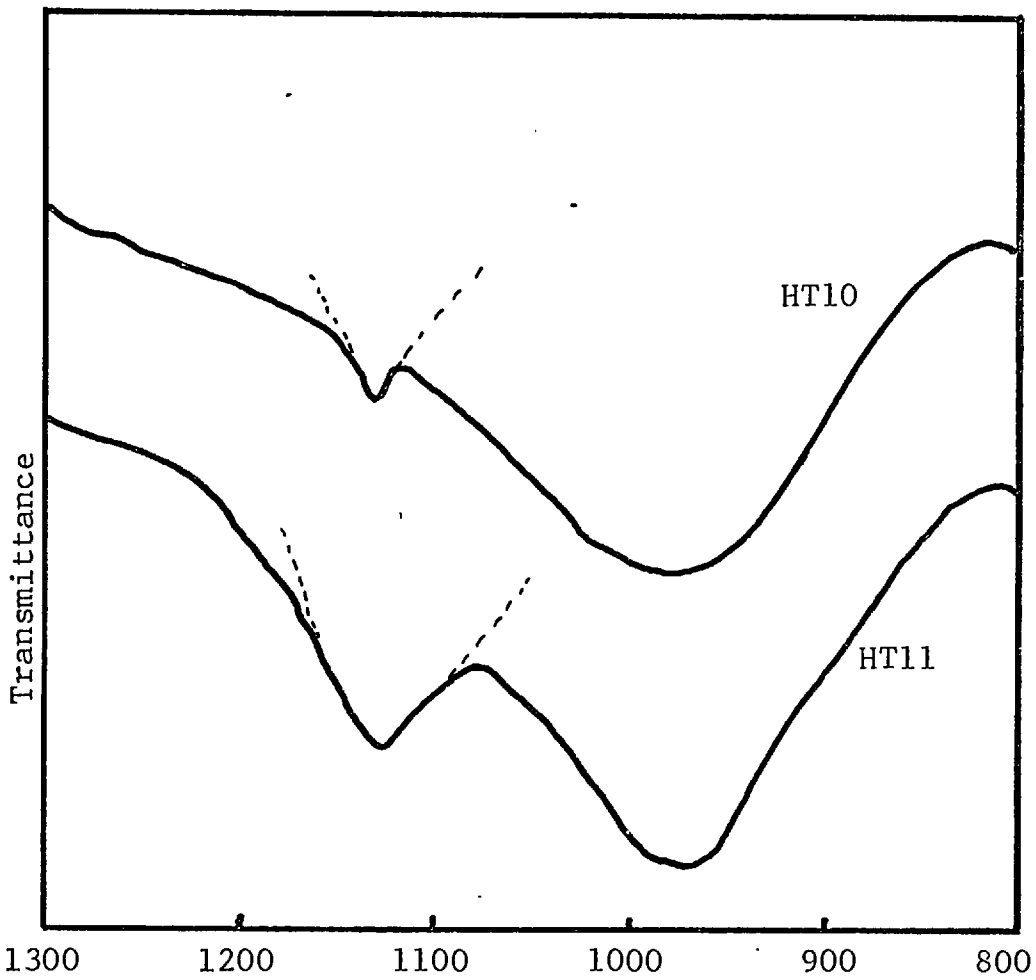


Figure 3.8

IR spectra of HT10 and HT11 in the region of the ClO_4^- and $(Al,Si)O_4$ stretching frequencies

decomposition of the perchlorate groups on heating can be followed by observing the amplitude of this peak. Figure 3.7 shows the decay of the perchlorate band after heating a perchlorate sodalite in argon for various periods of time at 900°C. As the chloride ion produced by the decomposition of the perchlorate ion has no vibration mode, the simultaneous increase of another band in the infra-red along with the diminution of the perchlorate peak could not be observed. Some disruption of the $(Al,Si)O_4$ framework can also be implied from the changes in the $1000cm^{-1}$ peak. The perchlorate peak changes lead to the possibility of making a quantitative estimate of the amount of chloride ion replaced by the perchlorate ion in HT10, by considering the relationship of the area of the $1119cm^{-1}$ peak of ClO_4 (Apc) to that of the aluminosilicate lattice peak (Aas) in as-grown HT10 and HT11, assuming the extent of perchlorate in HT11 approximates to 100%. The appropriate regions for the two spectra are superimposed in figure 3.8.

After estimation of the true band shape (broken line in figure) the respective ratios are (in arbitrary units):

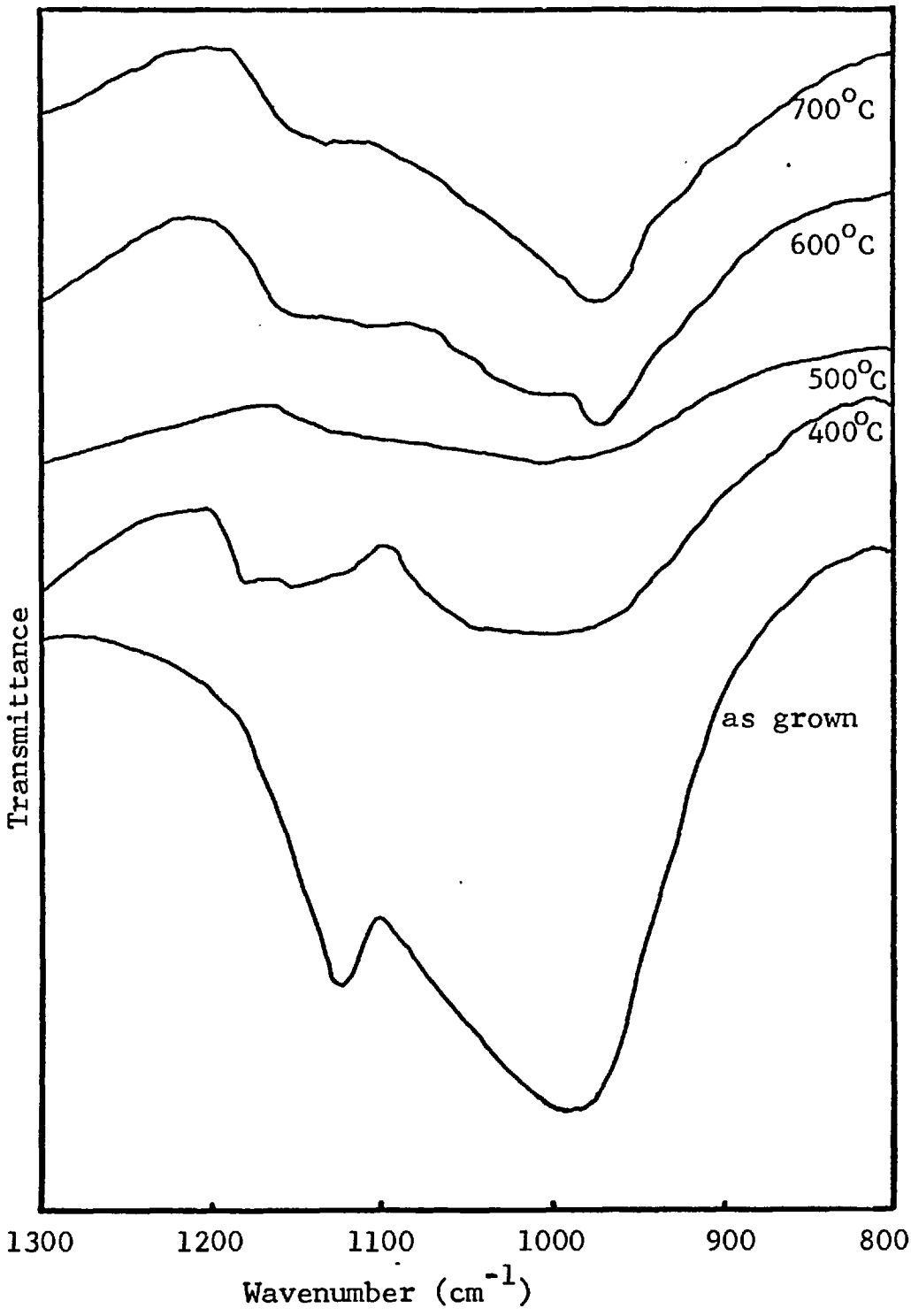


Figure 3.9

Variation of HT11 IR spectrum after heating at various temperatures for 4 minutes in argon

HT11 Aas = 571 Apc = 242

HT10 Aas = 427 Apc = 89

Then, the fraction of Cl^- sites filled by ClO_4^- in HT10 is therefore 0.489. As there is at least 5% error in these figures, taking them with those calculated from the work of Barrer and Cole (1970) who grew sodalite from kaolinite, these results justify the assumption made in section 2.5.3 that the salt take up of the product is under thermodynamic control rather than that of the starting materials. It may also be noted that the occurrance of the perchlorate peak at $1119cm^{-1}$ signifies that the radical is present as ClO_4^-, as one might expect from the stability of this radical and the lattice charge balance.

The $1119cm^{-1}$ peak cannot easily be observed in any of the spectra other than the as-grown material. This result suggests that at 900°C, decomposition of the perchlorate group is rapid. Thus if a sample of perchlorate sodalite is heated for 4 minutes at a series of temperatures between 400 and 900°C, significant decomposition appears to occur at 400°C (figure 3.9), and total decomposition occurs above

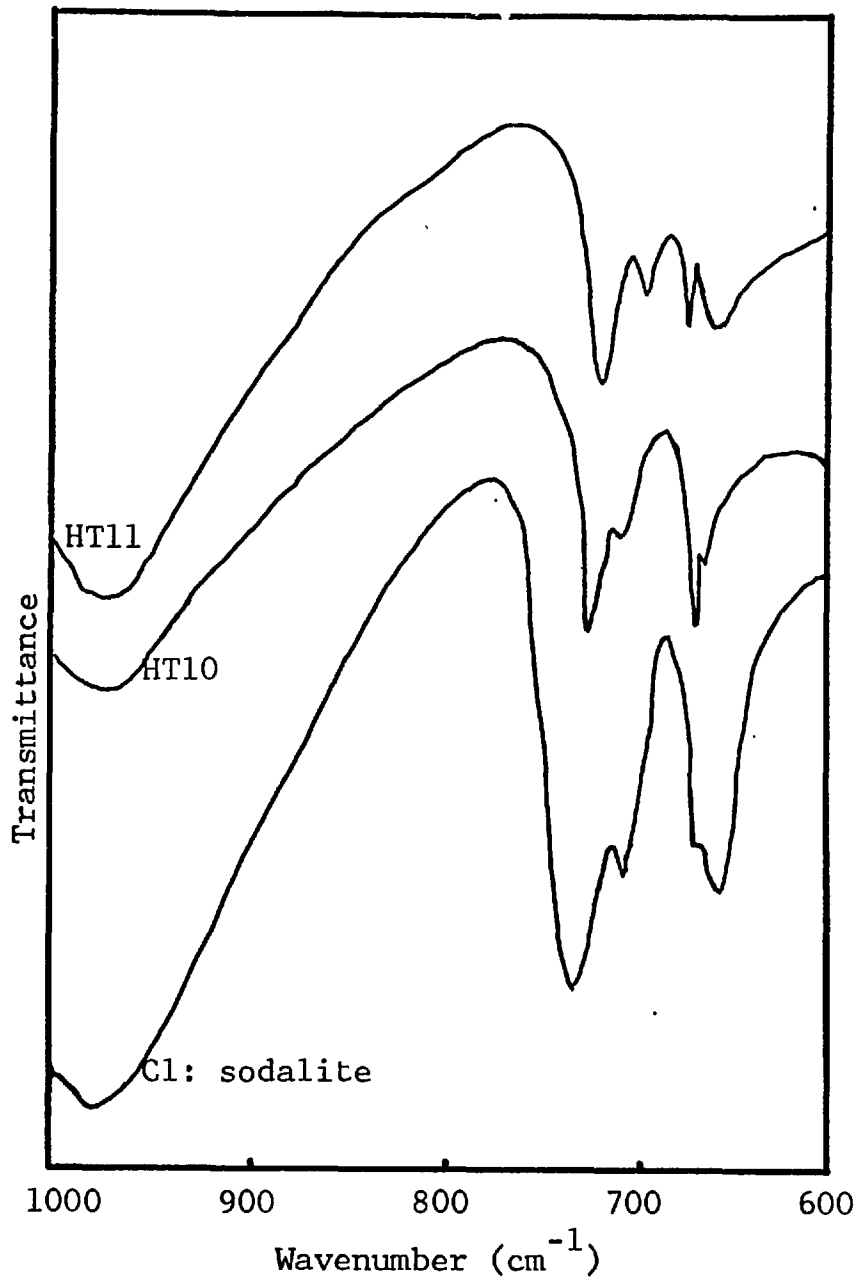


Figure 3.10

$(Al.Si)O_4$ IR bending modes in chlorosodalite, HT10 and HT11

this temperature. This result was not expected since pure crystalline $KClO_4$ decomposes at about 520°C and one would expect an 'encapsulated' salt to do so at a higher temperature as was found by Barrer and Cole (1970), who did not observe decomposition of perchlorate groups in sodalite grown from kaolinite, until approximately 650°C. The spectra also show disruption of the sodalite framework which seems to reorder after heating at the higher temperatures.

The aluminosilicate lattice bending modes between 600 and 800cm^{-1} are modified in HT11 (ClO_4: sodalite), though much less in material HT10, and not at all in unsubstituted materials. This effect is shown in figure 3.10 and is probably due to distortion of the bending modes by the large concentration of perchlorate groups. The materials also show this effect on heating, although heating for a long period up to 8 hours at 900°C produces materials which show bands nearer the 'normal' shape. This observation suggests that the bending modes are distorted by ClO_4^- groups and also possibly by the product of the decomposition, oxygen. When these groups have left the lattice, the distortions in the lattice can be annealed out.

4 ELECTRON PARAMAGNETIC RESONANCE (EPR)

4.1 Introduction

4.1.1 Paramagnetism and the resonance phenomenon

Any spinning or rotating charge behaves like a magnet with its poles along the axis of rotation; consequently electrons in atoms and molecules act as magnetic dipoles with a tendency to align themselves in the direction of an applied magnetic field. Very few stable molecules are paramagnetic because, whenever possible, the electrons tend to produce closed electron shells or pairs with opposed spin so that their magnetic dipoles cancel. Some compounds do exist which contain odd numbers of electrons, eg NO, NO_2, or whose molecule contains an even number of electrons, some of which have parallel spins, eg O_2; in such molecules there is a net magnetic moment and paramagnetic properties can be observed. Paramagnetic phenomena caused by the presence of unpaired electrons are more striking and diverse in the ions of the transition metals and in free radicals.

There are two main methods for studying paramagnetic

materials. The first involves measurements of bulk paramagnetic susceptibility and is based on measurement of the restoring force needed to maintain the orientation of magnetic dipoles against the disordering effect of thermal motion. It is not selective but relates only to the average over all the magnetic species in the sample. More recently the technique known as electron or paramagnetic resonance, electron paramagnetic resonance (epr) or electron spin resonance (esr) has been introduced.

Quantum theory shows that electrons can possess angular momentum only in integral multiples of a basic unit or quantum. It follows, therefore, that the associated angular magnetic moment must also be quantized, leading to a finite number of possible orientations with respect to a magnetic field. Each orientation represents a discrete energy level, and transitions between these levels may be induced, under appropriate conditions, by interaction with electromagnetic radiation. For a single unpaired electron there are only two possible orientations, with the axis of the magnetic dipole parallel or opposed (antiparallel) to the direction of the applied

magnetic field; the transition between them can be envisaged as the electromagnetic field reversing the direction of the magnetic dipole and hence the spin of the electron. When this occurs, there is an absorption of energy from the radiation which can be observed.

For a large number of species with a single unpaired electron, the frequency ν of the electromagnetic radiation which causes transitions is related to the magnetic field H acting on the sample by the equation 4.1

$$h\nu = g\beta H \qquad 4.1$$

where h is Plank's constant, β is the Bohr magneton (a factor for converting angular momentum to magnetic moment which has the value $\frac{e\hbar}{2m_e c} = 9.2732 \times 10^{-24} Jm^2 Wb^{-1}$

where e = electronic charge, $\hbar = \frac{h}{2\pi}$, m_e = electronic rest mass and c = speed of light) and g is a numerical factor, often approximately 2.

It is necessary to consider two results arising out of group theory: the Jahn-Teller theorem which states that any non-linear molecule with an orbitally degenerate ground state is unstable and tends to

distort in order to remove this degeneracy. Nothing in the elementary theory, however, tells us the direction of the resultant distortion, though this can often be deduced from spectroscopic data. Kramer's theorem states that if a system contains an odd number of electrons, a purely electrostatic field (such as encountered within an unconstrained crystal or molecule) cannot reduce the degeneracy of any level below two. Each degenerate level forms what is known as a Kramer's doublet, separable only by a magnetic field. Thus, one can, in principle, always observe electron resonance in such systems. Conversely, in a system with an even number of electrons, the degeneracy of the lowest orbital triplet or quintet may be removed by the crystal field, and the levels separated even without applied external magnetic field, an effect called zero-field splitting which is dealt with more fully in section 4.2.4. Electron resonance may or may not be seen depending on the extent of the splitting and the same factors as for the degenerate case (section 4.2.6).

4.2.1 Magnetic energy levels and the g-factor

The resonance phenomenon is shown in its simplest

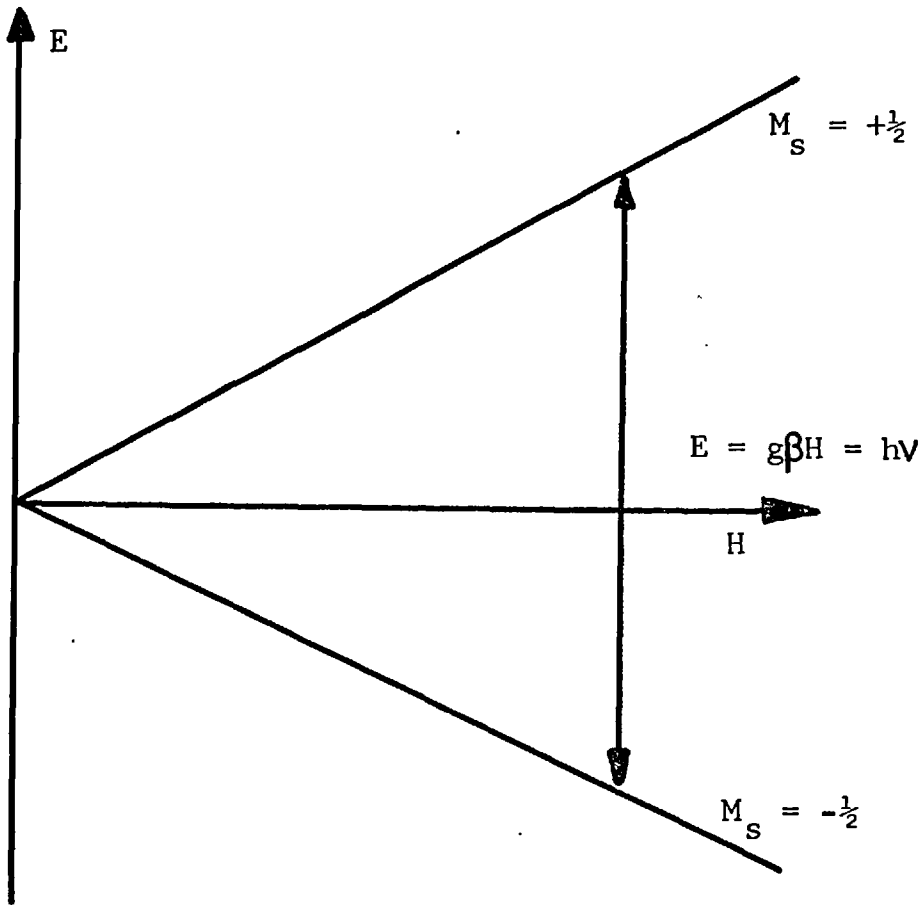


Figure 4.1

Magnetic (Zeeman) energy levels for a single unpaired electron ($S = \frac{1}{2}$) as a function of magnetic field

form by a set of non-interacting paramagnetic ions each possessing a single unpaired electron which has 2 possible energy states with M_J (magnetic quantum number) = M_s (spin quantum number) = $\pm \frac{1}{2}$. The two levels are degenerate, but are split by an applied magnetic field as shown in figure 4.1. In this case the g-factor or spectroscopic splitting factor represents the rate of divergence of magnetic energy levels with field. For commonly used fields (around 3400 gauss) the energy separation of the states corresponds to electromagnetic radiation of 9-10GHz in the microwave region.

In thermal equilibrium, the lower level is more densly populated than the upper levels and, since the transition probabilities in each direction are equal, there is a net absorption of energy $E = g\beta H = h\nu$. The interaction which causes the transition is between the magnetic dipole of the electron and the oscillating magnetic field intrinsic to the electromagnetic radiation.

In practice the situation is often less simple; the g-value may be anisotropic, orbital angular momentum

may influence the transitions observed, and a multitude of lines may be seen due to other magnetic nuclei close to the electron, or to the system having more than one unpaired electron.

These factors are discussed in following sections.

4.2.2 The Hamiltonian approach

A common approach to quantum mechanical problems is to express the interactions affecting the electronic energy levels in terms of Hamiltonian operators. When applied to the time-dependent Schrodinger equation this method yields eigenvalues which are the permitted energy levels, and, if the applied oscillating magnetic field is included, the relevant transition probabilities. The mathematics for this general approach is difficult, and perturbation theory is normally used. In this approach firstly the strongest interaction only is considered and applied to the wave equation to obtain the permitted energy levels. The next strongest interaction is then considered as a perturbation of the first, and so on. This procedure is valid only if the successive

interactions differ in magnitude by at least one or two orders of magnitude. With occasional exceptions this is the case in epr studies.

The general Hamiltonian, $\mathcal{H}$, for a species in a crystalline environment is:

$$\mathcal{H} = \mathcal{H}_E + \mathcal{H}_{LS} + \mathcal{H}_{SI} + \mathcal{H}_Q + \mathcal{H}_V + \mathcal{H}_{SH} + \mathcal{H}_{IH} \qquad 4.2$$

where the symbols have the following significance:

i $\mathcal{H}_E$ is a composite term expressing the total kinetic energy of the electrons, the coulombic attraction between the electrons and nuclei and the repulsion between the electrons

$$\mathcal{H}_E = \sum_i \left(\frac{p_i^2}{2m} - \frac{Ze^2}{r_i}\right) + \sum_{ij} \frac{e^2}{r_{ij}} \qquad 4.3$$

p_i is the momentum of the ith electron and r_i its distance from the nucleus. r_{ij} is the distance between electron i and electron j and Z is the nuclear charge. This equation gives energy levels with separations of the order of $10^5 cm^{-1}$ and normally only the lowest need be considered in epr work.

ii $\mathcal{H}_{LS}$ represents spin orbit coupling and takes the form

$$\mathcal{H}_{LS} = \lambda LS \qquad 4.4$$

if we consider only terms derived from the ground state from equation 4.3 where L and S are the free ion values of the orbital and spin angular momenta of the electrons and λ is the spin-orbit coupling constant with units of energy. The magnitude of this interaction is generally between 10^2 and $10^3 cm^{-1}$.

iii $\mathcal{H}_{SI}$ includes the magnetic interaction between each electron and (magnetic) nucleus and is given by

$$\mathcal{H}_{SI} = \sum_i a_i j_i I_i \qquad 4.5$$

where j_i is the total angular momentum of the ith electron and I_i is the nuclear spin. This interaction gives rise to the nuclear hyperfine levels (and their associated hyperfine lines). a_i is the hyperfine coupling constant (in frequency units).

The hyperfine levels have a separation of the order $10^{-2} cm^{-1}$. (see also section 4.2.5)

iv $\mathcal{H}_Q$ is the nuclear quadrupole term. These interactions are smaller than those above (about

$10^{-4}cm^{-1}$) and are commonly neglected. For nuclei with spin I greater than $\frac{1}{2}$ they shift the hyperfine levels to a small extent.

v The effect of the crystal field is described by

$$\mathcal{H}_V = \sum_i e_i V(r_i) \qquad 4.6$$

where $V(r_i)$ is the electrostatic potential at the ion with which each electron interacts. Simple perturbation theory may not be applicable in many cases for this term, since the magnitude of the crystal field varies widely between different crystals etc.

In an external magnetic field (H_o) the last two terms must be added.

vi $\mathcal{H}_{SH}$ gives the interaction of the angular momentum of the electrons with the field whilst $\mathcal{H}_{IH}$ gives the interaction of the nuclei with the field, having a magnitude of about $10^{-4}cm^{-1}$ and may be neglected except when considering second-order effects in the nuclear hyperfine interaction.

4.2.3 The spin Hamiltonian

The effect of an external magnetic field on the energy levels of paramagnetic species, after taking into account the crystal field and spin orbit coupling, can be expressed in terms of a g-factor with the same symmetry as the combined crystal field and Jahn-Teller distortion. Thus, the terms in the general Hamiltonian $\mathcal{H}_E$, $\mathcal{H}_{LS}$, $\mathcal{H}_V$ and $\mathcal{H}_{SH}$ can be replaced by a single term

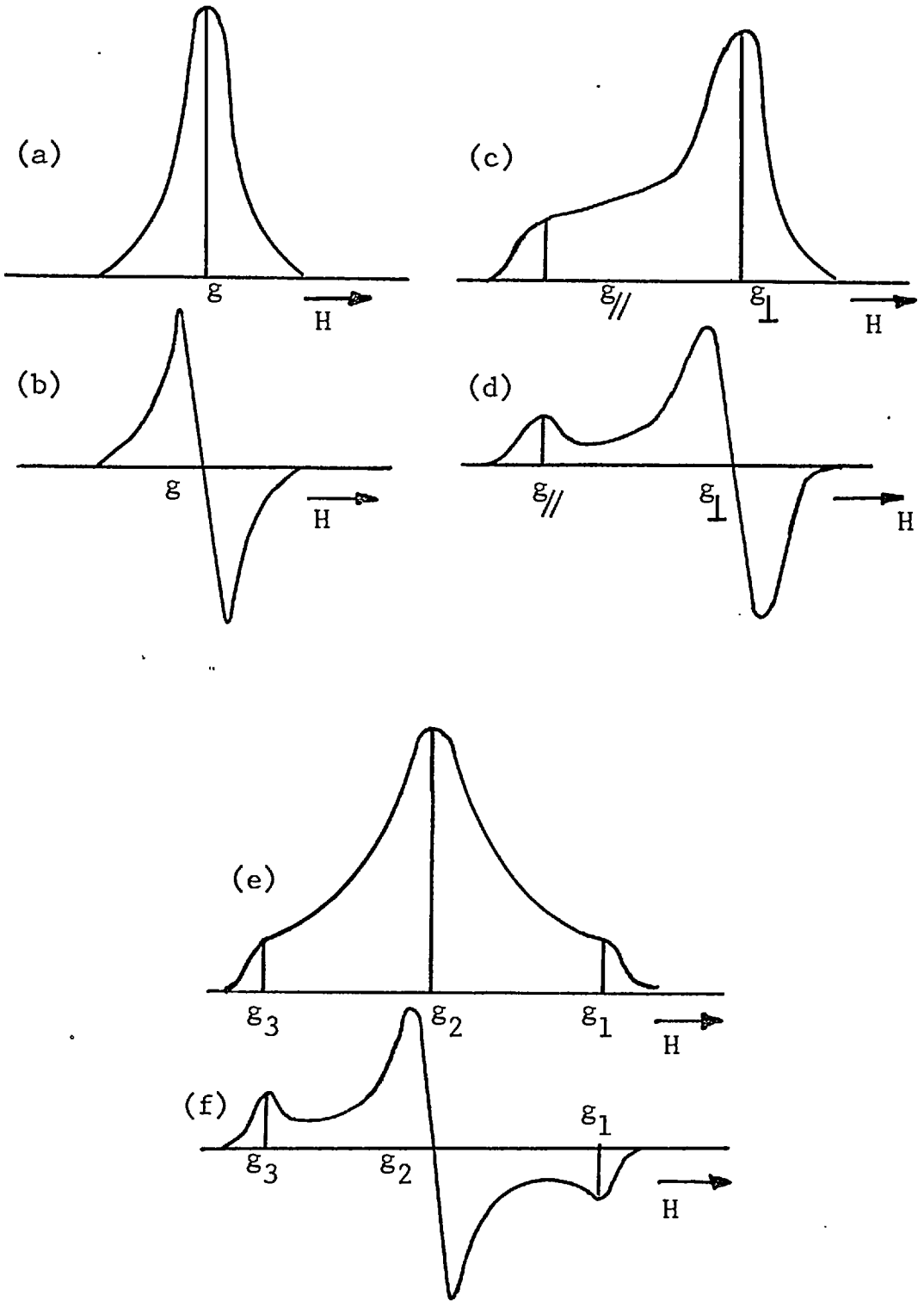
$$-\beta H_o \cdot \bar{g} \cdot S = -\beta \sum_i \sum_j H_i \cdot g_{ij} \cdot S_j \qquad 4.7$$

$\bar{g}$ is a 3 x 3 symmetrical tensor of the second order, and S is the effective spin. i and j each take the values x, y and z. Fortunately, the off-diagonal elements of the tensor are generally very small, and may be neglected except for the most refined analyses, thus $g_{xx} = g_x$, $g_{yy} = g_y$ and $g_{zz} = g_z$ giving for a non-symmetric system.

$$\beta H_o \cdot \bar{g} \cdot S = \beta (g_x H_x \hat{S}_x + g_y H_y \hat{S}_y + g_z H_z \hat{S}_z) \qquad 4.8$$

where $\hat{S}_x$, $\hat{S}_y$ and $\hat{S}_z$ are components of the effective spin along the x, y and z axes. For a system with axial symmetry

$$\beta H_o \cdot \bar{g} \cdot S = \beta g_{/\!/} H_z \hat{S}_z + \beta g_{\perp} (H_x \hat{S}_x + H_y \hat{S}_y) \qquad 4.9$$



	absorption spectra	1st derivatives
cubic symmetry	a	b
axial symmetry	c	d
rhombohedral symmetry (and less)	e	f

Figure 4.2

Epr lineshapes

where $g_{//}$ and $g_{\perp}$ are the components of the g-tensor respectively parallel and perpendicular to the field applied along the z axis. The resultant spectra and their first derivatives are shown in figure 4.2 for cubic, axial and rhombohedral (and below) symmetric cases; the positions for measurement of the g-factors are indicated. The precise shapes of spectra measured experimentally are governed by several other factors and these are discussed further in section 4.2.6.

The remaining terms of the general Hamiltonian are then $\mathcal{H}_Q$ and $\mathcal{H}_{IH}$ which are negligible in the present context, and $\mathcal{H}_{SI}$, which further splits the levels obtained from the spin Hamiltonian into nuclear hyperfine levels, is dealt with in section 4.2.5.

4.2.4 Fine structure: zero field splittings

There are many paramagnetic species with more than one unpaired electron and thus have in their ground state total spin S greater than $\frac{1}{2}$. Application of a magnetic field will split the ground state into 2S + 1 magnetic levels. Transitions will occur

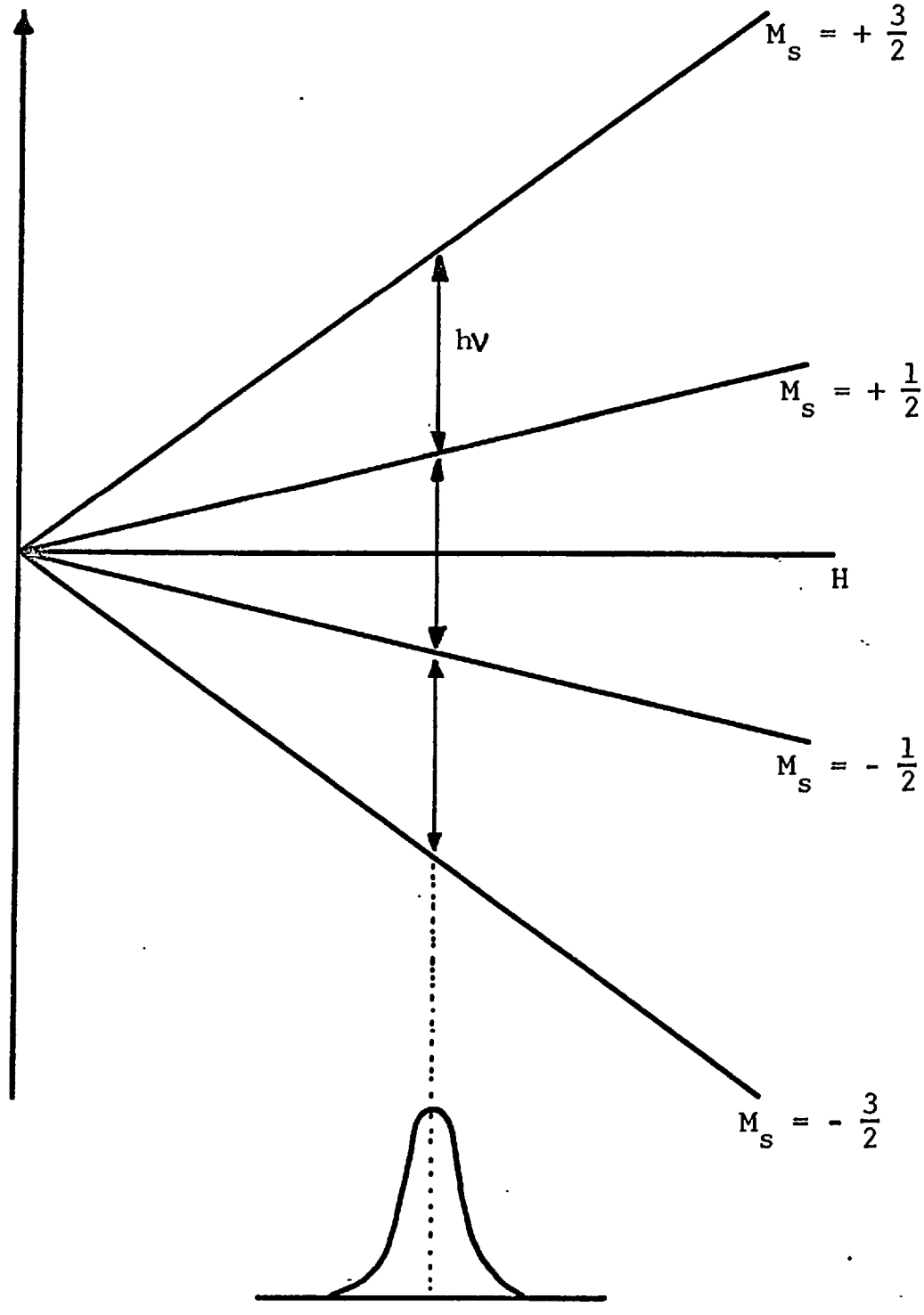


Figure 4.3

Energy levels for a system with spin $S = \frac{3}{2}$ and no zero-field splitting, and its epr absorption signal

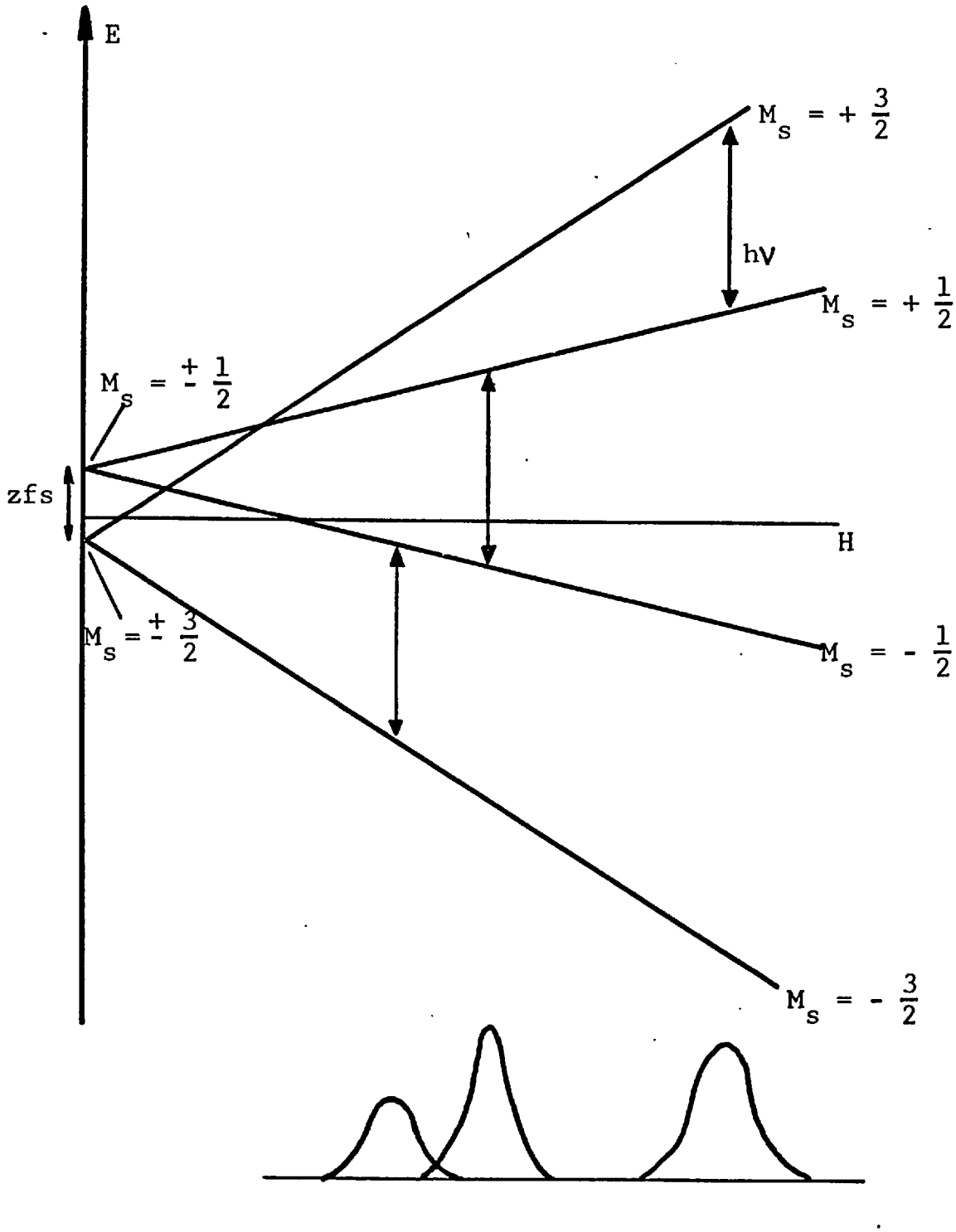


Figure 4.4

Energy levels for a system with spin $S = \frac{3}{2}$ with zero field splitting less than hν . There are 3 epr peaks, unequal in spacing and intensity

between these levels according to the selection rule ΔM_s (the spin quantum number) = ± 1. This simple model is shown in figure 4.3 for a system with spin $S = \frac{3}{2}$; all the transitions occur at the same frequency and a single line would be observed.

In general, however, paramagnetic species are studied in crystals where they are subjected to electrostatic fields. The crystal field alone can remove the degeneracy of the ground state within the limitations of Kramer's theorem giving rise to zero-field splitting (D). The situation for this system is shown in figure 4.4, again for a species with $S = \frac{3}{2}$. Here, transitions for which $\Delta M_s = \pm 1$ can be at different fields with constant frequency or conversely at varying frequency with constant field. These multiple transitions lead to fine structure in the absorption lines which need not be equally spaced or of equal intensity. Their relative positions will be dependent on the orientation of the crystal in the magnetic field since the crystal field has a symmetry which depends upon the symmetry of the crystal.

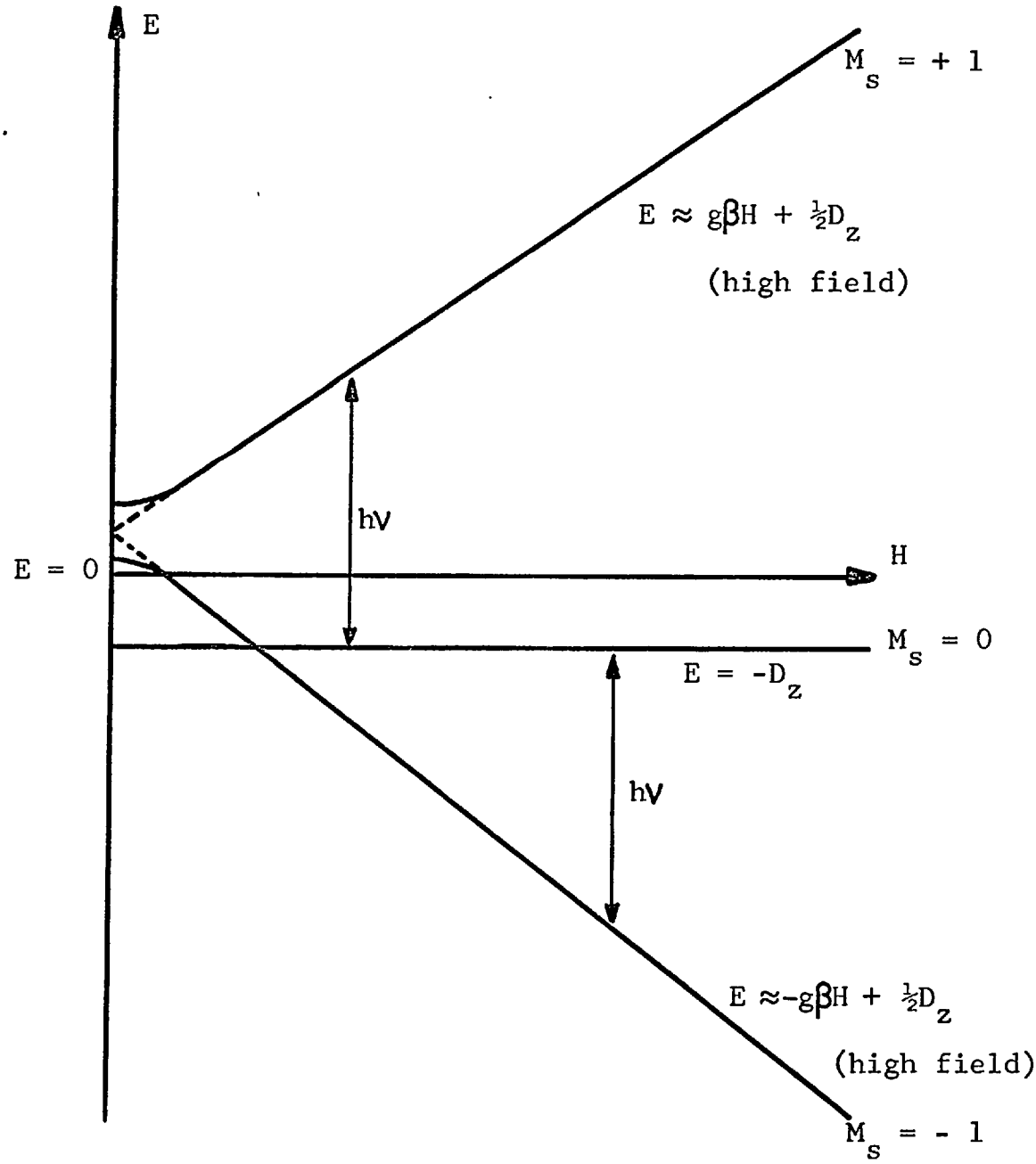


Figure 4.5

Energy levels for the FeO_4^{2-} ion in K_2CrO_4, with H parallel to the z axis. Note high field approximation

Since the magnitude of the zero-field splitting varies considerably, it is important to consider its magnitude in relation to the energy of the microwave radiation (in this study about $0.3cm^{-1}$, in the X-band).

A zero-field splitting less than the microwave energy will not in itself prevent observation of epr transition; the FeO_4^{2-} ion in a K_2CrO_4 lattice is a system of this type, having $D = 0.05cm^{-1}$. Figure 4.5 shows the situation for the ferrate (VI) ion with the applied field parallel to the z axis. Several cases also exist, however, for which the zero-field splitting is greater than the energy of the microwaves, so no epr absorption is observed. A system of this type is the V^{3+} ion with a $3d^2$ configuration, in which the zero-field splitting is $8cm^{-1}$.

So far we have been discussing single crystals, where the position and intensity of the signal is dependent on the direction of observation, because of anisotropy of the crystal field. In the case of fine powders, however, with which most of this study

is concerned, the observed spectrum consists of the lineshapes obtained from all the crystallite orientations contained in the powder, superimposed.

4.2.5 Nuclear hyperfine splitting

If either the nucleus of a paramagnetic species or the nuclei surrounding it possess a resultant angular momentum and therefore a magnetic moment, an interaction with the electronic magnetic moment can occur to produce additional energy levels which give rise to transitions observable as hyperfine structure. The nuclear spin is quantized and, in a magnetic field, for a nucleus of spin I, there will be $2I + 1$ values of M_I, the component of $\bar{I}$ (the nuclear magnetic moment) in the direction of the field, with values I, I - 1, ..., - I, analgous to the situation of a free electron in a magnetic field.

Under the usual epr conditions, ie for strong magnetic fields, over a few hundred gauss, the interaction of a nucleus with the field is considerably smaller than that of an electron and the nuclear spin is unaffected by the oscillating

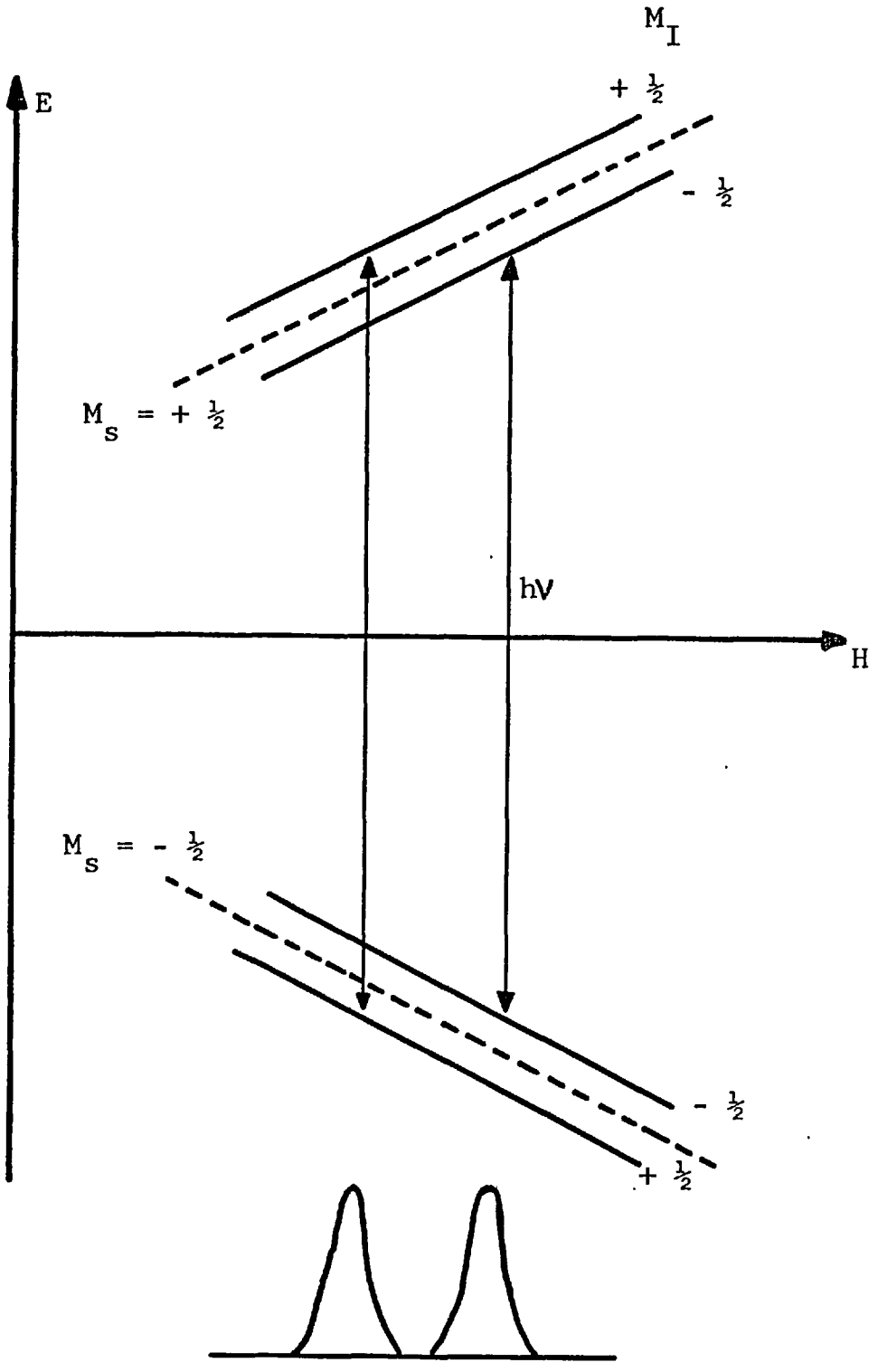


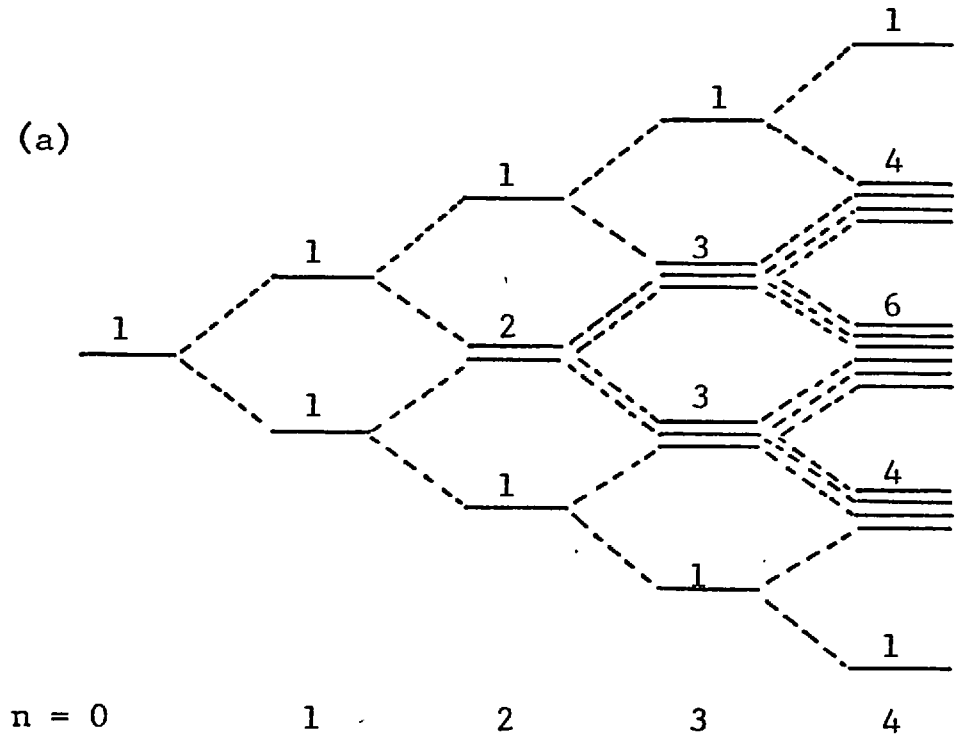
Figure 4.6

Energy levels for a system with electron spin $S = \frac{1}{2}$ and nuclear spin $I = \frac{1}{2}$, as a function of magnetic field.

The epr absorption peaks are of equal intensity

field of the microwaves; thus the nuclear and electronic angular moments are independently quantized and the selection rule for electron resonance transitions involving nuclear hyperfine interaction is $M_s = \pm 1$, $M_I = 0$. The energy levels of a system with $S = \frac{1}{2}$ and $I = \frac{1}{2}$ are shown in figure 4.6, as a function of magnetic field. Since the population difference between the nuclear levels is extremely small, eg less than 3ppm at 300°K, all nuclear spin orientations are very nearly equally probable, and the resonance lines are of equal intensity.

When more than one nucleus interacts with an electronic spin, each electronic level is initially split into $2I_i + 1$ levels by nucleus i; each of these levels is further split into $2I_j + 1$ levels by nucleus j, and so on. The total number of energy levels for a given value of M_s is $(2I_i + 1)(2I_j + 1)(2I_k + 1)$ etc. Since transitions occur without change in nuclear spin quantum number, this is also the maximum number of observable epr lines; however, some of the interacting nuclei will be magnetically equivalent, ie their hyperfine coupling constants



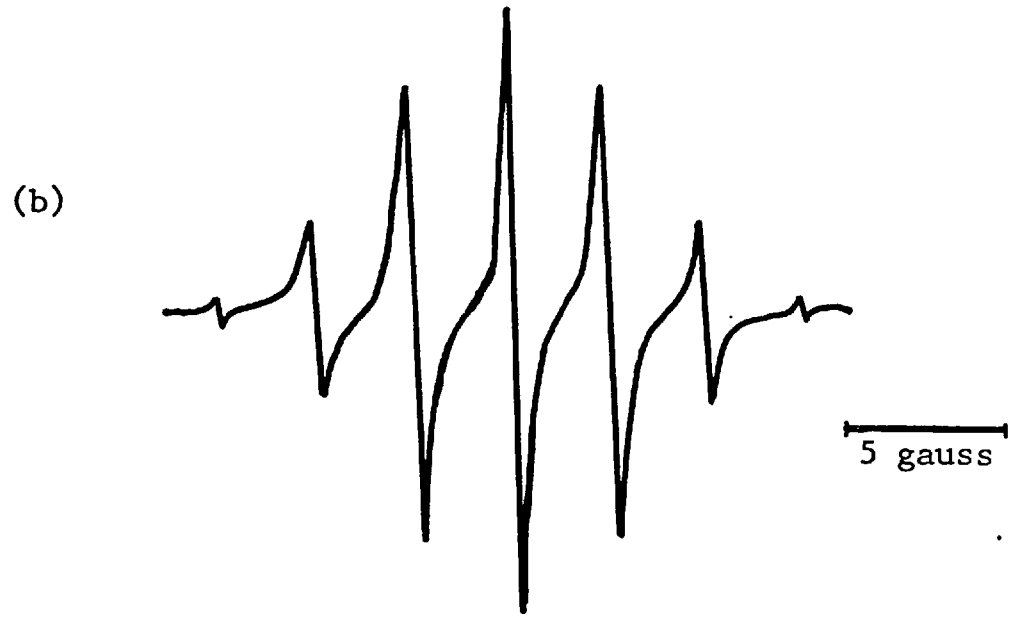


Figure 4.7

(a) Nuclear magnetic energy levels for radicals with 1, 2, 3 and 4 equivalent protons, showing the degeneracy of each level

(b) Epr spectrum of the benzene mono-anion $C_6H_6^-$

are identical. Examples of this would be a number of organic radicals containing magnetically equivalent protons ($I = \frac{1}{2}$). Each interacting proton causes a doubling of the number of hyperfine energy levels, so for n protons, the maximum number of levels is 2^n, but if all are equivalent, there are n + 1 levels (figure 4.7a). The degeneracies of the hyperfine levels represent the relative intensities of the transitions originating from each. Figure 4.7b shows the epr spectrum obtained by interaction of an electron with the six magnetically equivalent protons in the benzene negative ion $C_6H_6^-$; there are seven lines with relative intensities 1:6:15:20:15:6:1.

In general, for an unpaired electron interacting with n magnetically equivalent nuclei of nuclear spin I, there will be (2nI + 1) epr lines.

The electron-nucleus interaction occurs by two different mechanisms. The first mechanism is a classical interaction of two dipoles (μ_s and μ_I separated by a distance r). The combined spin and orbital angular momenta of the electron set up a

field at the nucleus which depends on their separation and the shape of the orbitals. The magnitude of the interaction depends on the angle between the radius vector (the line joining electron and nucleus) and the external field; it is therefore directional and is called the dipolar or anisotropic hyperfine interaction.

The second form of interaction is known as the Fermi or contact interaction and is non-classical, depending on the presence of a finite unpaired spin density at the position of the nucleus. Thus, only σ or s orbital electrons can show it since p, d and f etc orbitals have nodal planes through the nucleus. It can be used for finding the amount of s-character of a particular electronic state. This interaction is isotropic and does not depend on the applied field direction. Thus, the isotropic hyperfine interaction in the lattice of single crystals is retained in fluids, polycrystalline powders and glasses whereas the anisotropic components which also contribute fully in the lattice may be averaged to zero by the paramagnetic species reorientating sufficiently quickly in a fluid or by the

multiplicity of fixed orientations they can assume in the powder or glass. Hence, for disordered states, only isotropic interactions are important.

The nuclear hyperfine Hamiltonian term can now be combined in the spin Hamiltonian as

$$\mathcal{H}_{SI} = \sum_{i}^{n} hS.\mathbb{T}_i.I_j \qquad 4.10$$

where $\mathbb{T}_i$ is a tensor representing the coupling between the electron and nuclear spin angular momentum vectors of n nuclei of spin I_j. If only isotropic interactions are considered then this term becomes

$$haS.I \qquad 4.11$$

where a is the isotropic hyperfine coupling constant and replaces $\mathbb{T}_i$ of equation 4.10. a is a scalar quantity related to the unpaired spin density at the nucleus $\psi^2(0)$ by equation 4.12

$$a = -(8\pi/3)g_e g_I \beta\beta_I |\psi^2(0)| \qquad 4.12$$

g_I and β_I are the nuclear g-factor and magneton respectively.

Ignoring any nuclear quadrupole interactions ($\mathcal{H}_Q$) and contributions from direct interactions of the nucleus with the magnetic field ($\mathcal{H}_{IH}$), to a

reasonable approximation the spin Hamiltonian becomes

$$\mathcal{H} = -g\beta S.Ho + haS.I \qquad 4.13$$

and now represents the complete general Hamiltonian subject to the assumptions discussed above.

It is important to note that the hyperfine splitting is independent of the frequency of observation, which means that nuclear hyperfine interaction can be distinguished from the effects of differences in g-factors.

4.2.6 Line shape and relaxation

The population excess of the ground state ($M_s = -\frac{1}{2}$) over the upper state ($M_s = +\frac{1}{2}$) for a single spin system is very small; at 300°K, for g = 2 in a magnetic field of 3000 gauss, from the Boltzmann distribution function

$$n_{+\frac{1}{2}}/n_{-\frac{1}{2}} = \exp\left(-\frac{\Delta E}{kT}\right) = \exp\left(-\frac{h\nu}{kT}\right)$$

$$= \exp\left(-\frac{g\beta H}{kT}\right) = 1 - \frac{g\beta H}{kT} \text{ (since } g\beta H \ll kT) \qquad 4.14$$

'4.14' = 0.9986. The excess population is thus about 0.07%, and the epr phenomenon depends on this small

difference. Since the transition probability in either direction is equal, the two levels would quickly become equally populated and absorption of energy would cease. There are relaxation processes, however, which allow the electrons in the upper state to dissipate energy and return to the lower state; specifically we are concerned with spin-lattice relaxation. This is an interaction between the unpaired electron and its environment, which is called the lattice whether it is crystalline, 'amorphous' or fluid; the energy is dissipated by vibrations and rotations of the atomic environment.

The existence of the relaxation process has two other consequences. Firstly if it is too slow, saturation of the spin system can occur, ie the population difference between the spin states diminishes and the rate of absorption of energy, which depends on this factor, also diminishes. Secondly, the lines may be broadened because of the Heisenberg uncertainty principle, since any reduction in the lifetime of the upper state, by fast relaxation, acts to broaden the resonance

ie $E.\Delta t \approx h/2\pi$ or $\Delta\nu \approx \frac{1}{2\pi}\Delta t$ 4.15

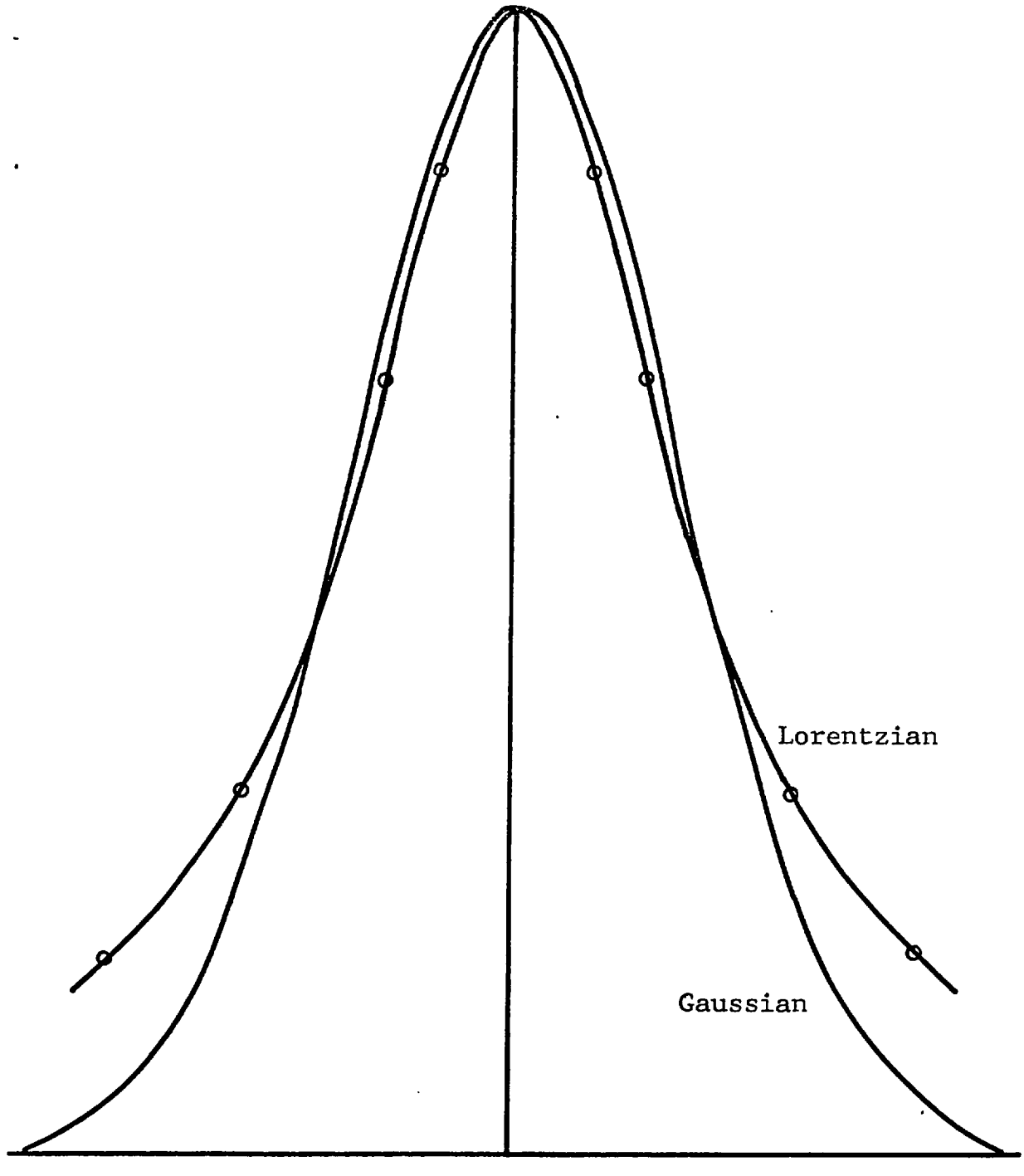


Figure 4.8

Lorentzian and Gaussian lineshape functions normalised to the same amplitude and width at half amplitude

Spin-lattice relaxation or lifetime broadening usually gives a Lorentzian lineshape, which is one of the most commonly considered basic lineshapes, Lorentzian and Gaussian, which are represented respectively by the functions

$$A_L = \frac{A_o}{1 + a^2 (H_o - H)^2} \qquad 4.16$$

and $$A_G = A_o \exp (-b^2 (H_o - H)^2) \qquad 4.17$$

and are superimposed in figure 4.8. The broadening may be homogeneous or inhomogeneous. The former, which includes lifetime broadening can also be produced by spin-spin or dipolar interactions in which each magnetic species produces a magnetic field at each of its neighbours. Transitions, therefore, occur over a range of frequencies corresponding to the variation of the local field. This effect normally gives a Gaussian lineshape. It can be much reduced by increasing the separation of the spins, ie by diluting with a diamagnetic species.

The effect of spin lattice relaxation can be reduced by lowering the temperature of observation, thus the line widths at room temperature of some rare-earth

ions is so great as to make resonance unobservable, but at $20^{o}K$ or $4^{o}K$ they can be observed.

Inhomogeneous broadening can be due to poor uniformity of the magentic field, resonances from different parts of the sample occurring at apparently different fields, but this is not common. Inhomogeneous broadening also results from inhomogeneity in the crystal lattice and from unresolved fine or hyperfine structure.

4.3 Equipment and procedure

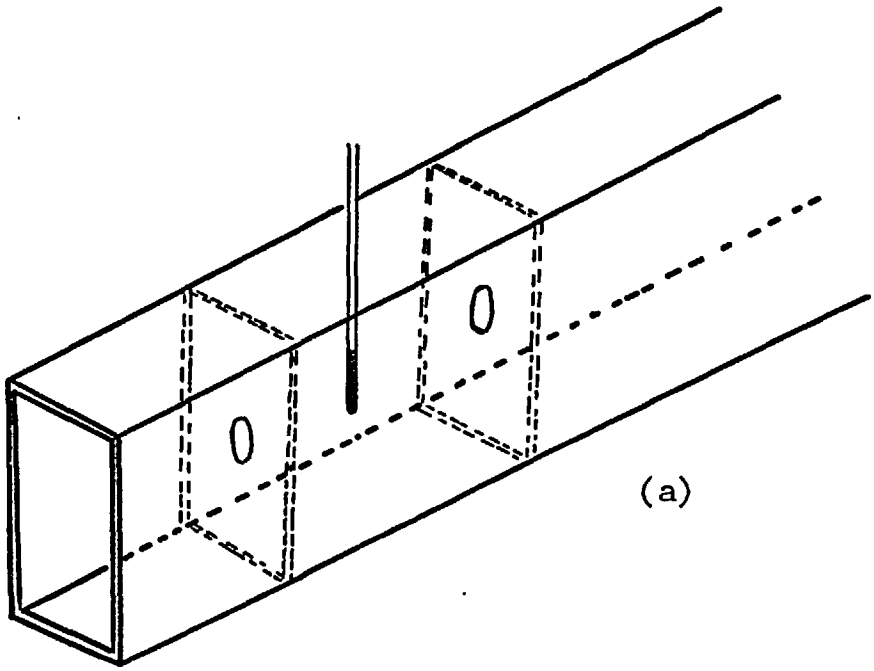
4.3.1 Basic features of epr spectrometers

It is clear from sections 4.1 and 4.2 than an epr spectrometer is essentially

i a source of microwave radiation of constant frequency and variable amplitude,

ii a means of applying this to the paramagnetic sample,

iii a means of measuring the power absorbed from the field, and



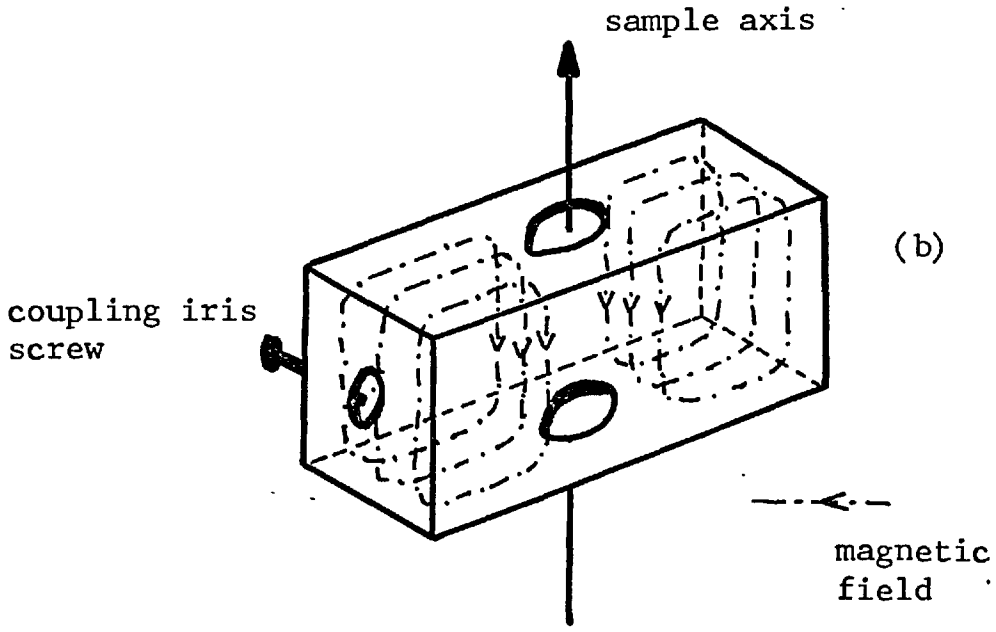


Figure 4.9

Resonant cavities

a Transmission type

b Reflection type

iv a homogeneous but variable magnetic field

For several reasons, mainly historical, most spectrometers use a microwave frequency of 9-10GHz or 3cm wavelength, which is in the X-band where the magnetic field required for samples with g = 2 is about 3300 gauss. The usual source of radiation is a klystron valve with some form of automatic frequency control giving microwaves which are transmitted along a waveguide, usually of rectangular section brass or copper tubing of dimensions appropriate to the radiation wavelength, via attenuators, phase shifters etc, to the resonant cavity which houses the sample. The cavity is in effect a blanked off section of waveguide with ultra flat walls plated in gold or silver to produce a highly conducting, corrosion free surface to the skin depth. Cavities are of two types, transmission types with a small hole in each end wall to transmit power in and out, and the more common reflection type which only requires one hole (figures 4.9). The power entering and leaving the cavity is controlled by a coupling iris, and when properly matched, no energy reflects back from the cavity.

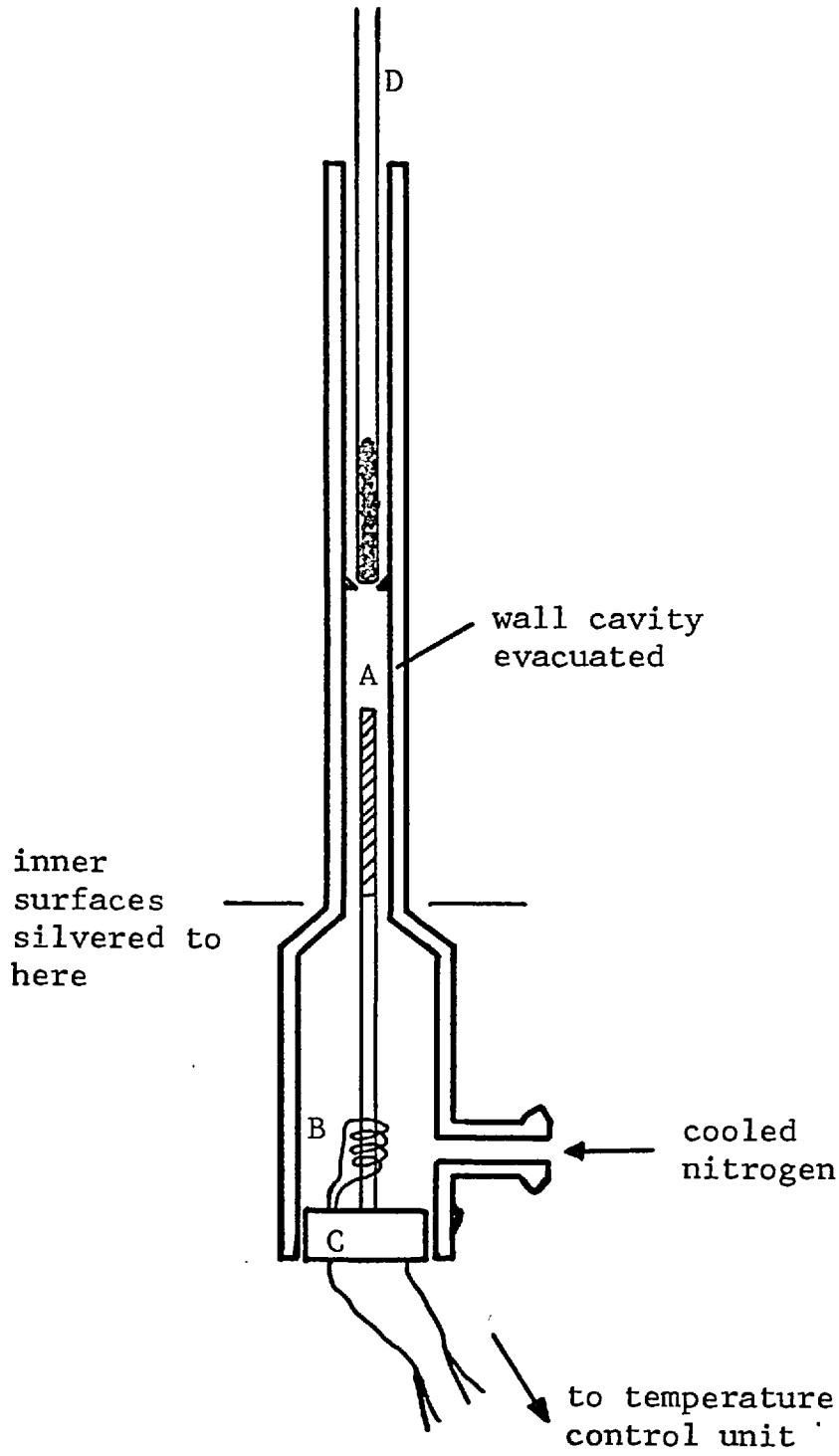


Figure 4.10

Low temperature silica sleeve

A Platinum resistance thermometer

B Heater coil

C Teflon lead through/plug

D Sample in silica tube

Absorption is generally detected by a semiconducting crystal detector which rectifies the microwaves to give direct current.

The most general means of producing the field is by means of an electromagnet since fields from zero to tens of thousands of gauss may be required. A large increase in sensitivity can be obtained by modulating the magnetic field sinusoidally and feeding the resultant output into a phase sensitive detector. The signal obtained in this way is plotted by a pen recorder or on an oscilloscope and is displayed to give the first derivative of the absorption line.

4.3.2 Experimental equipment

The spectrometer used was a Varian E-12 with an electromagnet producing fields up to 15 kgauss and a klystron which could deliver up to 200 mWatts in the X-band. The cavity was of the reflection type, used in the H_{102} mode with accessories including a silica, dewar-sleeve type sample holder through which temperature controlled nitrogen ($-170^{o}C$ - $+200^{o}C$) could be passed (figure 4.10) and a rotating, graduated chuck to take rods on which single crystals

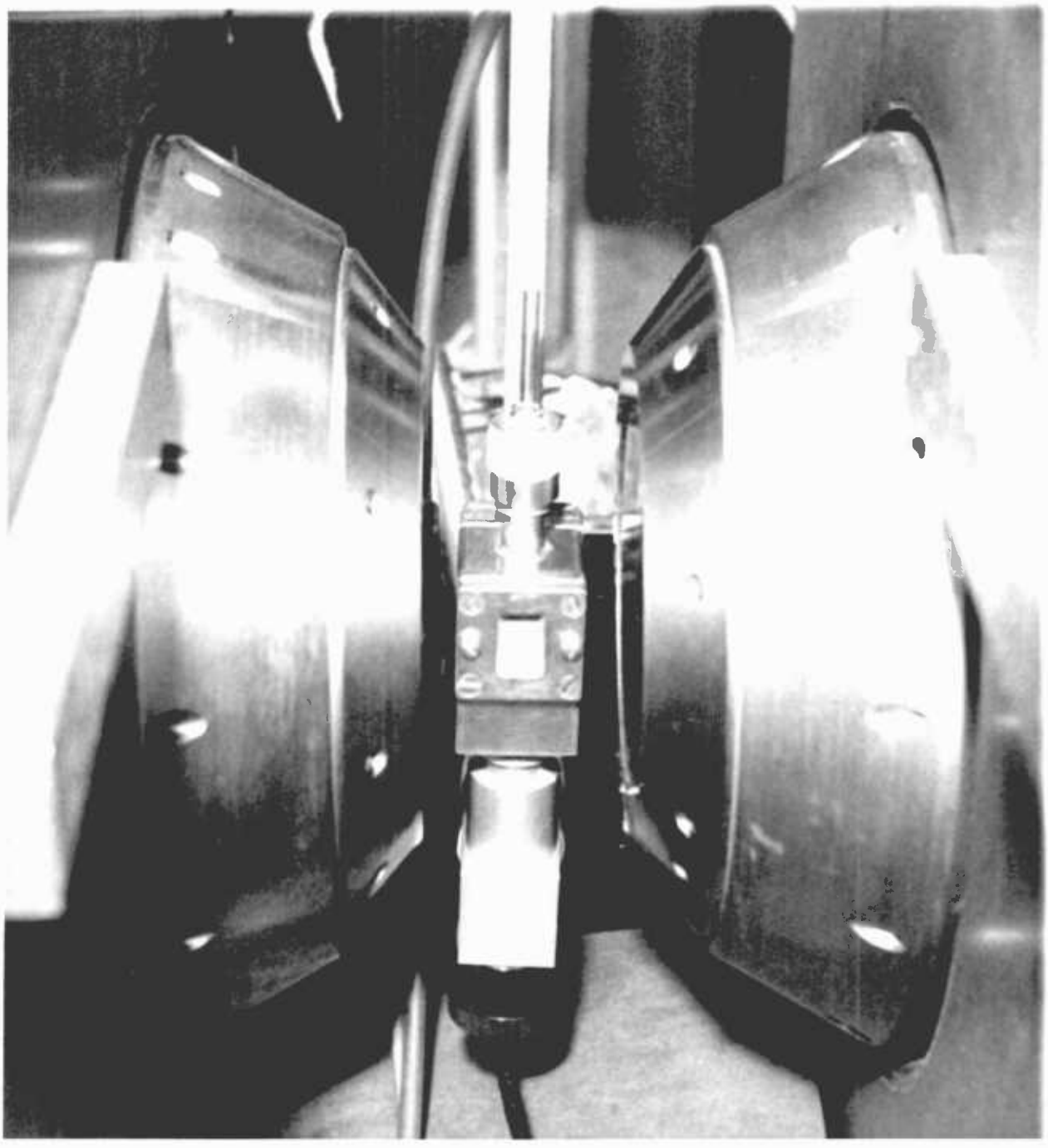


Figure 4.11

Low temperature epr sleeve in cavity,

between magnet poles

could be mounted. The magnetic field modulation coils are embedded in resin in the walls of the cavity. Powder and liquid samples were placed in the cavity in fused silica tubes (ID = 3mm); most glasses are not suitable since they normally contain paramagnetic ions. A photograph of the magnet poles with the resonant cavity and silica sleeve in position is shown in figure 4.11.

The limiting sensitivity of the system is about 10^{12} spins.

4.4 Epr results

4.4.1 Introduction

Epr spectroscopy is used in this study to test various hypotheses as to the nature of the electron donor centre. In this section we are concerned with the more fundamental results in elucidating the nature of this centre. However, other measurements will be mentioned in Chapter 5 as they become relevant to the discussion.

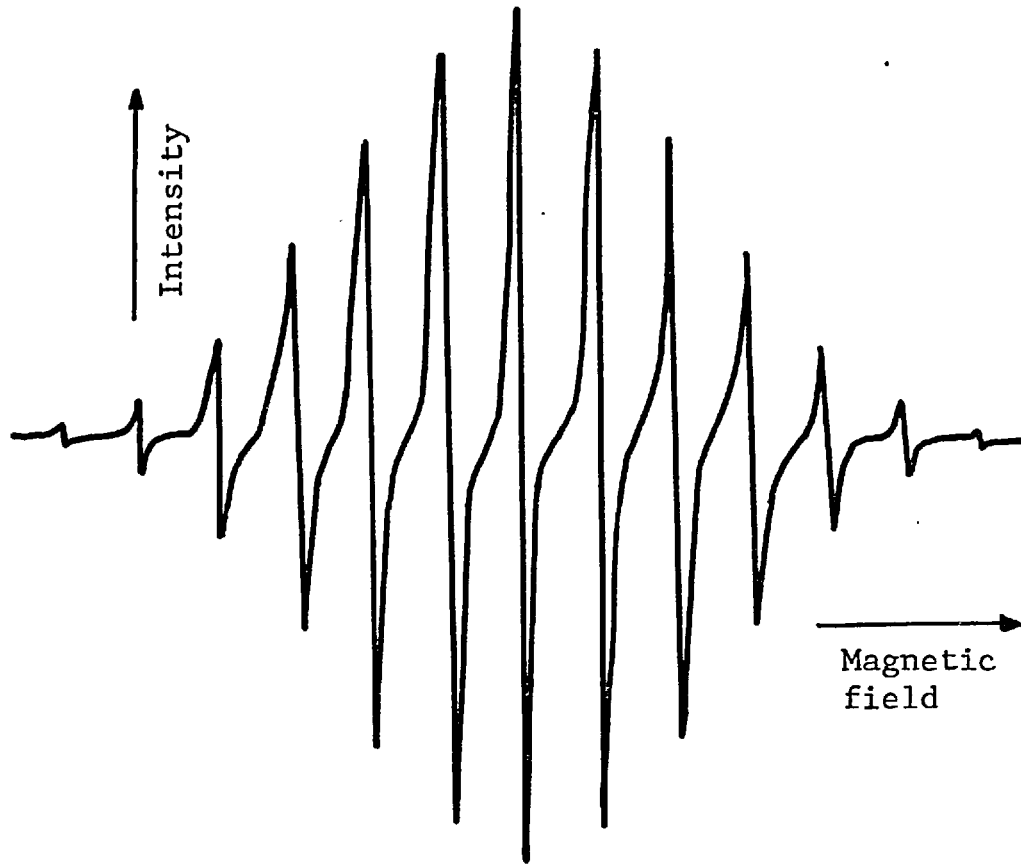


Figure 4.12

13 line F-centre epr signal in coloured sodalite

4.4.2 The coloured state

Sodalite after irradiation with UV or bombardment with electrons is coloured magenta and shows an electron resonance consisting of 13 lines (figure 4.12), first observed by Hodgson et al (1967). The lines of the resonance are the result of hyperfine interaction of a single unpaired electron with four nuclei of spin $\frac{3}{2}$ in a site with cubic symmetry. The theoretical intensity relationships of the lines for this interaction is 1:4:10:20:31:40:44:40:31:20:10:4:1, in good agreement with the observed ratios. Examination of the sodalite structure reveals that the site which satisfies these requirements is the halide vacancy, which is at the centre of a tetrahedron of sodium nuclei (Na^{23}, $I = \frac{3}{2}$, natural abundance = 100%). The photochromic sodalites investigated in this work all showed the characteristic 13-line epr spectrum in their coloured state.

4.4.3 Pre-radiation state

Epr spectra of all the sodalites studied were obtained from the uncoloured material and some

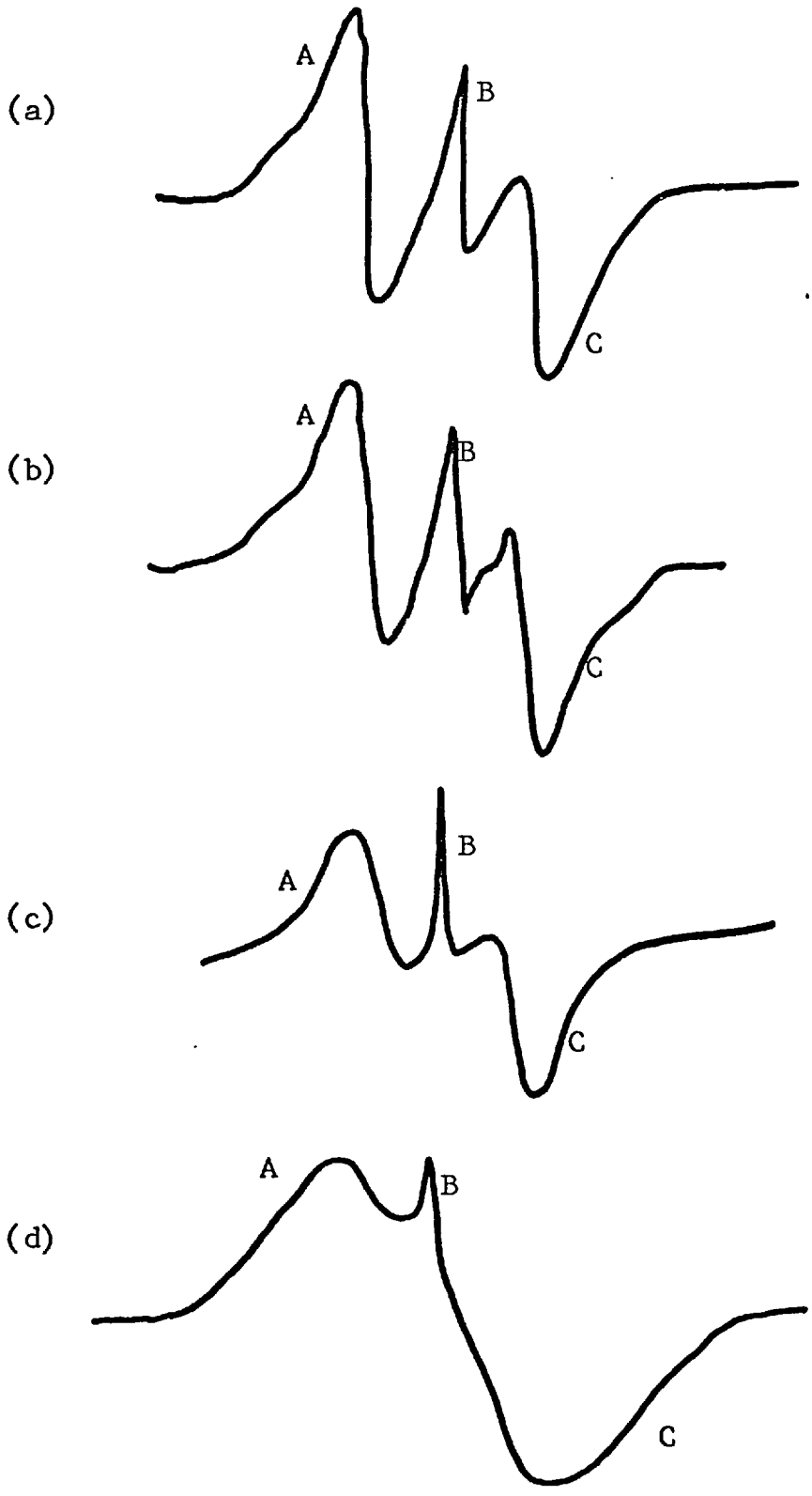


Figure 4.13

Epr spectra of

a as grown undoped hydrothermal sodalite

b activated undoped hydrothermal sodalite

c flux melt sodalites, and

d sodalite grown from kaolinite

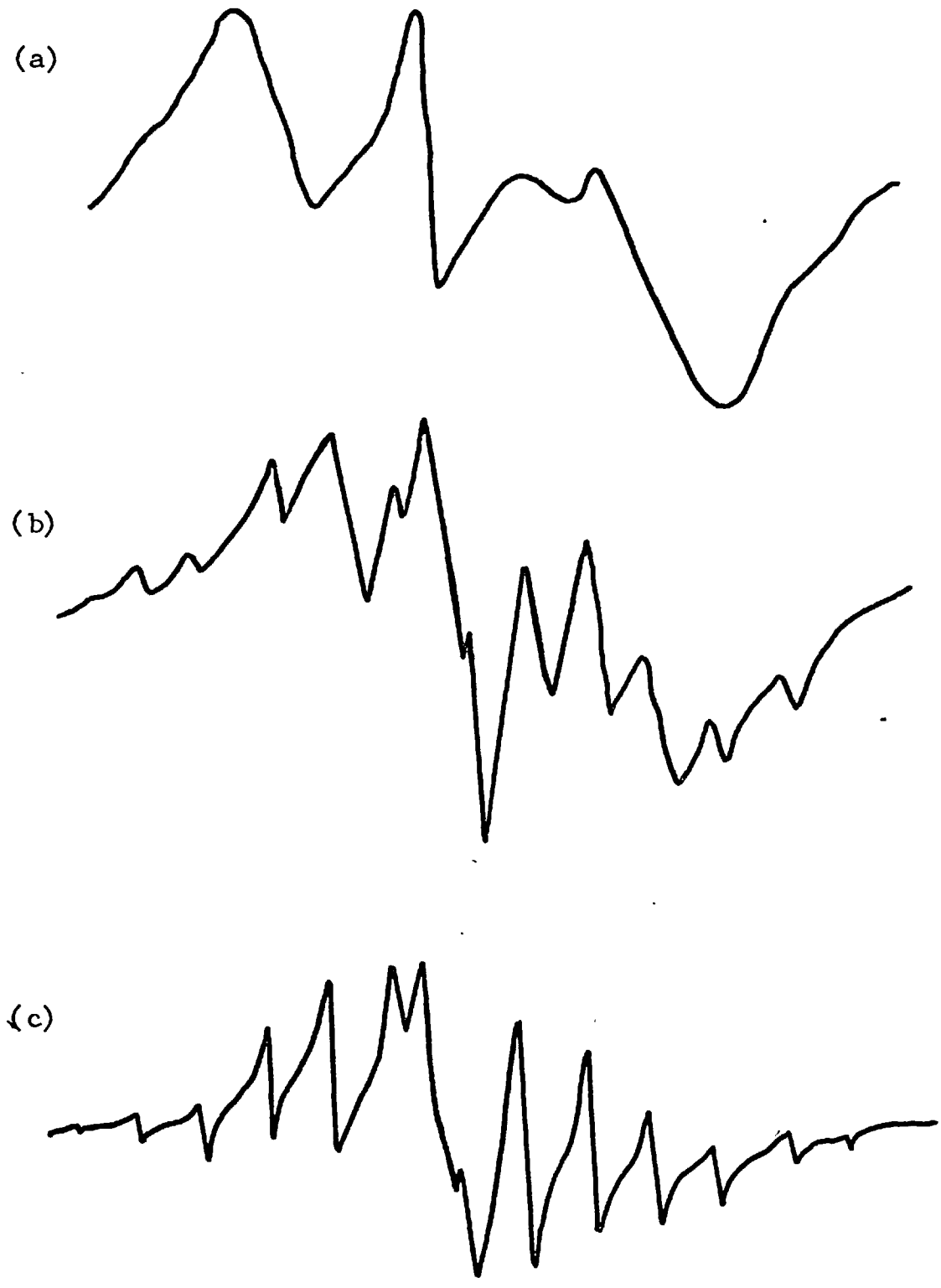


Figure 4.14

Epr spectra of sodalite HT10

a heated in argon at 900°C for 11 hr

b as a + UV irradiated for 2 hr

c as a + UV irradiated for 7 hr

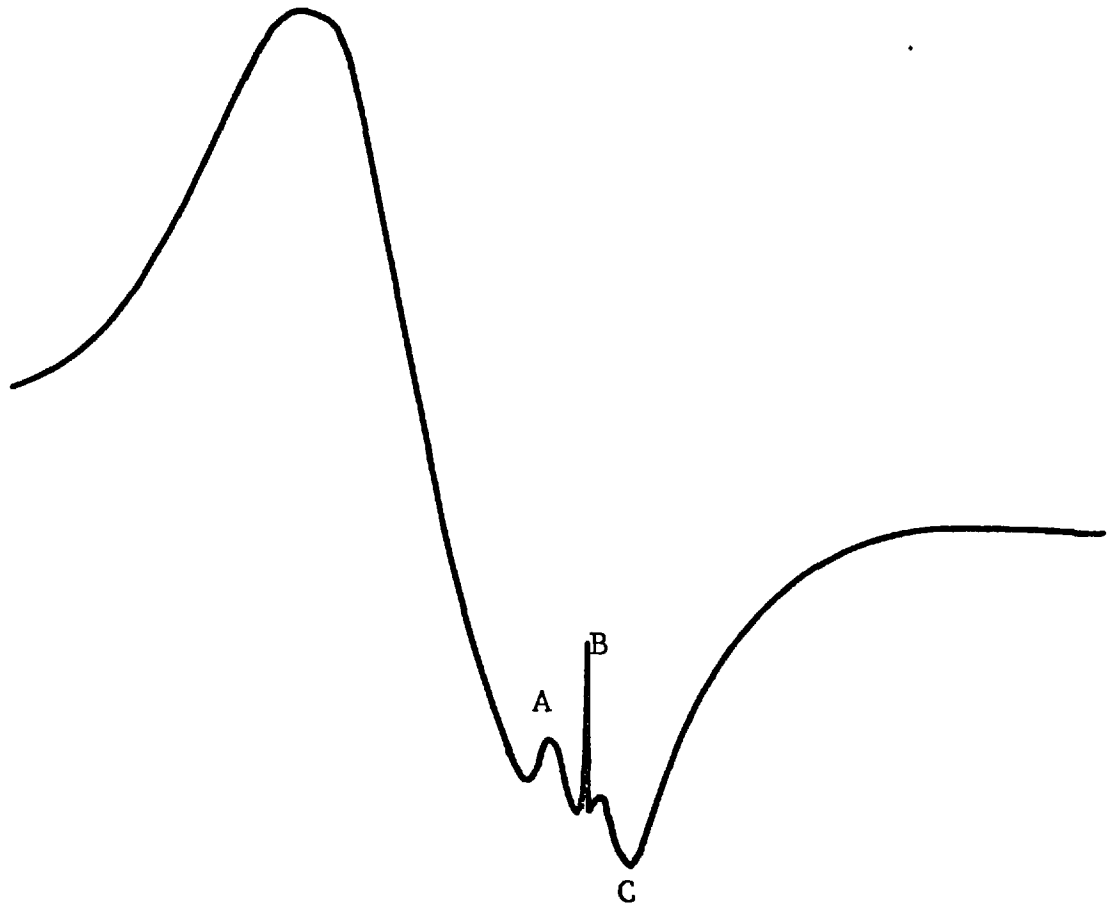


Figure 4.15

Epr spectrum of a typical hydrothermally grown sodalite between 0 and 6500G, showing large ferromagnetic impurity signal with the smaller three line signal superimposed

typical spectra are shown in figure 4.13, for as-grown and activated, undoped materials grown by hydrothermal techniques, sodalites grown by flux melt techniques and those grown from kaolinite. Clearly in each case the salient features are the peaks marked A, B and C with g-factors of about 2.065, 2.017 and 1.930 respectively. Irradiation of these materials with UV results in the lines A and C breaking up and eventually disappearing as the red colouration develops, whilst the F-centre type signal mentioned above begins to dominate the pattern (figure 4.14); at the same time the line B becomes difficult to detect. It can be identified by eliminating the F-centre lines, since these lines arise because of hyperfine interaction and are equally spaced.

4.4.4 Ferromagnetic impurities

For many of the materials studied the epr spectrum showed a broad resonance line centred on about $g = 2.23$ with $w_{\frac{1}{2}}$ (full width at half height) of about 800 gauss (figure 4.15). Lines of this type are characteristic of ferromagnetic materials and the fact that it is not observed in all samples

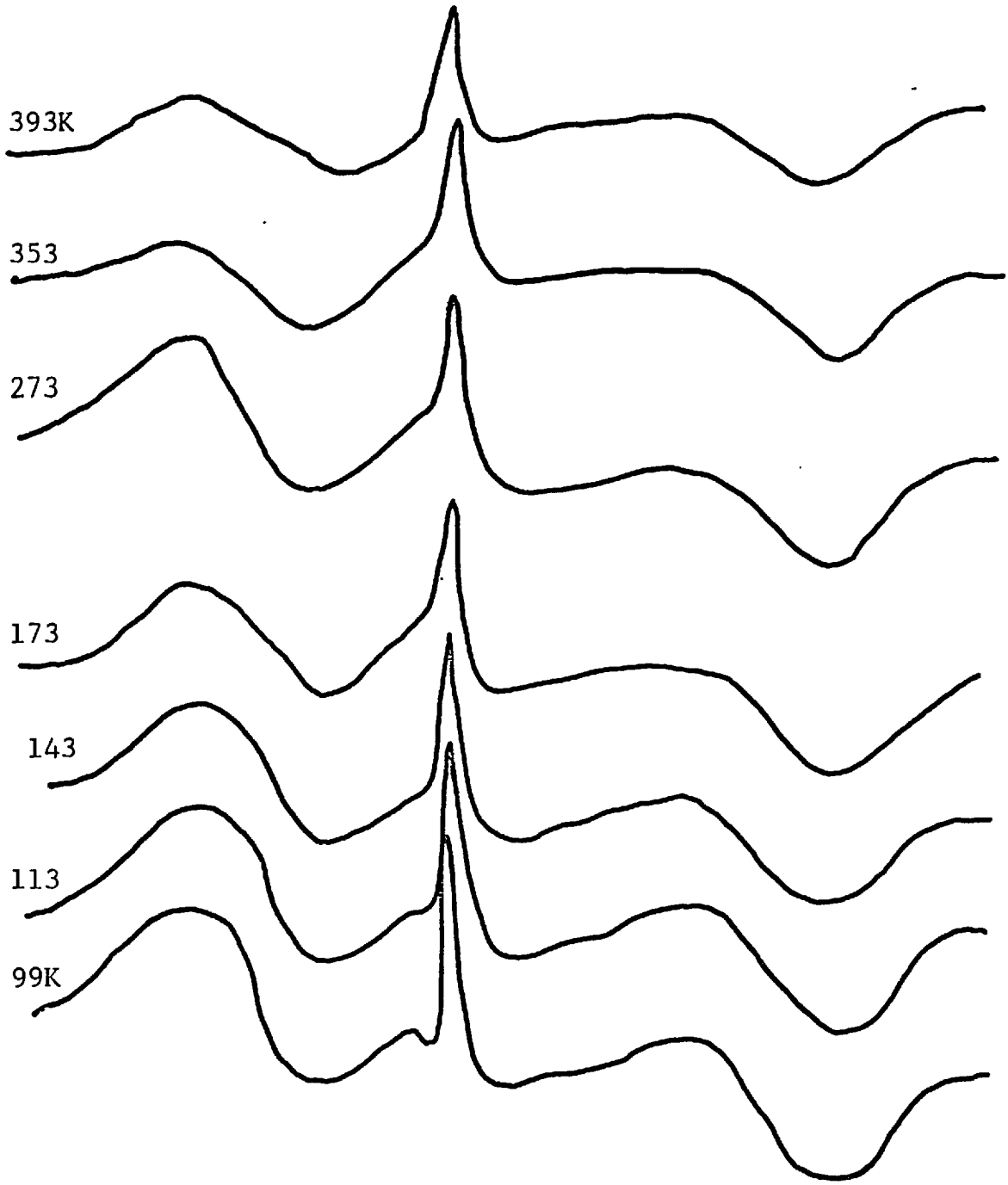


Figure 4.16

Epr spectra at various temperatures of flux melt sodalite LV16

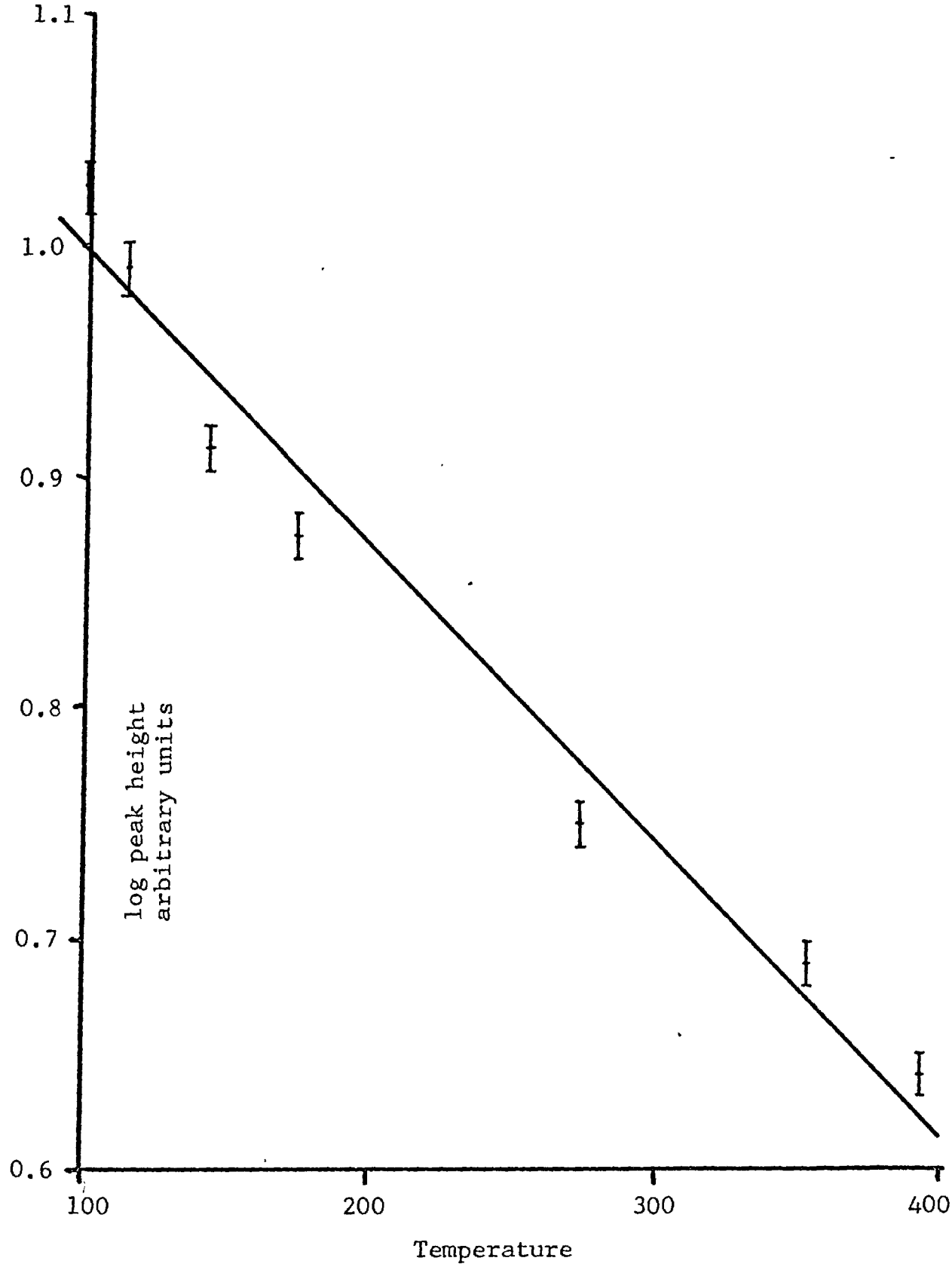


Figure 4.17

Log relative peak heights vs temperature for peak A of the epr spectrum of flux melt sodalite LV16

indicates that the ferromagnetic species is sometimes present as an impurity. The photoactive centre, ie that giving rise to signals A and C, gives rise to a much less intense signal than that arising from the ferromagnetic impurities, being only about 5-10% of the intensity. It appears that the photochromism is unaffected by the presence of the broad band and hence of the ferromagnetic impurity. This band was not studied in detail though some flux melt materials were grown with iron and nickel impurities.

4.4.5 Variable temperature studies

The epr spectra of a flux melt sodalite, taken at temperatures between -174°C and 120°C are shown in figure 4.16, normalised to the same receiver gain. Figure 4.17 shows log of the relative peak heights plotted against temperature. Peak size decreases approximately linearly with increasing temperature, due to increasing spin lattice interactions.

It was observed that the incidence of photochromic activity in sodalites at liquid nitrogen temperature (77°K) was very slow compared with the room



Figure 4.18

Epr spectra of partially perchlorate chlorosodalite

a As grown

b After heating at 900°C in argon for ½ hr

temperature activity, which, taken in conjunction with the variation of intensity of epr signal with temperature, suggests that the formation of the colour centre involves a phonon assisted relaxation from an excited vibration state. This observation will be discussed further with reference to configuration co-ordinate diagrams in Chapter 5.

4.4.6 Perchlorate sodalites

The hydrothermally grown materials HT11 ($Na_6Al_6Si_6O_{24}2NaClO_4$) and HT10 ($Na_6Al_6Si_6O_{24}2NaCl(ClO_4)$) both gave electron resonance signals as grown.

HT10 which as mentioned in Chapter 2 is photochromic when activated in air as well as inert gas, gives the 'normal' epr lines found for undoped sodalites in the as-grown state and after activation in argon or air (figure 4.18). The same pattern persists even after heating the material for eleven hours in argon or air at 900°C, and irradiation with ultra-violet of any of the material which has been heated to 900°C in argon or air for more than a few minutes produces the F-centre 13-line epr signal together with the original sharp peak B (figure 4.18).

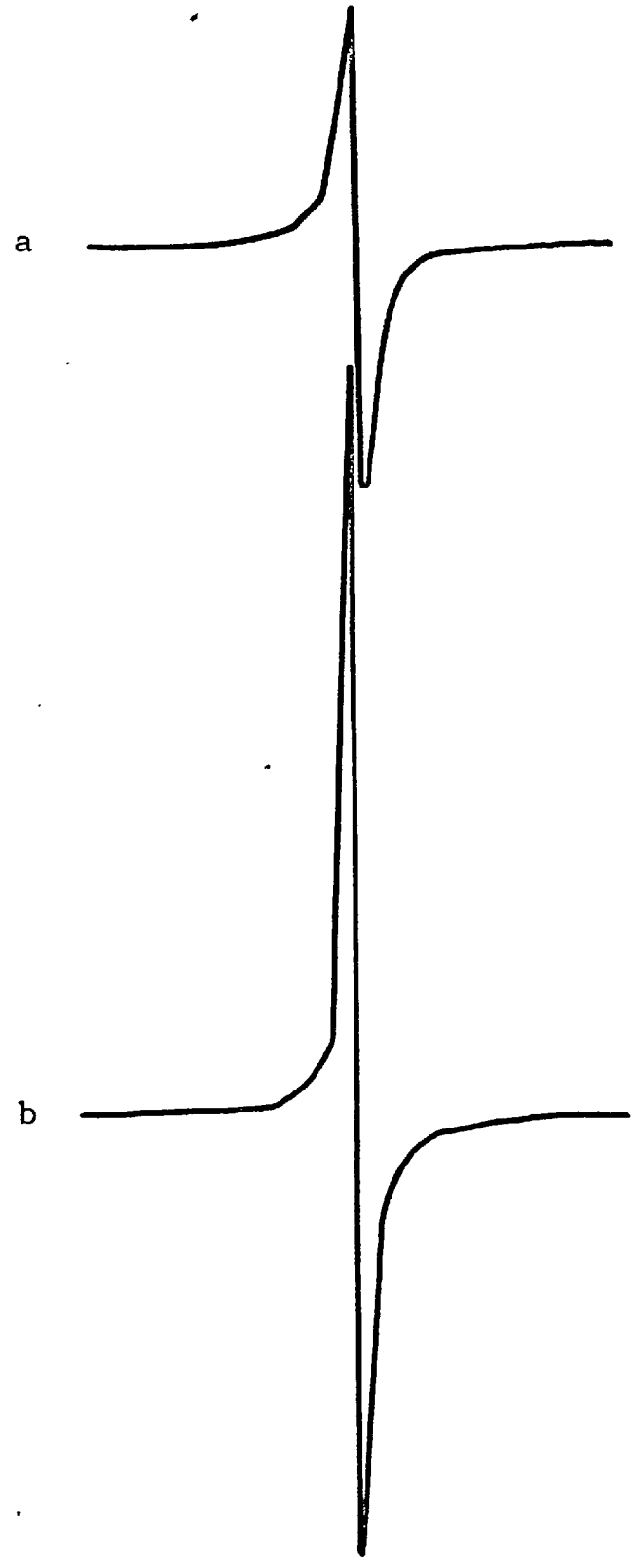


Figure 4.19

Epr spectra of material HT11

a As grown (microwave power 20mW)

b After 16 minutes at 900°C in argon (microwave power 0.2mW)

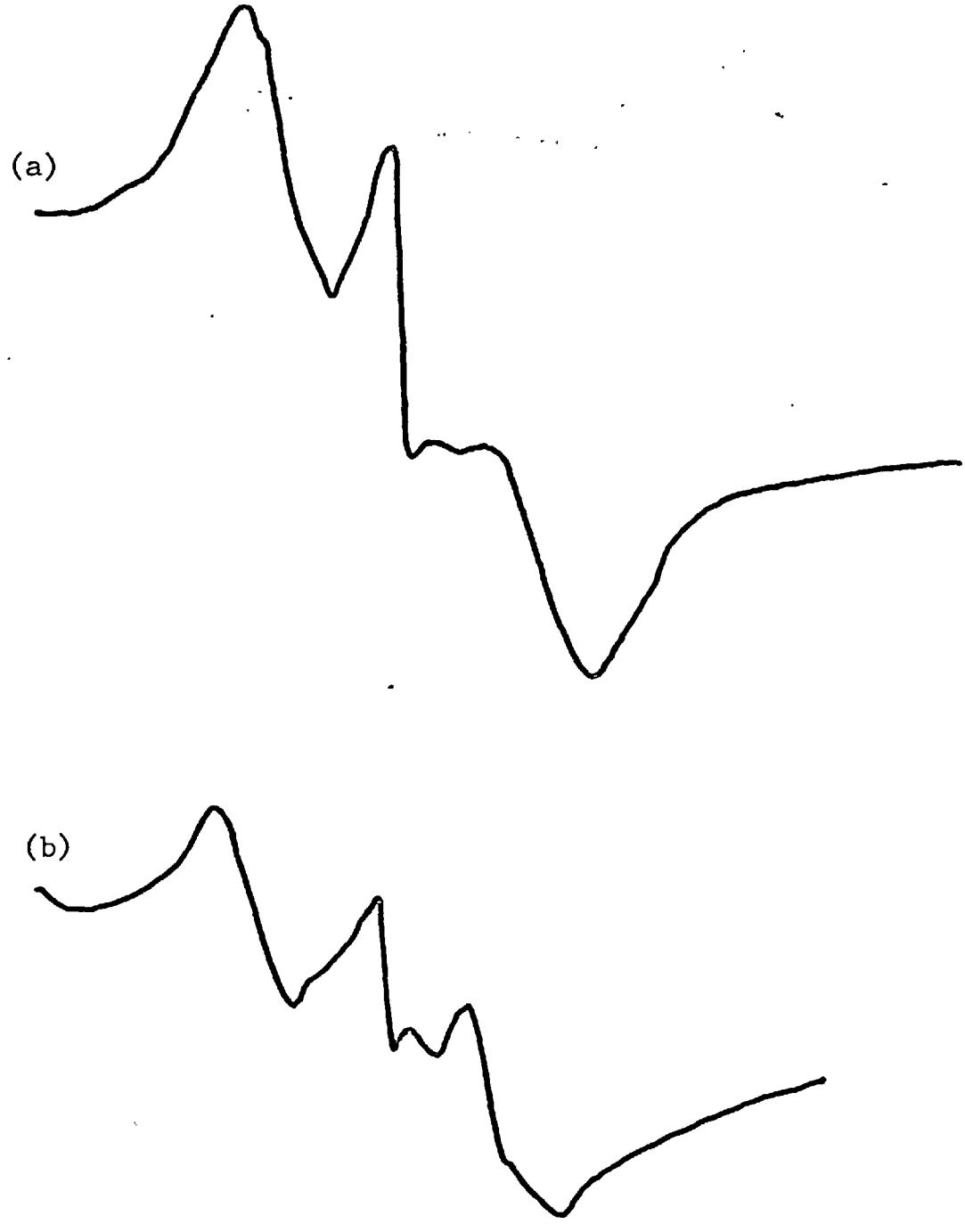


Figure 4.20

Epr spectra of HT11 heated to 900°C in argon

a for 2 hours

b for 4 hours

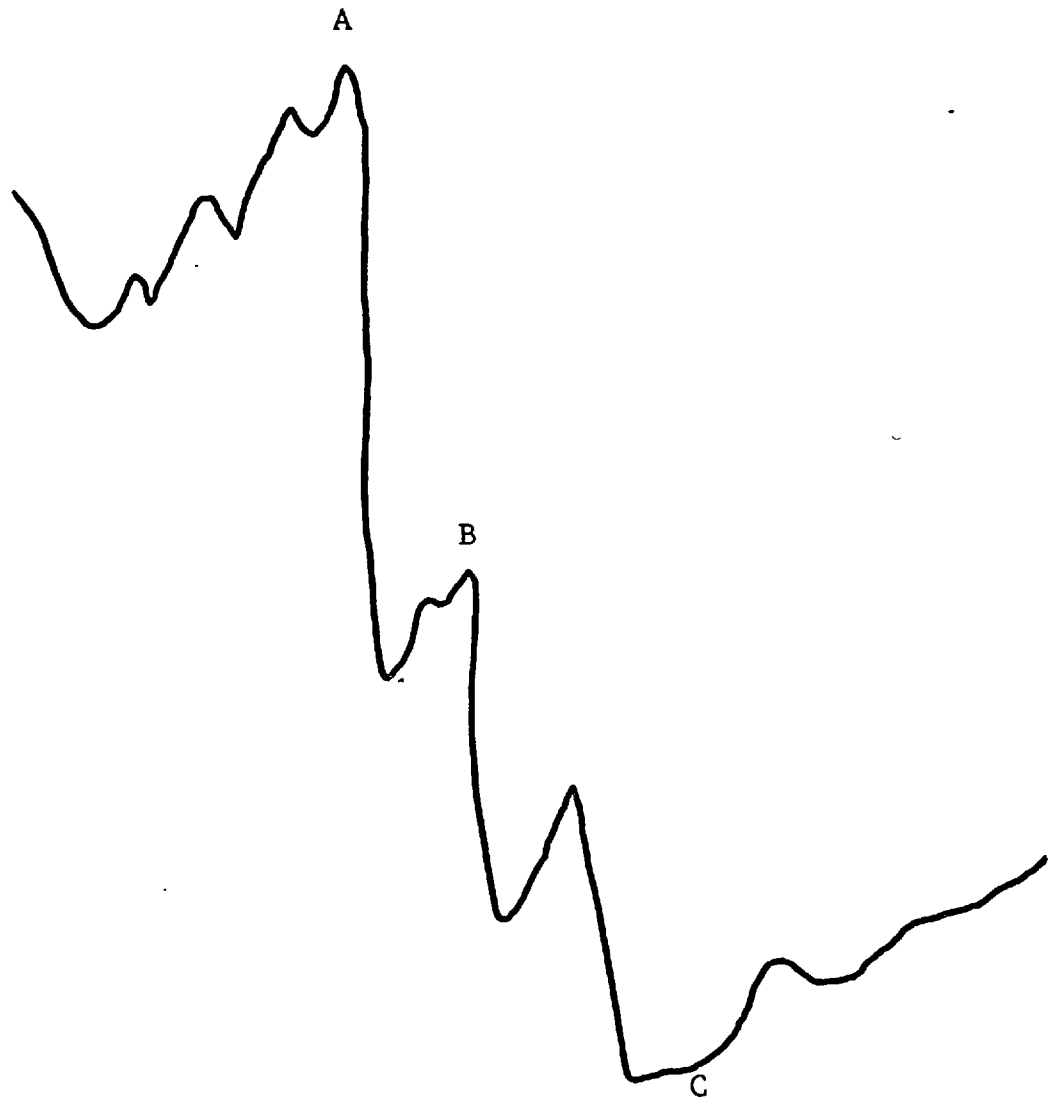


Figure 4.21

Epr spectrum of HT11 heated to 900°C in argon for 8 hours

The ordinate scale is ½ those of figure 4.20; the signal is therefore much weaker

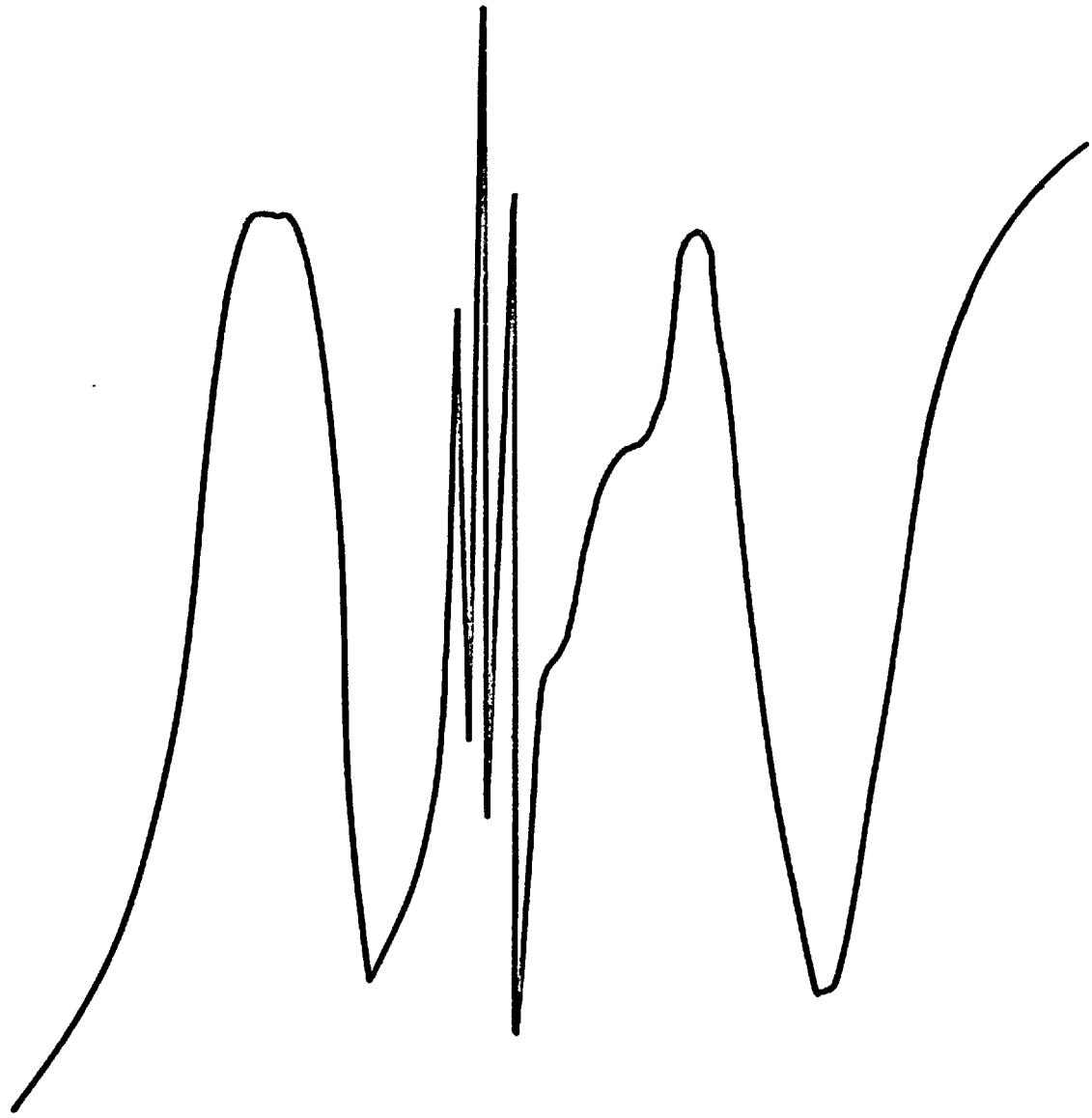


Figure 4.22

Epr spectrum of naturally occurring sodalite from the Kola peninsula, USSR

The HT11 as-grown epr signal on the other hand consists of a single symmetrical line centred on g = 2.017 (figure 4.19). Heat treatment of the material at 900°C for less than about 30 minutes causes the signal strength to increase dramatically and become asymmetric. However, on heating for longer periods in argon, air or oxygen, the more complex three line signal gradually develops (figure 4.20), though the products from long periods of heating have only a relatively weak signal B (figure 4.21).

4.4.7 Other sodalite materials

Several other sodalites were studied by epr techniques; two were grown by Bye (1970) whilst others were naturally occurring photochromic sodalites from Burma, India, Canada and the USSR kindly donated by the Geological Museum.

A typical spectrum from the natural mineral is shown in figure 4.22, given by hackmanite from the Kola peninsula, USSR. Whilst peaks A and C are present, there is a triplet in place of B.

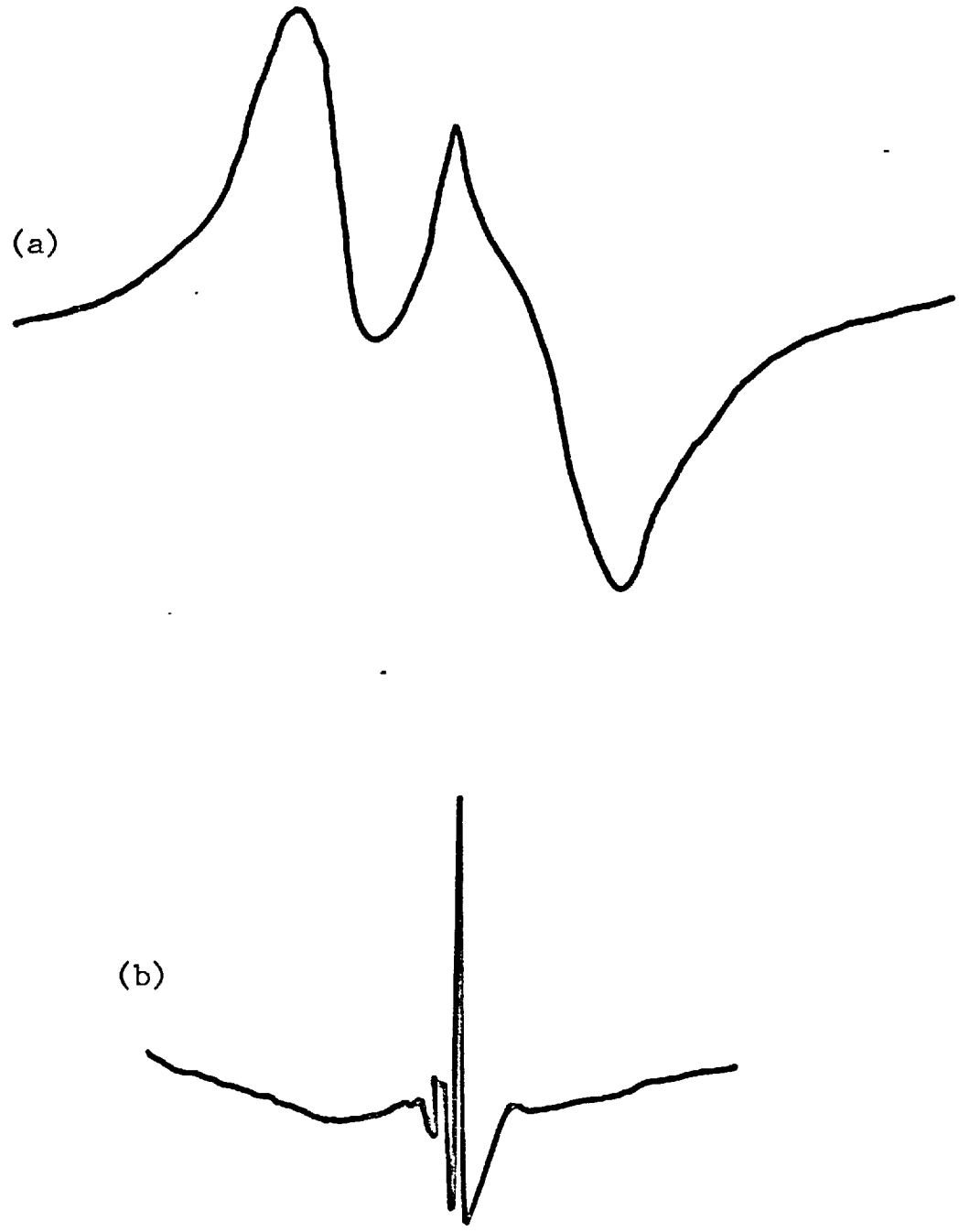


Figure 4.23

Epr spectra of sodalites hydrothermally grown by Bye (1970)

a As-grown, undoped, crushed crystals

b Selenium doped powder, fired in hydrogen

The sodalites grown by Bye gave different spectra (figure 4.23). An undoped powder made by crushing single crystals had a normal three-line spectrum, with the B line slightly broadened whereas a selenium doped material fired in hydrogen gave a two line signal, similar to the signals given by the sodalites of Hodgson et al (1967).

4.5 Discussion: epr

Since the colour of photochromic sodalite arises from an electronic transition of a trapped electron in a centre similar to an F-centre, one of the following possible mechanisms of the photochromism is indicated, where P = a paramagnetic centre, D = a diamagnetic centre, V_x = a vacancy at an x atom site and F = the F-type centre

$$D + V_{Cl} \xrightarrow{UV} P + F \qquad 4.18$$

$$D(I) + 2V_{Cl} \xrightarrow{UV} D(II) + 2F \qquad 4.19$$

$$P(S = \tfrac{1}{2}) + V_{Cl} \xrightarrow{UV} D_? + F \qquad 4.20$$

$$P(S = s) + nV_{Cl} \xrightarrow{UV} P(S = s-n) + nF \qquad 4.21$$

Another mechanism appears to be possible

$$F^- + V_{Cl} \xrightarrow{UV} 2F \qquad 4.22$$

but this mechanism is a special case of 4.18.

The three line epr signal obtained with most of the materials studied in the as-grown or activated states, which, on irradiation with UV, gives the thirteen line spectrum of the F-centre plus the central line B, suggests:

1 that the source of the trapped electron is a centre which also gives rise to lines A and C, and

2 that this electron source centre is paramagnetic, ruling out mechanisms 4.18 and 4.19 above.

One source of the electron which has been suggested is an iron species but this can now be eliminated as the direct source on two counts:

1 the high purity sodalites grown by Bye (1970) which were photochromic, and

2 large signals were observed in the epr spectra of some sodalites, from ferromagnetic impurities (figure 4.15) which were most probably due to iron or possibly nickel. Either of these impurities could have entered the materials

during growth from the autoclave.

The ferromagnetic type signals were invariant under UV irradiation, whilst the lines A and C diminished and eventually gave way to the F-centre signal. The ferromagnetic species is not, therefore, photoactive.

The epr spectrum of selenium doped, hydrothermally grown sodalite activated in hydrogen, was found to be similar to the epr signals given by the materials prepared by Hodgson et al (1967). However, for most of the sodalites in this study the three line spectrum of figure 4.13 is obtained. Together these facts suggest that more than one mechanism can cause photochromism in sodalite, agreeing with Bye (1970). In this study the active centre of interest is the one responsible for the signals A and C of the three line signal.

It is probable that the source of electrons in heat treated HT11 is the same as for the majority of other sodalites in this study, ie the centre which gives rise to epr lines A and C. The signals from it are relatively weak, however, compared with the



Figure 4.24

Epr spectrum of HT11 heated to 900°C in O_2 for ½ hour

very strong g = 2.017 line and expansion of the ordinate scale does not help since the very strong line blots out any signals in the positions of A and C. They can just be seen, nevertheless, in figure 4.24.

The spectrum of a sodalite grown from kaolinite (figure 4.13d) shows considerable broadening as compared to signals from sodalite materials grown from other methods. This observation is explained by X-ray powder diffraction which shows that the sodalites prepared by this technique are poorly crystallised, which causes broadening of the signal from inhomogeneities in the environment of the centre giving the signal.

5 PHOTOCHROMIC ACTIVITY IN SODALITES

5.1 Introduction

In Chapter 4 the possibility that the donated electron giving rise to photochromism came from an iron species was shown to be false. Ballentyne and Bye (1970) from optical measurements on high purity sodalite cast definite doubts that the source of the electron was a sulphur centre but it was suggested that divalent anions in chlorine sites could both cause more chlorine vacancies ('latent' F-centres), and be the electron source for photochromic activity. For the sodalites grown in this study, this situation only exists if the same divalent paramagnetic anion is formed in the presence of a wide variety of dopants and growth media which seems unlikely. Sulphur centres can also be eliminated as being the photoactive centre since the epr signal from this centre is considerably smaller in sulphur doped (as sulphide), flux-melt sodalite than in a non-sulphur doped one with comparable photochromic activity (figure 5.1).

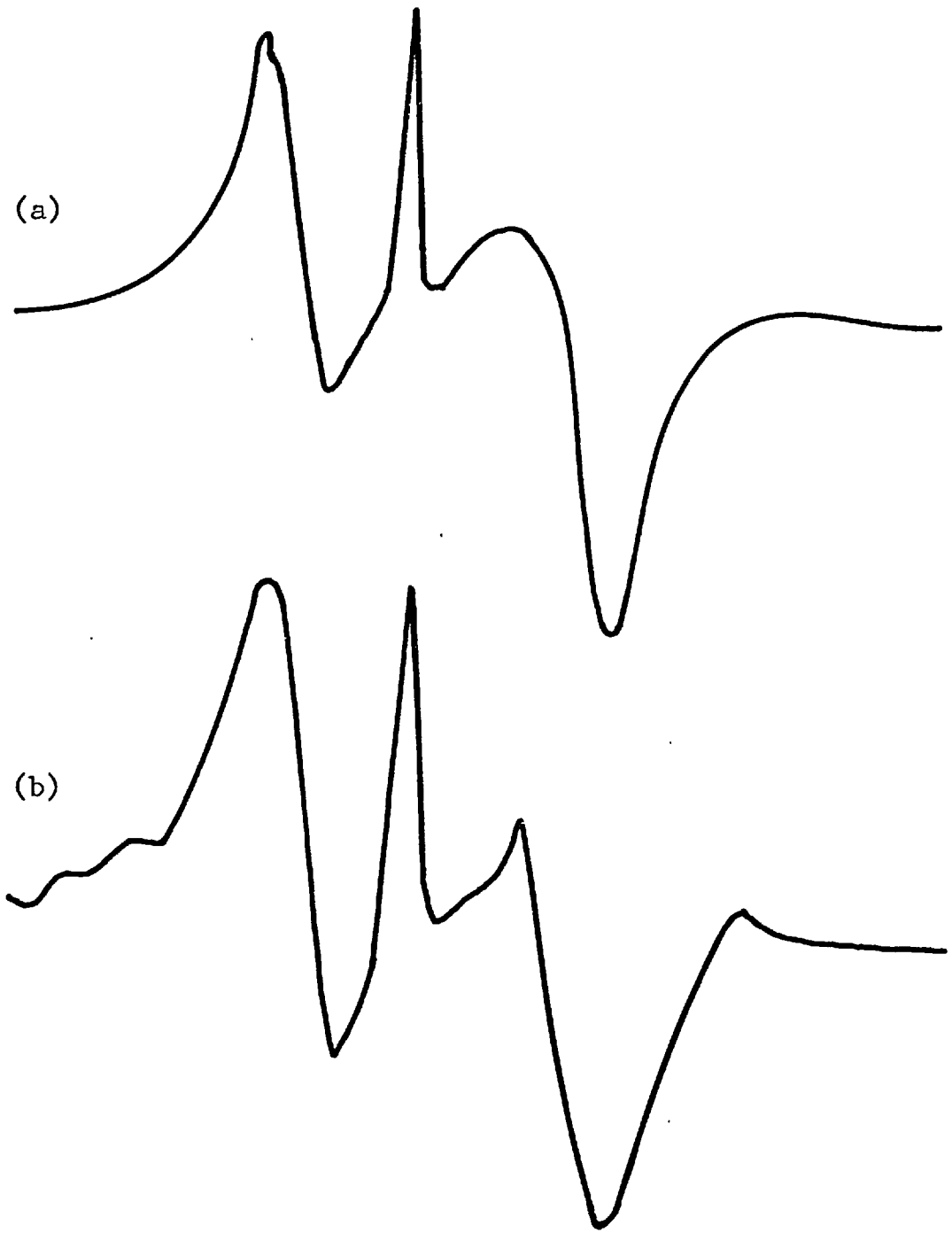


Figure 5.1

Epr spectra of flux-melt grown sodalites as grown

a undoped

b sulphur doped

The signal in (b) appears to be slightly stronger, but the microwave power used to produce it was a factor of 10 greater than for (a)

In an attempt to elucidate the parameters of the photoactive centre, theoretical lineshapes were calculated with the aid of the CDC 6400 computer of the Imperial College Computer Centre. The programs used are described below but the relevant results are introduced as appropriate.

5.2 Computer simulation of epr powder spectra

Two programs for calculation of epr spectra were obtained from the chemistry department of Imperial College, and, after some modification, were suitable for the purposes of this study. The programs were called SHAPE 5 and SPINGT½.

5.2.1 SHAPE 5

This program can be used to calculate the lineshapes given by paramagnetic species in powders and glasses. The calculation is performed using the procedure of Kneubühl (1960) and the following assumptions are made:

1 electron spin of the paramagnetic species $S = \frac{1}{2}$, ie one unpaired electron

2 the paramagnetic species are randomly orientated throughout the powder or glass

3 no hyperfine splitting is present

4 the only broadening considered is that due to anisotropy of the g-factor.

The procedure can be extended to mobile liquids by including the effects of Brownian motion.

The parameters fed into the program as data for the Kneubühl part of it are g-values, linewidths, microwave frequency and the idealised line shape to be used (Gaussian or Lorentzian). The line positions are first calculated, hyperfine shifts, also fed in as data, are applied to them, and they are then convoluted according to the shape function to give practical spectra. The program is shown in Appendix I.

The experimental spectrum, which is introduced in the data, and the computed curve are normalised and plotted superimposed.

5.2.2 SPINGT½

The listing of the SPINGT½ main program and subroutines is given in Appendix I. The program calculates electronic energy levels of the ground state of paramagnetic species from parameters fed in as data to form a spin Hamiltonian and plots out their epr powder spectra. The calculation is performed using the procedure of Bowers and Owen (1955). Initially it is assumed that no nuclear interaction terms are present in the Hamiltonian, ie I = 0; then with a strong magnetic field parallel to the z axis (chosen as the axis of quantization), matrices are set up representing the Hamiltonian of the system and eigenvalues are extracted by subroutine EIGEN from the secular determinant associated with the energy matrix. For the corresponding terms with the x and y axes as the directions of quantization, respectively, the matrix is transformed as required by Bowers and Owen, who also provide for the subsequent introduction of hyperfine interactions. After calculation, the spectrum is normalized to the experimental spectrum which is fed in as data, and the two curves are plotted superimposed.

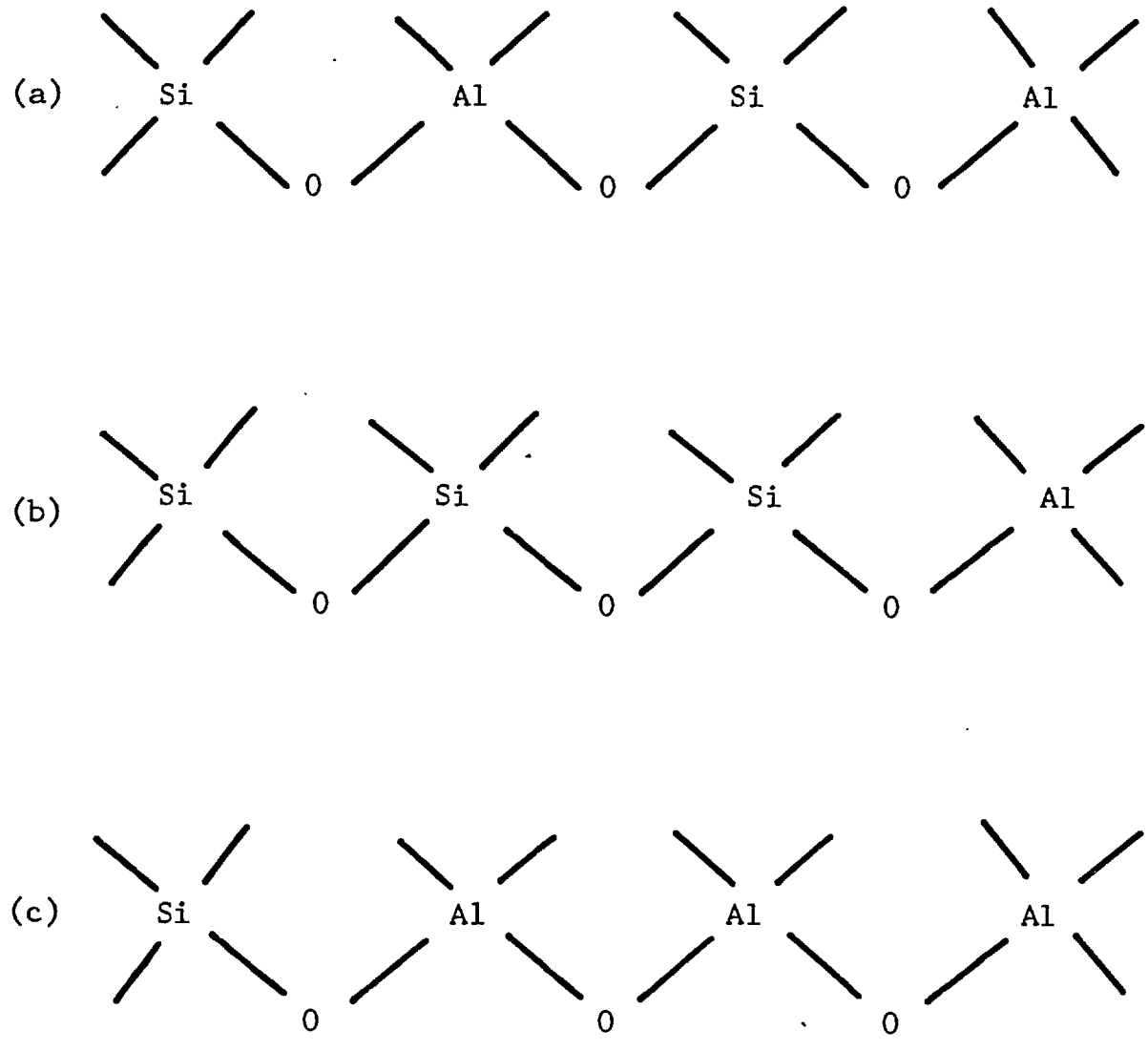


Figure 5.2

a 'Normal' aluminosilicate lattice

b Si substituted for Al

c Al substituted for Si

5.3 The source of the electron

The electron source centre appears to be of the type which could be formed in a variety of sodalites grown under a wide range of conditions. This requirement seems to indicate a centre of the structural disorder type, or, recalling the two salient peaks in the epr signal of the centre, one involving an atom of nuclear spin $\frac{1}{2}$ or an atom of zero nuclear spin in a triplet state in axially distorted cubic symmetry.

5.3.1 Antistructure disorder model

The normal sequence of atoms in the sodalite aluminosilicate lattice is shown schematically in figure 5.2a. Suppose, however, an aluminium atom exchanged with a silicon atom. The new atomic sequences resulting from this exchange are shown in figures 5.2b and 5.2c. This type of disorder is not expected from structural work by Pauling (1929) on aluminosilicate structures; however, here we are concerned only with disorder on a microscopic scale (parts per million) which may well occur. Also Yamaguchi et al (1968) has found that sulphur containing sodalites made by sintering give deeper

photochromic colouration if made with silicon substituted for some aluminium, and Kohn and Benjamin (1961) have suggested the degree of general disorder in silica minerals as an influence on their colouration. Also epr studies by Bershov and co-workers (1969) have shown the presence of partial disordering of the distribution of aluminium atoms in naturally occurring single crystals of sodalite, between the two structural positions of aluminium and silicon.

The substitution of silicon for aluminium in the lattice should produce an electron donor centre as there is one electron in excess of that required for normal bonding; (cf the donor atom in an n-type extrinsic semiconductor, though in the present case the 'donor' level is much lower in the band gap, cf the U-levels of Medved (1954)).

The disorder can be represented in Kröger-Vink notation by equation 5.1, and assuming equilibrium

$$Si_{Si} + Al_{Al} \rightleftharpoons Si'_{Al} + Al^{\bullet}_{Si} \qquad 5.1$$

conditions exist, the equilibrium constant K for 5.1 is

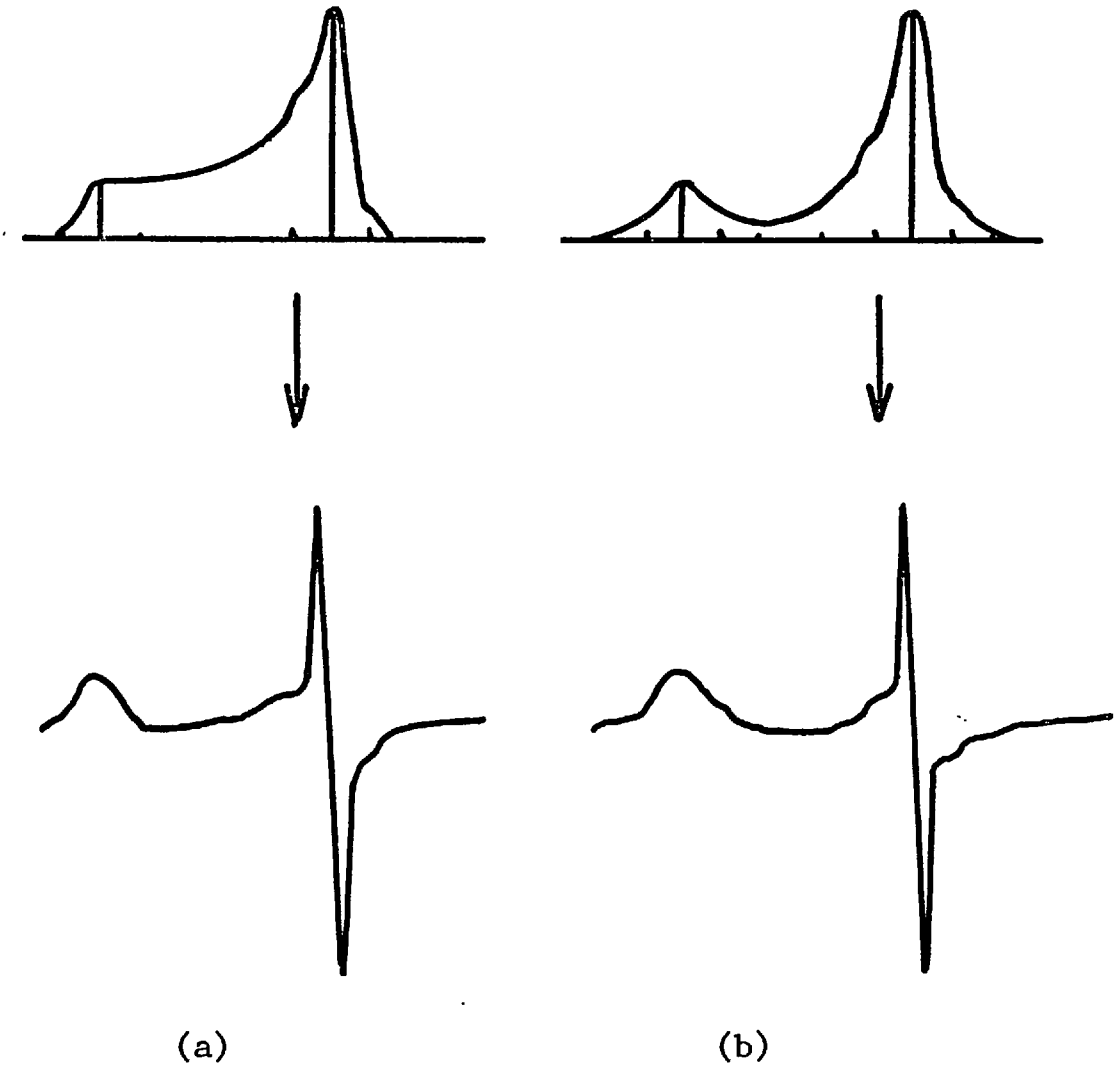


Figure 5.3

Expected epr absorption and first derivative lineshapes for the antistructure disorder model in sodalite

a with an unpaired electron on a silicon atom

b with an unpaired electron on an oxygen atom

$$K = \frac{\left[Si'_{Al}\right]\left[Al^{\bullet}_{Si}\right]}{\left[Si_{Si}\right]\left[Al_{Al}\right]} = \left[Si'_{Al}\right]\left[Al^{\bullet}_{Si}\right] \qquad 5.2$$

since the degree of disorder is such that the silicon and aluminium on their own sites exhibit approximately unit activity. Then using $\Delta G = -RT\ln K$ (or $-kT\ln K$) a free energy change for the disorder process can be calculated; at 300K for 1ppm Si_{Al}, $\Delta G = 16.5$ kcalmole^{-1} or 0.71 ev and for 100ppm Si_{Al}, $\Delta G = 11.0$ kcalmole^{-1} or 0.48 ev. The concentration of the electron donor is between these wide limits, giving the limits of the free energy change for this type of disorder.

The epr spectrum resulting from the structure in figure 5.2 would exhibit axial symmetry. The electron giving the resonance signal could either be on the misplaced silicon atom, or on an adjacent oxygen atom. In the former case, each of the axial lines would consist of a central line, relative strength 19, with two hyperfine lines, relative strengths ½ (figure 5.3a); the hyperfine lines arise from the isotope Si^{29} of natural abundance 4.7%. In the case of the electron sited on an oxygen atom the axial lines are each split into

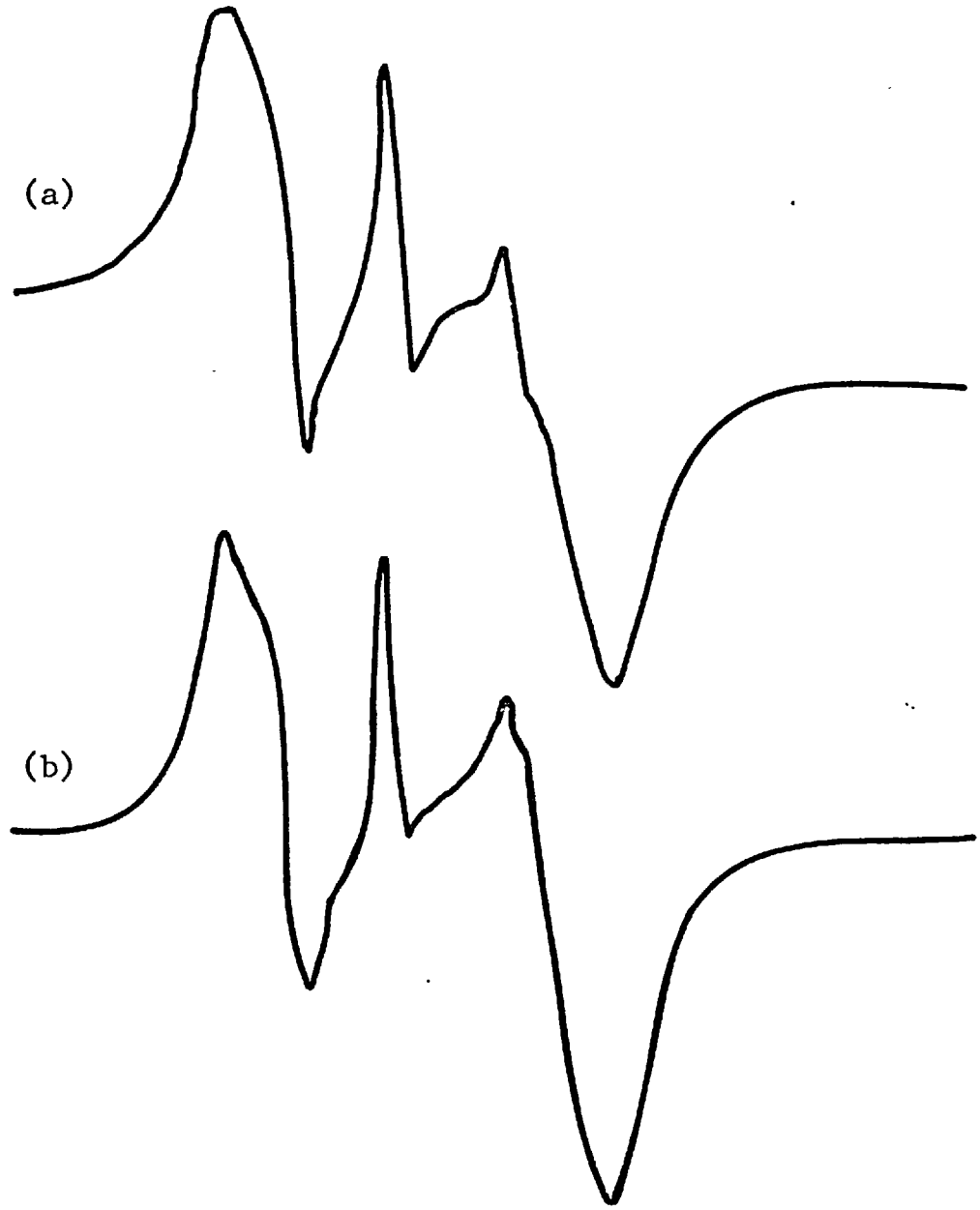


Figure 5.4

Epr spectra of sodalites grown from feedstocks with:

a excess silica

b excess alumina

both after heating at 900°C in argon for ½ hour

5 lines of approximate relative strengths 1:19:382: 19:1, arising from splitting by 4.7% Si^{29} at each of two silicon sites (figure 5.3b). Of these two possibilities the electron on oxygen is probably the most likely, as this centre has already been observed in smoky quartz (O'Brien 1955).

The antistructure disorder model was found wanting in two respects:

1 sodalites were grown by hydrothermal techniques with excesses of silica and alumina, producing materials HT14 and HT15 respectively. As far as could be determined, these had the same, normal activation characteristics and epr spectra (figure 5.4);

2 neither of the epr spectra in figure 5.3 show much resemblance to the experimental curves.

5.3.2 Models involving other centres

The experimental epr spectra of the sodalites studied could be approximated (neglecting the centre line B) by a species with electronic spin ½ with cubic site symmetry and hyperfine splitting by a nucleus with

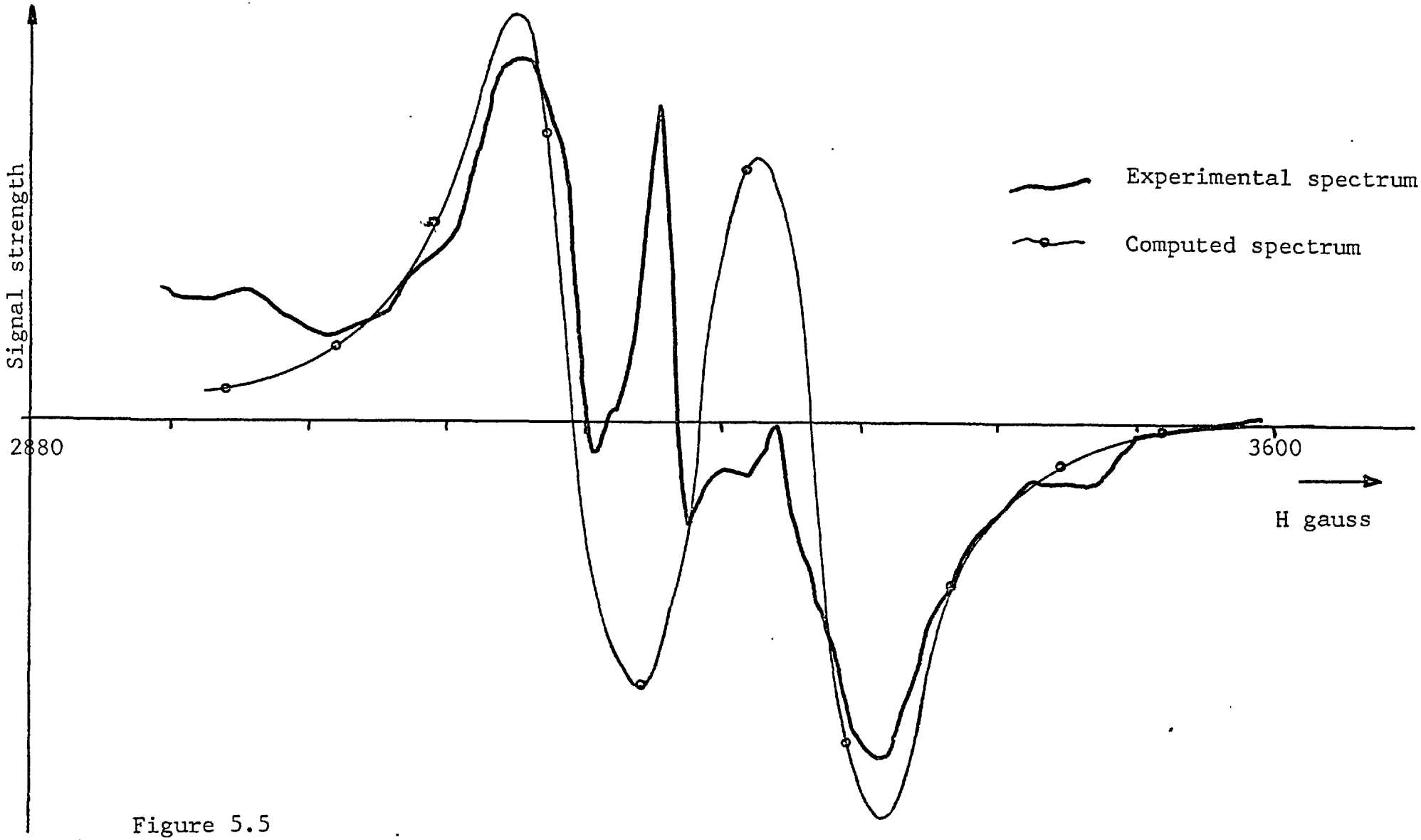


Figure 5.5

Best fit computed curve for the epr spectrum of a typical sodalite using SHAPE 5



Figure 5.6

Epr spectrum of as-grown deuterated sodalite

$I = \frac{1}{2}$. Computer program SHAPE 5 was employed to produce the best fit shown in figure 5.5. Since there is no line in the middle of the experimental epr spectrum of the photoactive centre the hyperfine interaction could only be with nuclei of $I = \frac{1}{2}$ with a natural abundance of approximately 100%. The only nuclei satisfying these requirements are H^1, F^{19}, P^{31} and Tm^{169}, and the only one of these which could occur consistently in all the various sodalites is H^1. In an attempt to eliminate this possibility, sodalites were grown hydrothermally substituting NaOD for NaOH, and D_2O for water in the growth vessel and during washing. Its epr spectrum in the region of 3400 gauss is shown in figure 5.6, which clearly shows that there are no significant changes from the spectra of sodalites from hydrogen containing media. If hydrogen had been involved in the photoactive centre, deuterium would have substituted for it during deuterated hydrothermal growth and the hyperfine splitting due to hydrogen ($I = \frac{1}{2}$), would have been replaced by that due to deuterium ($I = 1$). The possibility of the electron donor centre being one involving hyperfine interaction can therefore be eliminated; the two line signal must therefore derive

from a centre involving a nucleus or nuclei with zero nuclear spin but with zero field splitting, giving rise to a spectrum displaying fine structure.

The work on high purity sodalites by Ballentyne and Bye (1970) and an earlier part of this study (section 5.1) eliminated all the species which could satisfy the above requirements except centres containing oxygen. These centres will now be considered.

5.3.3 Oxygen containing centres

In table 5.1 are listed centres containing oxygen which might reasonably be expected to occur in sodalite.

Centres with more than one hydrogen atom can be discounted immediately since these species would give more than two principal lines in an epr spectrum, and the deuterated hydrothermal growth work with subsequent epr measurements of section 5.3.2 eliminates all the centres involving one hydrogen atom, leaving only the pure oxygen centres.

Table 5.1

O^+		HO^+		HO_2^+	
O^o	(atomic oxygen)	HO^o		HO_2^o	
O^-		HO^-	(hydroxyl)	HO_2^-	(hydroperoxide ion)
O_2^+	(oxygenyl)	H_2O^+		$H_2O_2^+$	
O_2^o	(molecular oxygen)	H_2O	(water)	$H_2O_2^o$	(hydrogen peroxide)
O_2^-	(superoxide)	H_2O^-		$H_2O_2^-$	
O^{2-}	(oxide)	H_3O^+			
O_2^{2-}	(peroxide)				

Oxide (O^{2-}) and peroxide (O_2^{2-}) have no unpaired electrons and would not give epr signals; moreover, removal of an electron from them to form an F-centre would give species with odd numbers of electrons which could, in principle, give epr signals. The photoactive centre in sodalite has properties opposed to those of O^{2-} and O_2^{2-} and they need not, therefore, be considered further.

O^+ and O_2^+ would require excessive energy to ionise

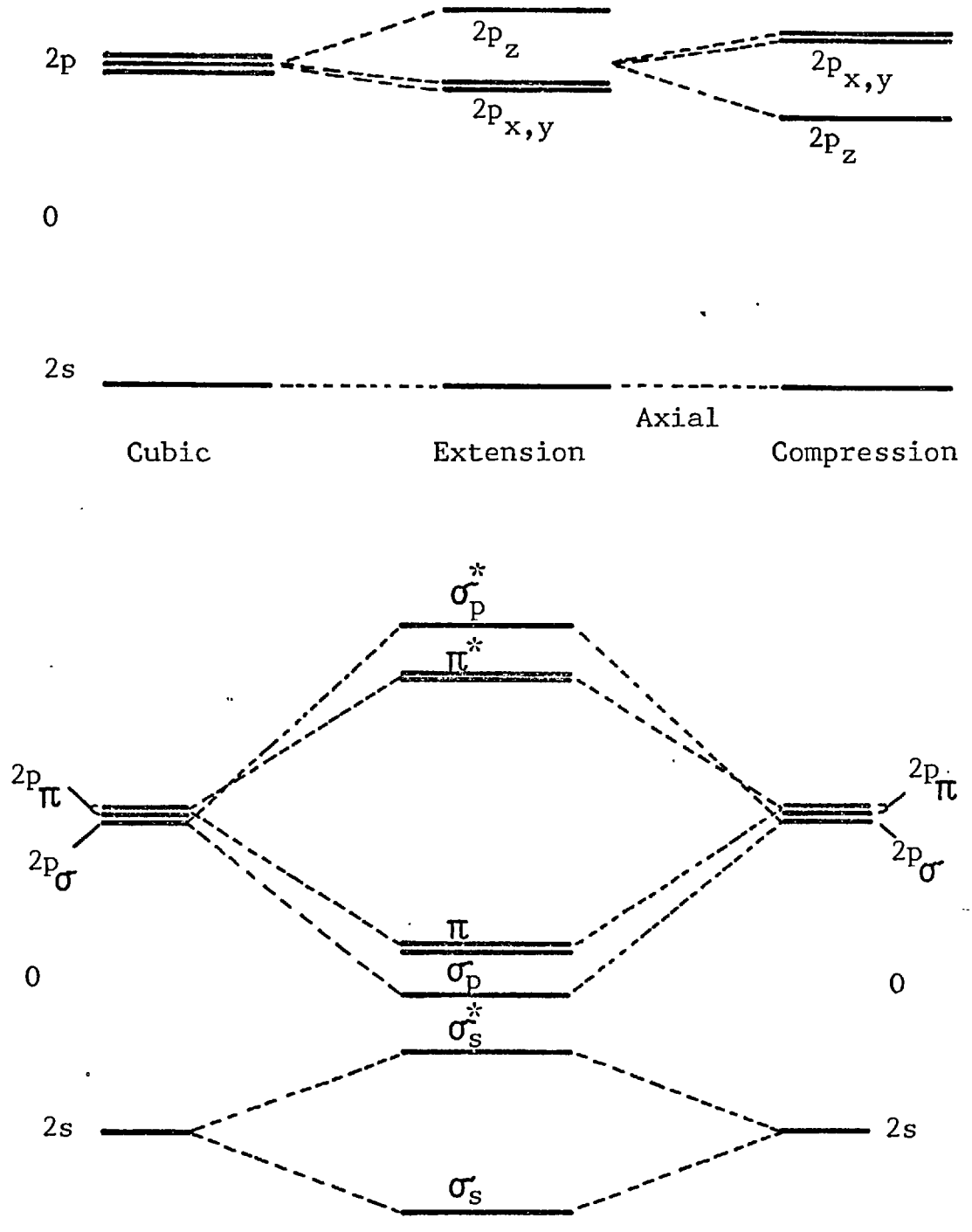


Figure 5.7

Top - highest atomic orbitals of oxygen in various site symmetries

Bottom - highest molecular orbitals of O_2 species

them and, according to their site symmetry, would have one unpaired electron, though from the atomic and molecular orbital energy level diagrams for oxygen (figure 5.7), O^+ could have three unpaired electrons in cubic or spherical symmetry. Results from the SHAPE 5 computer program show that a single unpaired electron species is not the source of the epr signal under investigation which eliminates O^- and O_2^- with 7 and 13 electrons respectively giving one unpaired electron each, regardless of site symmetry (figure 5.7).

Knowledge of the lineshapes generally encountered in epr spectra and section 5.3.2 suggest that the centre responsible for the experimental epr two line signal is a triplet state (S = 1) species with axial symmetry producing some zero field splitting which rules out the O^+ centre even in an isotropic site and leaves only O^o and O_2^o, ie atomic and molecular oxygen. Computer program SPINGT½ was therefore employed to elucidate the parameters of the centre.

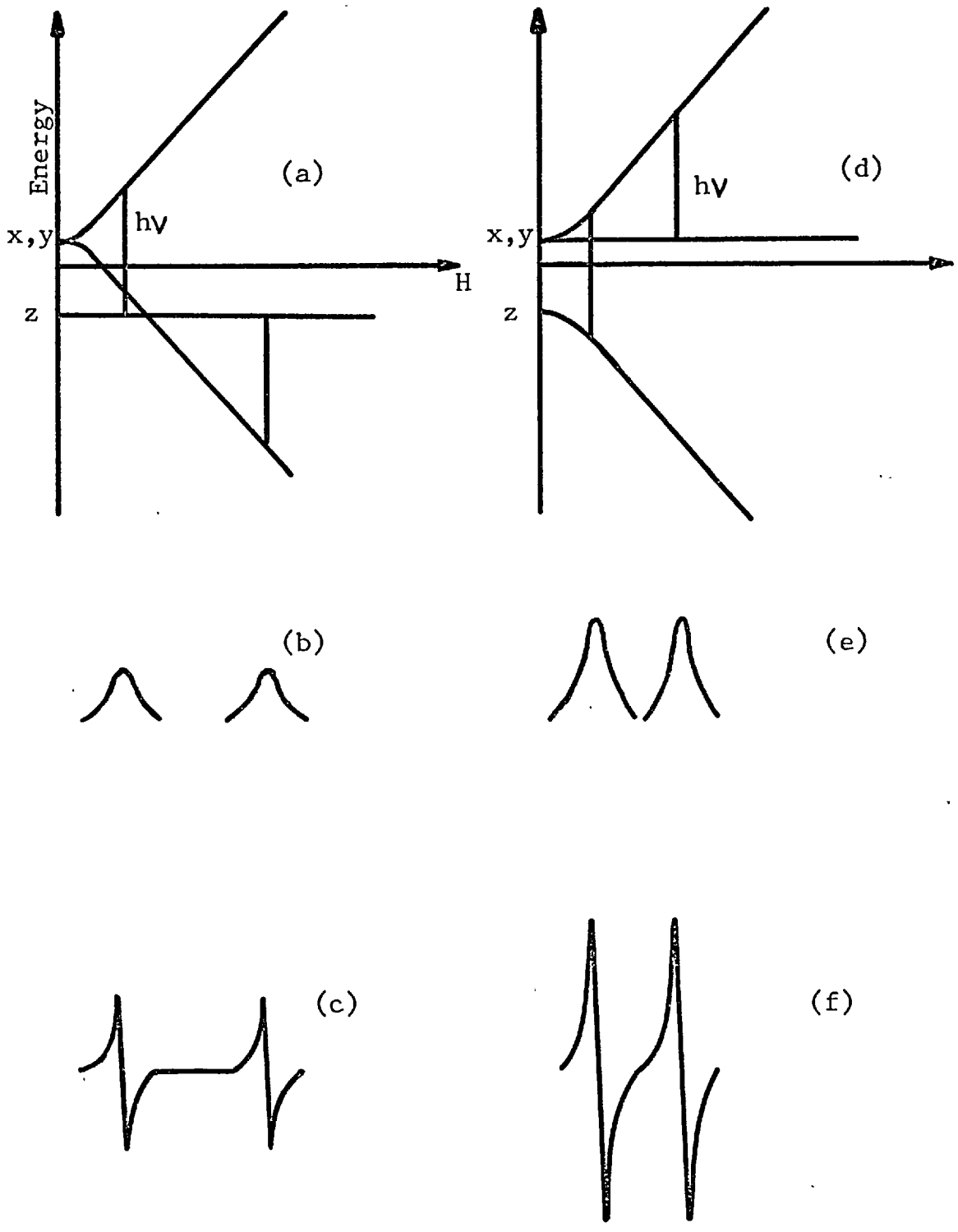


Figure 5.8

Triplet state species with zero-field splitting and axial symmetry

a and d Energy levels vs field diagrams
b and e The corresponding epr absorptions
c and f The corresponding epr spectra

a, b, c Magnetic field in z direction
d, e, f Magnetic field in x or y directions

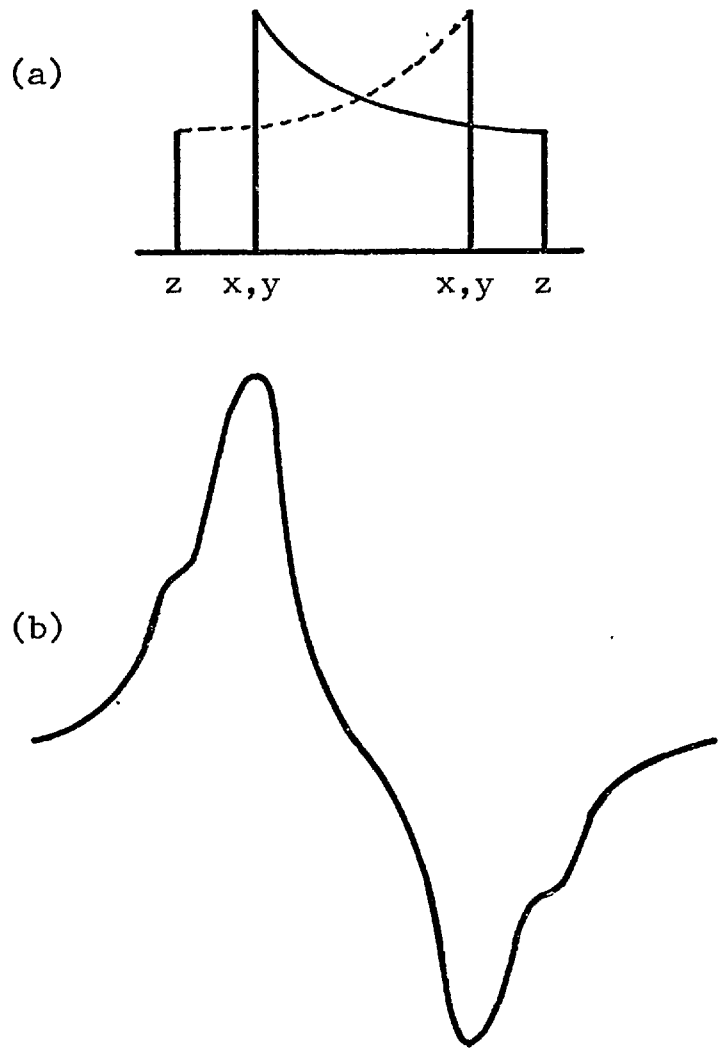


Figure 5.9

Triplet state species with zero-field splitting and axial site symmetry in a polycrystalline material

a Absorption lines

b 1st derivative epr spectrum

5.3.4 Reconstruction of the epr powder spectrum of the photoactive centre

For a single crystal containing a paramagnetic species with S = 1 and axial symmetry about the crystallographic z axis (figure 5.8), when the magnetic field is along the z axis, the energy level versus field diagram (a) shows the epr spectrum will be as in b, giving the first derivative curve c. But, for the field along the x or y crystallographic axes (d), the absorption spectrum is shown in e and its first derivative in f. In a polycrystalline material, a component of the field is along each axis of each crystallite. A combination of the four lines should therefore be seen to give the first derivative curve shown in figure 5.9 for a well resolved case. For a less well resolved spectrum, it is easy to envisage the spectrum obtained generally for the majority of sodalites in this study (neglecting for the present the sharp 'non-contributing' line).

The curve computed by SPINGT½ in best agreement with an experimental curve chosen at random is shown

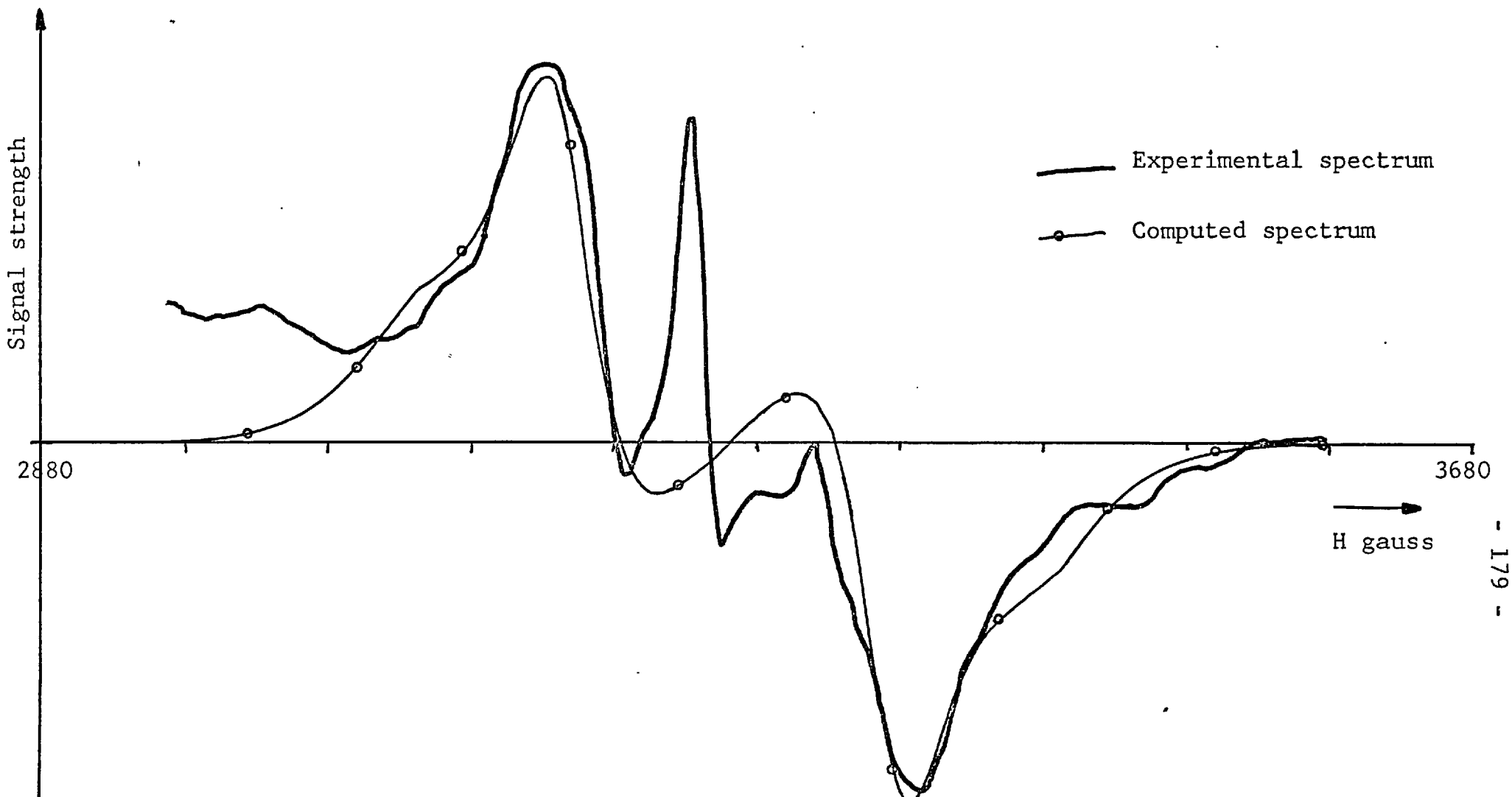


Figure 5.10.

Best fit computed curve for the epr spectrum of a typical sodalite chosen at random using program SPINGT½

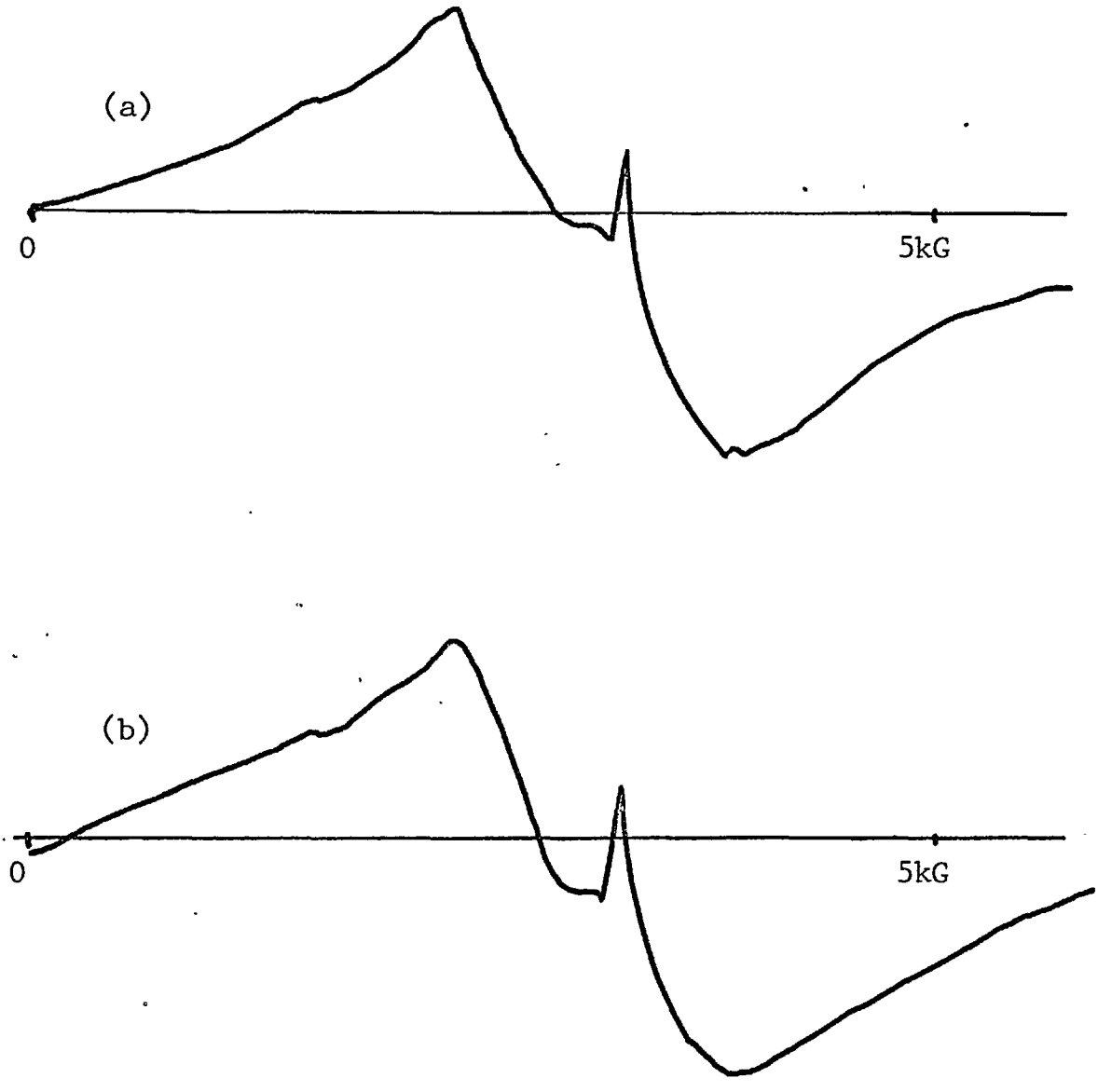


Figure 5.11

Epr spectra of:

a Oxygenated dionized water (-50°C)

b Oxygenated iso-propyl alcohol (-50°C)

in figure 5.10 together with the experimental spectrum. The degree of agreement leads one to suppose that the active centre in the materials under study is in a spin triplet ground state in an axially symmetric crystal field with a g-factor of 2.0051 and a zero field splitting D = 0.0165cm^{-1}. In principle both the centres O° and O_2° still under discussion can satisfy these requirements.

5.4 Oxygen in other media

Boiled deionized water and GPR grade iso-propyl alcohol were oxygenated from a compressed oxygen cylinder and their epr spectra taken at -50°C (figure 5.11). They show the same lineshape as the photoactive centre, though considerably broadened.

Oxygen gas dissolves in water to about 3.5% at room temperature, and to about 2.5% in lower alcohols. The dissolved oxygen would give epr signals but water and alcohols in the liquid state, being polar, will absorb microwave power from the resonant cavity. This effect can be prevented by freezing the solution which holds the solvent molecules effectively

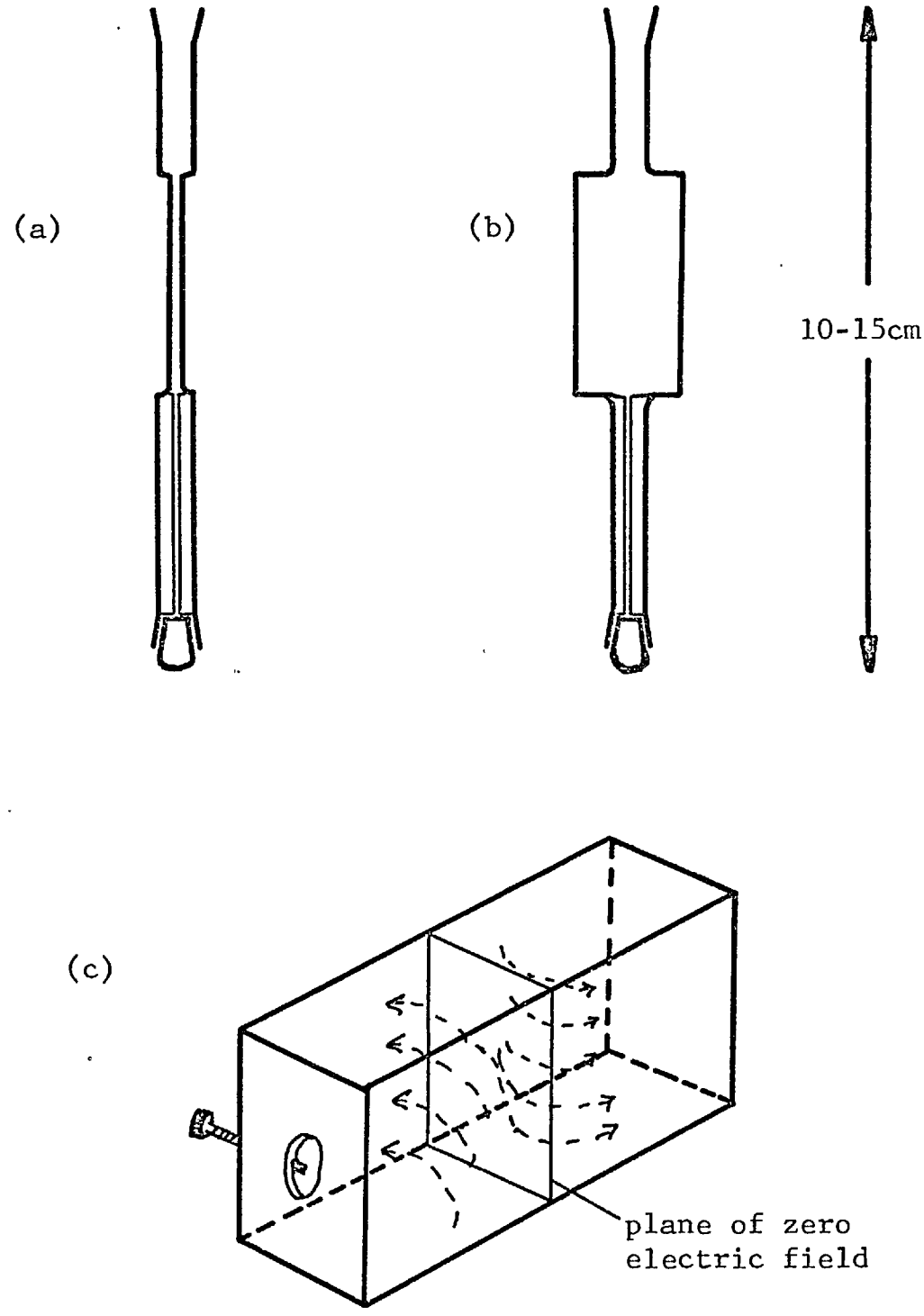


Figure 5.12

(a) side elevation and (b) elevation of a flat silica cell for epr measurements on polar liquids

(c) epr resonant cavity showing electric field; note plane of zero field

stationary as a lattice for the oxygen. The problem can also be overcome by using a flat silica cell (figure 5.12) to contain the sample in the planar region shown in the resonant cavity where the net electric field is zero.

The epr spectra shown in figure 5.11 therefore consist of signals given by oxygen molecules held in a rigid isotropic lattice (since the solvent molecules are frozen in random orientations). The spectrum is that of a triplet state species in an axial field, despite the fact that the lattice is isotropic; the axial field must therefore arise from the oxygen molecule itself. The shoulders which should be present at the outer edges of the lines from molecules in which components of the field are along their z axes cannot be seen, but this omission may be due to broadening which makes observation impossible at $-50^{o}C$, as their intensity is very low. Another possibility is that their position is nearly coincident with the position of the two centre lines. To summarise, this experiment appears to indicate that oxygen molecules can themselves produce a large enough axial perturbation from cubic symmetry to

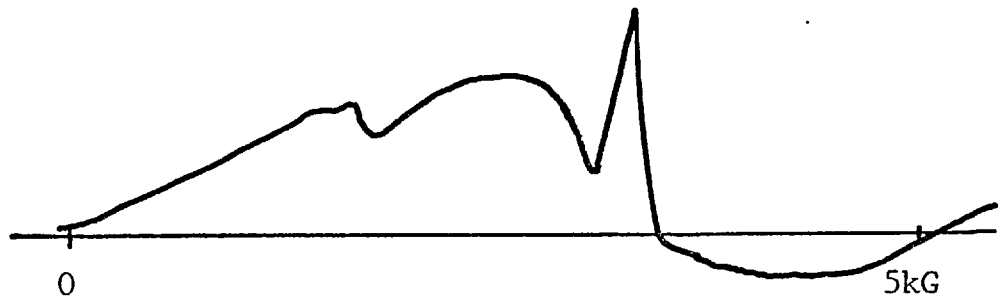


Figure 5.13

Epr spectrum of oxygenated dionized water at -50°C after UV irradiation for several hours also at -50°C. (Same machine settings as for figure 5.11)

produce an axially symmetric zero-field splitting and therefore the fine structure seen in the photochromic centre.

As an extension of this work, an oxygen solution in deionized water at about -50°C was irradiated with the ultra-violet radiation used for colouring sodalites. After 2-3 hr the epr spectrum shown in figure 5.13 was obtained. Clearly the O_2 has been decomposed by the ultra-violet, as expected. Since chemical reactions can be regarded merely as electronic rearrangements, the electrons of O_2 can be rearranged by UV radiation.

5.5 Oxygen in sodalite

The most likely position for most anionic or uncharged species in the sodalite lattice is a chlorine vacancy which has cubic symmetry. As seen in the last section, an oxygen molecule in this site would produce an axial crystal field at the parametric centre of the site, arising from its own axial symmetry. Conversely an oxygen atom in the same site will not have axial site symmetry unless the surrounding tetrahedron of sodium ions exhibits

Jahn-Teller distortion (Pake 1962).

At this point a reconsideration of the epr spectra of the material HT11 (figures 4.19, 4.20, 4.21), a perchlorate sodalite, may prove useful. On heating a perchlorate salt or perchlorate sodalite (Barrer and Cole 1970) oxygen is evolved according to the reaction 5.3

$$ClO_4^- \xrightarrow{\text{heat}} Cl^- + 4\,O \qquad 5.3$$

In the free salts the oxygen is liberated as molecular O_2; however, probably in the sodalite lattice and initially for the free salt, the oxygen will be free atoms, later combining to produce molecules as the concentration of O rises. Atomic oxygen could give rise to the single line in the as-grown spectrum of HT11, since the Jahn-Teller theorem does not predict the direction or extent of the distortion which relieves orbital degeneracy. (As shown in the previous section the single line could not be from O_2). If this single line at $g = 2.017$ is due to oxygen atoms, then on heating the as-grown material to activate it, this line would be expected to increase in intensity as

observed, if the atomic oxygen evolved is responsible for it. Further heating would allow some atoms to diffuse out of the lattice and some to form molecules, which gradually become more noticable in the epr spectrum. Thus O_2 may be responsible for the photoactive centre signals A and C, and O atoms for the single line B.

5.5.1 Formation of oxygen centres

Whilst the formation of the O_2 centres in material HT11 from O^o centres can be relatively easily followed using the epr spectrum of the material, a separate mechanism must be postulated for O_2 formation in the majority of hydrothermally grown sodalites; the most probable type is shown in equation 5.4.

$$2OH^- \rightleftharpoons O + H_2O + 2e^- \qquad 5.4$$

The standard electrode potential for this half reaction, E^o, is -1.043v, the standard free energy change is thus positive ($\Delta G^o = -nFE^o$), and the reaction will go to the left at standard temperature (25^oC) and pressure (1 atmosphere) and for unit activity of the species reacting. In an autoclave

during hydrothermal growth these are not the relevant conditions. However, the Nernst equation (5.5) can be applied to correct for the differences in temperature and concentrations.

$$E = E^{o} + \frac{RT}{nF} \cdot \ln \frac{ox}{red} \qquad 5.5$$

where:

E = electrode potential of reaction under conditions of interest

E^{o} = electrode potential of reaction under standard conditions

R = the gas constant (8.3143 $JK^{-1}mol^{-1}$)

T = absolute temperature

n = number of electrons involved in the reaction

F = Faraday constant (96,487 colomb $g.equiv^{-1}$)

ox = product of activities of oxidised species

red = product of activities of reduced species

These last two apply to the reaction 5.6

$$\text{oxidised species} + e^{-} \rightleftharpoons \text{reduced species} \qquad 5.6$$

In applying the Nernst equation here the following assumptions are made:

1 since the number of 'molecular' species on each side of equation 5.4 are equal, the pressure

will not directly affect the chemical equilibrium

2 $T = 400^{o}C = 673K$, the temperature typically used for hydrothermal growth

3 the activity of the H_2O present was approximated to its molarity, ie 29.6

4 for NaOH the activity coefficient was estimated from existing data (Weast 1971) as 0.728 giving the activity of OH^- in a typical hydrothermal growth run as 2.323

5 the concentration of oxygen atoms is the same in the growth medium as the crystallised product, giving a concentration of approximately 10ppm; since this species is present in high dilution its activity coefficient is taken as unity and the activity of $O \simeq 10^{-5}$/Avogadro's number = 1.660×10^{-29}.

When these figures are substituted into 5.5 we have $E = +0.829v$ thus the sign of the electrode potential has changed, and for the conditions of hydrothermal growth used reaction 5.4 has a free energy change of -1.600×10^{5} $Jmol^{-1}$ and the reaction will tend to

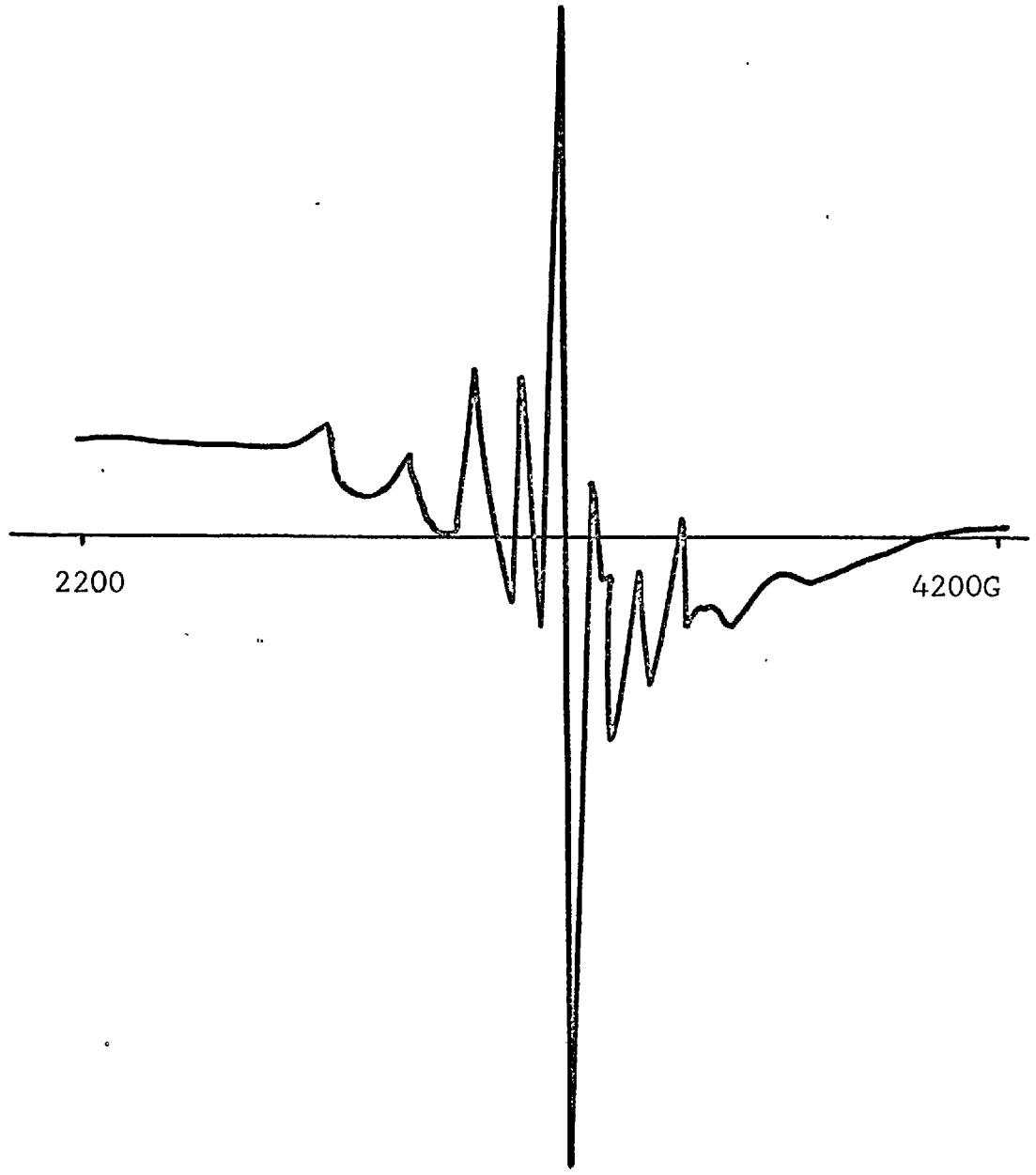


Figure 5.14

Epr spectrum of as grown vanadate doped, hydrothermally grown, sodalite

go to the right.

Evidence for this mechanism is as follows:

1 the existence of free electrons in the growth system would make it highly reducing

2 sodalite grown hydrothermally using a sodium chromate doped growth mixture has a definite green tinge showing reduction of yellow chromate (Cr VI) in the system to the green chromium III

3 sodalite grown hydrothermally using a sodium vanadate doped growth mixture has an epr spectrum (figure 5.14) showing hyperfine structure which can be assigned to V^{51} (natural abundance 99.76%, $I = \frac{7}{2}$), despite poor resolution. This observation implies than an electron resides (at least partially) on the vanadium ion and we therefore have a d^1 configuration or vanadium IV, ie the vanadium V in $NaVO_3$ present originally is reduced. Thus there is some evidence for the reaction 5.4 or a similar reaction producing oxygen atoms and a reducing species occurring, followed by 5.7

$$O^o + O^o \longrightarrow O_2 \qquad 5.7$$

These reactions would produce O_2 photoactive centres together with excess O^o, giving the double epr signals of figure 4.13

O_2 cannot definitely be said to be the photoactive centre unequivocally since it is possible that O^o or O_2 in a sodalite lattice could be free to rotate, which would produce rotational fine structure in an O_2 spectrum, but none in the epr signal of oxygen atoms. However, it seems unlikely that the dumb-bell shaped oxygen molecule would be free to rotate in the tetrahedral cavity with sodium ions at the apices which constitute the chlorine vacancy.

5.5.2 Non-photochromic sodalites

Sodalites have been grown, particularly by flux-melt techniques, which give the 'usual' photochromic centre epr signal, but which are not photochromic. However, these were grown from fluxes containing large excesses of V_2O_5 and it is probable that the chlorine vacancies are 'blocked' by VO_3^- groups, preventing formation of F-centres. This type of blocking process could well explain the inactivity

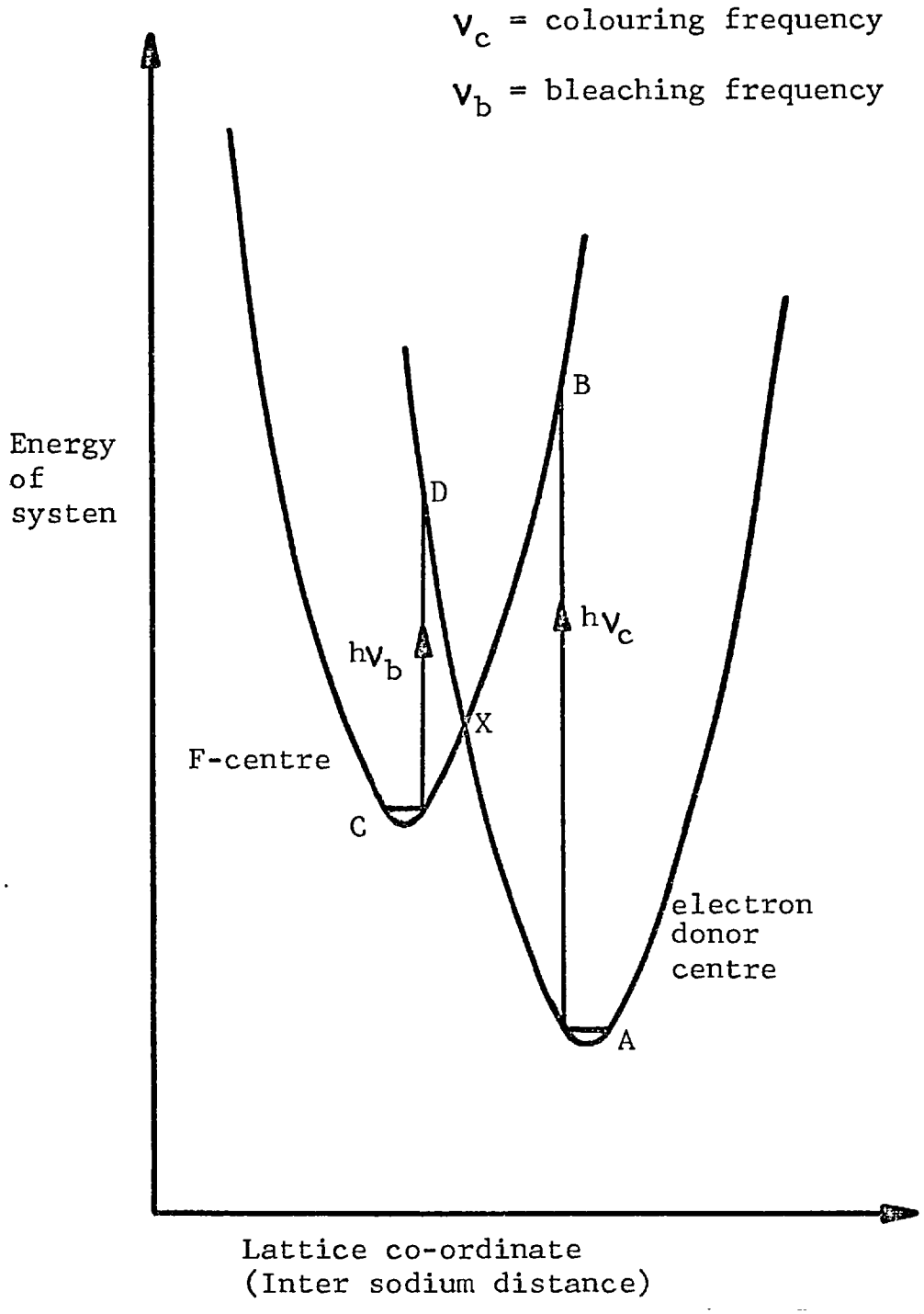


Figure 5.15

Possible configuration co-ordinate diagram for the photochromic process in sodalite. Confirmation of this scheme, or the more usual one via the conduction band, could be made by (a) F-centre luminescence, or (b) photoconductivity measurements

of many sodalites as being due to a lack of chlorine vacancies and suggests that the activation process is the formation of chlorine vacancies by allowing labile blocking species to escape through the lattice, out of the crystal.

5.6 Photochromism energetics - configuration co-ordinate diagrams

A commonly accepted mechanism for the photochromic process is that an electron is excited by UV radiation into the conduction band and from there falls into the F-centre. However, an alternative scheme is that given by a configuration co-ordinate or Frank-Condon diagram (figure 5.15) in which the electronic energy levels are approximated by parabolic potential wells of definite lattice configuration which have discrete vibrational levels. Electronic transitions occur, according to the Frank-Condon principle, sufficiently quickly that the transition is vertical on the diagram, ie the atoms do not have time to change position.

If we consider the 'photochromic' electron in uncoloured sodalite at room temperature, it would be

in the state marked A in the diagram. Absorption of UV sends the electron into a vibrationally excited state of the F-centre (B), which then decays to the room temperature state (C) thermally; in other words the decay is phonon assisted. Optical bleaching of sodalite on absorption of green light causes the transition C ⟶ D, followed by thermal decay back to state A. Hence, thermal bleaching is explained in terms of this mechanism.

A further transition mechanism can also be postulated from the configuration co-ordinate diagram. If a suitable pulse of heat is given to state A, taking its vibrational level above X, then on decay, as the heat is lost by lattice vibration, from point X the electron could come to rest in either state A or C; since the latter is the coloured state, thermal colouration could be possible. The heating effect could be obtained from an electron beam, so this mechanism could explain the cathodochromic effect. Activation of sodalite by electron beam could also be the result of a local heating effect, the heat in this case 'boiling out' chlorine ions and chlorine vacancy blocking species such as H_2O etc. Removal of

atoms and structural and compositional disruption by electron beams has also been reported in alkali silicate glasses (Borom and Hanneman 1967).

5.7 New photochromic materials

It would be of great interest and technological significance if a material could be produced with the advantages of all the materials considered in this work, and few, if any, of the disadvantages. Excluding organic materials as the solution (because of the relative ease of their chemical and photo-degradation), leaves homogeneous inorganic photochromic substances, since heterogeneous ones have the intrinsic problem of a resolution limit.

Thus we seek an inorganic homogeneous photochromic material with the following requirements:

1 a rigid reproducable crystal structure with cavities or vacancies suitable for (2) and (3)

2 an electron donor which can part with its electron on irradiation with the appropriate wavelength, in the environment of (1)

3 an electron acceptor site

(2) and (3) would have different net absorption bands before and after irradiation. These requirements are of course met by many existing materials, but, in addition, ease of forming would greatly enhance the usefulness of the new material. All existing materials with this property are inhomogeneous, and also a plastic state seems to negate requirement (1) above. A possible solution to this would be a material which could be moulded, drawn etc in one state, then processed in some way to give a crystalline condition. Possible areas of search for this kind of material are glass ceramics, crystallised by heat treatment, and (inorganic) liquid crystals.

5.8 Conclusions

The photochromism of most of the sodalite materials grown in this study has been shown possibly to be due to oxygen atoms or molecules in the lattice, O_2 being favoured because of its intrinsic axial symmetry, which relates quite well to the O^{2-} centres suggested by Ballentyne and Bye (1970). However, it is almost certain that other centres can act as electron donors in photochromic sodalite.

Charge compensation for the chlorine vacancies (latent F-centres) is probably by divalent impurity anions and also sodium vacancies, since NaCl has been found in the gases arising during activating sodalite (Phillips 1970).

An explanation has been given for the cathodochromic effect in terms of localised (pulsed) heating effect using Frank-Condon or configuration co-ordinate diagrams, which also satisfactorily explain optical colouring and bleaching and thermal bleaching in an empirical fashion. Electron beam activation is also explained in terms of a heating effect.

Perchlorate doped chlorosodalites have been produced by hydrothermal growth for which the time required for activation is less critical than for previous sodalites and which need not be activated in a reducing or inert atmosphere.

REFERENCES

Allinikov S (1970) Tech Report AFML-TR-70-246

Amodei J and Bosomworth D R (1969) J Appl Opt 8 2473

Ballentyne D W G and Bye K L (1970) J Phys D 3 1438

Band K, Fisher J H and Johns A J (1973) private communication

Barrer R M and Cole J F (1970) J Chem Soc (A) 1516

Barrer R M, Cole J F and Sticher H (1968) ibid 2475

Barrer R M, Cole J F and Villiger H (1970) ibid 1523

Bershov L V, Martirosyan V O, Platonov A N and Tarashchan A N (1969) Neorg Mat 5 1780

Bessent R G and Runciman W A (1966) Brit J Appl Phys 17 991

Borom M P and Hanneman R E (1967) J Appl Phys 38 2406

Bosomworth D R and Geritsen H J (1968) Appl Opt 7 95

Bowers K D and Owen J (1955) Repts Prog Phys 18 304

Britten A J (1964) Ordnance Nov-Dec

Butcher J and White E A D (1964) Min Mag 33 974

Bye K L (1970) PhD Thesis London U p-31

Bye K L and White E A D (1970) J Crystal Growth 6 355

Carson A N (1965) Tech Doc Report AD-617-961

Cohen A J and Smith H L (1962) Science 137 981

Compton W D and Rabin H (1964) Sol St Phys 16 121

Duncan R C Jr, Faughnan B W and Phillips W (1970) Appl Optics 9 2236

Faughnan B W, Staebler D L and Kiss Z J (1971)
Appl Sol St Science 2 107

Faughnan B W and Kiss Z J (1968) Phys Rev Letts 21 1331

Faughnan B W and Kiss Z J (1969) IEEE J Quantum Electronics
QE5 17

Fyler N F (1964) US Patent no 3,148,281

Goldstein E (1896) Zeit f Instrumentkunde 16 211

Gorog I (1970) Appl Opt 9 2243

Hodgson W G, Brinen J S and Williams E F (1967)
J Chem Phys 47 3719

Holser W T and Kennedy G C (1959) Am J Sci 257 71

Hughes G and Hankins H C A (1972) IERE Conf Proc no 25 p-81

Kazan B and Knoll M (1968) 'Electronic Image Storage'
Academic, New York pp 182-185

Kirk R D (1954) J Electrochem Soc 101 461

Kirk R D (1955) Am Min 40 22

Kiss Z J (1969) IEEE J Quantum Electronics QE5 12

Kiss Z J and Yocom P N (1964) J Chem Phys 41 1511

Kneubühl F K (1960) J Chem Phys 33 1074

Kohn H W and Benjamin B M (1961) Am Min 46 218

Laudise R A (1963) 'The Art and Science of Growing Crystals'
Wiley, New York p-252

Laudise R A and Ballman A A (1961) J Phys Chem 65 1396

Laudise R A, Crocket J H and Ballman A A (1961)
J Phys Chem 65 359

Laudise R A and Kolb E D (1969) Endeavour 28 114

Laudise R A and Nielson J W (1961) Sol St Phys 12 141

Lee O I (1936) Am Min 21 764

Luth W C and Tuttle O F (1963) Am Min 48 1401

MacNevin W M and Ogle P R (1954) J Am Chem Soc 76 3846

Marais M M (1968) CNET - Gp PEC 'Séminaire de Chimie de l'Etat Solide' - Paris 8 avril

Medved D B (1954) Am Min 39 615

Megla G K (1966) Appl Opt 5 945

Milkey R G (1960) Am Min 45 990

Morey G W (1957) Economic Geology 52 225

Muller R and Milberg M E (1968) J Am Ceram Soc Bul 47 401

Nakamoto K (1970) 'Infrared Spectra of Inorganic and Coordination Compounds' 2nd edn, Wiley-Interscience New York

O'Brien M C M (1955) Proc Roy Soc 231A 404

Pake G E (1962) 'Paramagnetic Resonance' W A Benjamin Inc New York p-55

Pauling L (1929) J Am Chem Soc 51 1010

Phillips W (1970) J Electrochem Soc 117 1557

Phillips W and Kiss Z J (1968) Proc IEEE 56 2072

Rabenau A and Rau H (1969) Philips Tech Rev 30 89

Radler R (1962) Tech Doc Report ASD-TDR-62-305

Radler R (1963) Tech Doc Report ASD-TDS-63-172

Segall B, Ludwig G W, Woodbury H H and Johnson P D Phys Rev 128 76

Staebler D L and Kiss Z J (1969) Appl Physics Letts 14 93

Swank R K (1964) Phys Rev 135A 266

Taylor M J (1970) Physics Bulletin 21 485

Taylor M J, Marshall D J and Evans H (1971) J Phys and Chem Solids 32 2021

Tubbs M R and Wright D K (1971) Phys Stat Solidi a7 155

Van Heerden P J (1963) Appl Opt 2 393

Weast R C (1971) Editor 'Handbook of Chemistry and Physics' 52nd edn, Chemical Rubber Co, Cleveland USA, p-D-123

Welber B (1965) J Chem Phys 42 4262

Williams E F, Hodgson W G and Brinen J S (1969) J Am Ceram Soc 52 139

White E A D (1965) 'Techniques of Inorganic Chemistry' Vol IV, Wiley, New York p-252

White E A D (1971) Brit Patent Appl no 43422/71

Yamaguchi G and Kubo Y (1968) Bull Chem Soc Jap 41 2641

APPENDIX I

SHAPE 5

```
 72/11/03 UNIVERSITY OF MINNESOTA 6000 FORTRAN COMPILER KRONOS 2.0.8 PSR9       73/04/12. 00.46.23.
       MNF(T,R=2,B=LENT)
  0001008       1*       PROGRAM CALTAP (INPUT,OUTPUT,TAPE5=INPUT,TAPE6=OUTPUT,TAPE27,
SEQ     1* NOTE - PROGRAM STATEMENT IS NON STANDARD        ****************************************
                        XTAPE25)
                      C
                      C     THIS CALCULATES ANISOTROPIC ESR SPECTRA FOLLOWING THE ANALYTIC
                      C      SOLUTIONS OF KNEUBUHL J CHEM PHYS 1960 VOL33 P1074
                      C     GAUSSIAN OR LORENTZIAN LINESHAPES CAN BE CHOSEN AND THE COMPUTED
                      C      SPECTRUM IS PLOTTED ON THE CALCOMP PLOTTER
                      C      THE EXPERIMENTAL SPECTRUM IS READ IN , NORMALISED TO THE COMPUTED
                      C   ONE , AND PLOTTED ON THE SAME AXES .  UP TO THREE SETS OF DATA CAN BE
                      C   FED IN .
                      C
  0102018       2*        COMMON    INSTAR(1000),HSTAR(1000),DNOH(1000),FH(1000),DFH(1000),I
                         1H(2000),GFH(1000),GDFH(1000),H(2000),TOTL(2000),S(1000),X(1000),Y(
                         110(),D(2,7))
  0102018       3*        INTEGER RANGE,HILIM,OLIM
  0102018       4*        REAL N,NU
                      CALL START(2)
  0102018       5*        CALL PLOT(1.0,1.0,-3)
                      C   READS NUMBER OF GRAPHS TO BE DRAWN - MAXIMUM THREE
  0102128       6*        READ(5,1000)NGRA
  0102218       7*   1000 FORMAT(I1)
                      C   STARTS LOOP FOR GRAPHS
  0102218       8*        DO 40 IG=1,NGRA
                      C   SETS HYPERFINE COUNTER TO ZERO
  0102308       9*        IHYP=0
                      C   CLEARS TOTL 1 - 2000
  0102308      10*        DO 1 I=1,2000
  0102348      11*      1 TOTL(I)=0
                      C   READS EXPERIMENTAL SPECTRUM - STARTING FIELD, FINISHING FIELD AND
                      C   NUMBER OF POINTS, THEN SIGNAL STRENGTH S IN ARBITRARY UNITS.
                      C   IDATA IS NORMALLY ZERO - IF IT IS GREATER THAN ZERO THE PROGRAM
                      C   DOES NOT LOOK FOR NEW VALUES OF S AND USES THE LAST SET OF S READ IN.
  0102528      12*        READ(5,1007)IHSTRT,IHEND,NDATA,IDATA
  0102648      13*   1007 FORMAT(4I5)
  0102648      14*        IF(IDATA.GT.0)GO TO 2
  0102658      15*        READ(5,1008)(S(I),I=1,NDATA)
  0103118      16*   1008 FORMAT(13F6.1)
                      C   CALCULATES STEPLENGTH
  0103118      17*        RR=IHEND-IHSTRT
  0103128      18*        DN=NDATA-1
  0103158      19*        DH=RR/DN
                      C   ALL INTEGRAL FIELD VALUES EXCEPT IHSTRT AND IHEND ARE IN MILLIGAUSS
  0103168      20*        IDH=1000.*DH+0.5
  0103213      21*        DH=IDH
  0103228      22*        DH=DH/1000.
                      C     THE INPUT PARAMETERS ARE READ IN, THE END OF DATA BEING INDICATED
                      C   BY GX=0 ON THE LAST CARD.   NU IS IN KMCS.
                      C   CENTRED SYMBOLS ARE DRAWN ON THE CALCULATED LINESHAPE, AND LPT
                      C   DETERMINES THE REPEAT CYCLE.  E.G. FOR LPT=4 A SYMBOL IS DRAWN ON
                      C   EVERY 4TH POINT
SEQ    22* CAUTION - RESULT - DH TO LEFT OF = APPEARED TO LEFT OF PREVIOUS =    ********************
  0103238      23*     2  READ(5,1001)GX,GY,GZ,AX,AY,AZ,NU,HILIM,LOLIM,N,GAU,LPT
  0103478      24*   1001 FORMAT(3F6.4,3F6.2,F7.3,2I3,2F3.1,I3)
                      C    WHENEVER INPUT IS COMPLETE GO TO PLOTTER
  0103478      25*        IF(GX.EQ.0.)GO TO 28
                      C   RETAINS LPT
SEQ    25* COMMENT - IS FLOATING POINT EQUALITY TO BE EXPECTED      ********************************
```

```
0103548      26*        IPT=LPT
                    C   READS HYPERFINE SPLITTINGS IN GAUSS
0103568      27*        READ(5,2000)HYPX,HYPY,HYPZ
0103628      28*   2000 FORMAT(3F8.3)
                    C   ADDS ONE TO HYPERFINE COUNTER
0103628      29*        IHYP=IHYP+1
                    C   WRITES G VALUES, LINEWIDTHS, FREQUENCY, HYPERFINE SHIFTS, AND
                    C   STEPLENGTHS
0103638      30*        WRITE(6,1002)GX,GY,GZ,AX,AY,AZ,WO,HYPX,HYPY,HYPZ,DH
0104048      31*   1002 FORMAT(1H0,17HEXPERIMENTAL DATA /4X,2HGX,8X,2HGY,8X,2HGZ,8X,2HAX,8
                     1X,2HAY,8X,2HAZ,5X,9HFREQUENCY,5X,23HHYPERFINE SPLITTINGS,8X,10HSTE
                     2PLENGTH/11F10.5)
                    C   CALCULATE FIELD CORRESPONDING TO G-VALUES
0104048      32*        AX=1./AX
0104058      33*        AY=1./AY
0104068      34*        AZ=1./AZ
0104078      35*        P=714.443*WO
0104118      36*        HX=P/GX+HYPX
0104138      37*        HY=P/GY+HYPY
0104168      38*        HZ=P/GZ+HYPZ
                    C   ALL INTEGRAL FIELD VALUES EXCEPT IHSTRT AND IHEND ARE IN MILLIGAUSS
0104218      39*        IHX=HX*1000.+0.5
0104248      40*        IHY=HY*1000.+0.5
0104278      41*        IHZ=HZ*1000.+0.5
                    C   EVALUATE LENGTH OF DNDH VECTOR *HSTAR*
0104318      42*        RANGE=(IHX-IHZ)/IDH+1
0104358      43*        SUM=0.
                    C   SET HSTAR TO FIELD VALUES HZ THROUGH HX
                    C   AND EVALUATE ARGUMENTS OF ELLIPTIC INTEGRAL
0104368      44*        DO 5  I=1,RANGE
                    C   ALL INTEGRAL FIELD VALUES EXCEPT IHSTRT AND IHEND ARE IN MILLIGAUSS
0104468      45*        IHSTAR(I)=IHZ-IDH+I*IDH
0104548      46*        HSTAR(I)=IHSTAR(I)
0104608      47*        HSTAR(I)=HSTAR(I)/1000.
                    C   DO NOT CALCULATE DNDH AT HY WHERE WE HAVE AN INFINITY
SEQ    47* CAUTION - RESULT - HSTAR TO LEFT OF = APPEARED TO LEFT OF PREVIOUS =          **********
0104648      48*        IF(IHSTAR(I).EQ.IHY)GO TO 5
                    C   DO WE TRANSFER TO HIGH FIELD EQUATION
0104728      49*        IF(IHSTAR(I).GT.IHY)GO TO 3
                    C   LOW FIELD ARGUMENT OF ELIPTIC INTEGRAL
0104778      50*        SQK=((HX*HX-HY*HY)*(HSTAR(I)*HSTAR(I)-HZ*HZ))/((HY*HY-HZ*HZ)*(HX*H
                     1X-HSTAR(I)*HSTAR(I)))
0105168      51*        CALL H174(SQK,ELIP)
                    C   LOW FIELD CALCULATION OF DNDH
0105238      52*        DNDH(I)=((N*HX*HY*HZ)/(3.1416*SQRT(HY*HY-HZ*HZ)))*(ELIP/(HSTAR(I)*
                     1HSTAR(I)*SQRT(HX*HX-HSTAR(I)*HSTAR(I))))*2.
0105548      53*        GO TO 4
                    C   HIGH FIELD ARGUMENT OF ELIPTIC INTEGRAL
0105568      54*     3  SQK=((HY*HY-HZ*HZ)*(HX*HX-HSTAR(I)*HSTAR(I)))/((HX*HX-HY*HY)*(HSTA
                     1R(I)*HSTAR(I)-HZ*HZ))
0105768      55*        CALL H174(SQK,ELIP)
                    C   HIGH FIELD CALCULATION OF DNDH
0106038      56*        DNDH(I)=((N*HX*HY*HZ)/(3.1416*SQRT(HX*HX-HY*HY)))*(ELIP/(HSTAR(I)*
                     1HSTAR(I)*SQRT(HSTAR(I)*HSTAR(I)-HZ*HZ)))*2.
                    C   ACCUMULATING DNDH
0106348      57*     4  SUM=SUM+DNDH(I)
0106448      58*     5  CONTINUE
                    C   CHECKS TO SEE IF DISTANCE IHZ - IHY IS AN INTEGRAL NUMBER OF
                    C   STEPLENGTHS  I.E. IS DNDH TO BE CALCULATED AT IHY .  IF SO, IT IS
```

```
                      C   CALCULATED BY DIFFERENCE.
     0106518      59*        ZY=IHY-IHZ
     0106528      60*        YCALC=ZY/OH
     0106548      61*        IYCALC=YCALC
     0106558      62*        YCINT=IYCALC
     0106568      63*        IF(YCINT.NE.YCALC)GO TO 14
   SEQ    63* COMMENT - IS FLOATING POINT EQUALITY TO BE EXPECTED        ********************************
     0106608      64*        INT=YCINT+1.
     0106628      65*        ONOH(INT)=N-SUM+(ONOH(1)+ONOH(RANGE))/2.
                      C   ALL INTEGRAL FIELD VALUES EXCEPT IHSIRT AND IHEND ARE IN MILLIGAUSS
     0106758      66*     14 HILIM=HILIM*1000
     0107013      67*        LOLIM=LOLIM*1000
                      C    UNLESS FIRST HYPERFINE LINE , COLLECTS PREVIOUS VALUES OF HILIM
                      C    AND LOLIM ( IN ILIM AND OLIM ) AND ADJUSTS SO THAT NEW SPECTRUM
                      C    FITS ON TO LAST ONE CORRECTLY
     0107038      68*        IF(IHYP.LQ.1)GO TO 7
     0107058      69*        LOLIM=OLIM
   SEQ    69* CAUTION - VARIABLE OR ARRAY - OLIM NOT DEFINED AT THIS POINT        **********************
     0107098      70*        HILIM=ILIM
   SEQ    70* CAUTION - VARIABLE OR ARRAY - ILIM NOT DEFINED AT THIS POINT        **********************
     0107078      71*        IZ=JHZ-IHZ
   SEQ    71* CAUTION - VARIABLE OR ARRAY - JHZ NOT DEFINED AT THIS POINT        **********************
     0107108      72*        LOLIM=LOLIM-IZ
     0107128      73*        IX=JHX-IHX
   SEQ    73* CAUTION - VARIABLE OR ARRAY - JHX NOT DEFINED AT THIS POINT        **********************
     0107148      74*        HILIM=HILIM+IX
                      C    LOW FIELD LIMIT OF SPECTRUM
     0107158      75*     7 IHLO=IHZ-LOLIM
                      C    HIGH FIELD LIMIT OF SPECTRUM
     0107208      76*        IHHI=IHX+HILIM
                      C   STORES PRESENT VALUES OF HILIM AND LOLIM
     0107228      77*        OLIM=LOLIM
     0107238      78*        ILIM=HILIM
                      C    TOTAL WIDTH OF SPECTRUM
     0107248      79*        IDELTA=(IHHI-IHLO)/IOH+1
     0107318      80*        IF(IHYP.EQ.1)GO TO 10
                      C  WRITES ERROR MESSAGE IF PRESENT SPECTRUM NOT COMPATIBLE WITH
                      C  PREVIOUS ONE
     0107338      81*        IF(IDELTA.NE.IDELH1)CALL ERROR(IDELTA,IDELH1)
   SEQ    81* CAUTION - VARIABLE OR ARRAY - IDELH1 NOT DEFINED AT THIS POINT      **********************
                      C    EVALUATING THE COEFFICIENTS OF THE LINEWIDTH QUADRATIC USING
                      CRAMERS RULE
     0107428      82*     10 VZ=1.
     0107448      83*        VY=IHY-IHZ+1000
     0107478      84*        VY=VY/1000.
   SEQ    84* CAUTION - RESULT - VY TO LEFT OF = APPEARED TO LEFT OF PREVIOUS =   **********************
     0107508      85*        VX=RANGE
     0107528      86*        IF(VY.EQ.VX)VX=VX+1.
   SEQ    86* COMMENT - IS FLOATING POINT EQUALITY TO BE EXPECTED        ********************************
     0107568      87*        DENOM=(VY*VZ*VZ-VZ*VY*VY)-(VX*VZ**2-VX*VY**2)+(VX**2*VZ-VX**2*VY)
     0107678      88*        DELX=(AX*VY*VZ**2-AX*VZ*VY**2)-(VX*AY*VZ**2-VX*AZ*VY**2)+
                            1(VX**2*AY*VZ-VX**2*AZ*VY)
     0110058      89*        DELY=(AY*VZ**2-AZ*VY**2)-(AX*VZ**2-AX*VY**2)+(VX**2*AZ-VX**2*AY)
     0110238      90*        DELZ=(VY*AZ-AY*VZ)-(VX*AZ-VX*AY)+(AX*VZ-AX*VY)
     0110308      91*        C1=DELX/DENOM
     0110328      92*        C2=DELY/DENOM
     0110338      93*        C3=DELZ/DENOM
                      C   CHOOSES GAUSSIAN OR LORENTZIAN SHAPE
     0110358      94*        IF(GAU.GT.1.)GO TO 12
```

```
                      C    CLEAR F(J)
     0110408      95*       DO 6 J=1,IDELTA
     0110473      96*     6 FH(J)=0
                      C    CONVOLUTE DNDH WITH LORENTZIAN FUNCTION
     0110658      97*       DO17 I=1,RANGE
     0110743      98*       A=C1+FLOAT(I)*C2+FLOAT(I)**2*C3
     0111003      99*       DO 9 J=1,IDELTA
     0111118     100*       IH(J)=IHLO-IOH+J*IOH
     0111178     101*       H(J)=IH(J)
     0111233     102*       H(J)=H(J)/1000.
SEQ    102* CAUTION - RESULT - H TO LEFT OF = APPEARED TO LEFT OF PREVIOUS =    **********
     0111278     103*       IF(IH(J).GT.IHHI) GO TO 17
     0111368     104*       B=H(J)-HSTAR(I)
     0111478     105*       DFH(J)=((4.*A**3)/(3.1416))*(DNDH(I)*B)/((1.+A*A+B*B)**2)*DH*(-1.)
SEQ    105* CAUTION - MULTIPLY OR DIVIDE BY 1     **********************************************
     0111718     106*     8 FH(J)=FH(J)+DFH(J)
     0112028     107*     9 CONTINUE
     0112078     108*    17 CONTINUE
                      C    ACCUMULATE HYPERFINE COMPONENTS
     0112138     109*       DO 11 I=1,IDELTA
     0112228     110*    11 TOTL(I)=TOTL(I)+FH(I)
                      C   WRITES FIELD VALUES AND INTENSITIES
     0112468     111*       WRITE(6,1005)
     0112548     112*  1005 FORMAT(1H0,62HMAGNETIC FIELD VALUES AND INTENSITIES FOR LORENTZIAN
                         1 LINESHAPE/)
     0112548     113*       WRITE(6,1004)(H(I),TOTL(I),I=1,IDELTA)
     0113058     114*  1004 FORMAT(1X,4(F9.1,F12.7))
                      C   CHOOSES GAUSSIAN OR LORENTZIAN SHAPE
     0113058     115*       IF(GAU.LT.1.)GO TO 29
     0113078     116*    12 DO 13 J=1,IDELTA
     0113178     117*    13 GFH(J)=0
     0113358     118*       DO 22 I=1,RANGE
     0113448     119*       A=C1+FLOAT(I)*C2+FLOAT(I)**2*C3
     0113508     120*       DO 23 J=1,IDELTA
     0113618     121*       IH(J)=IHLO-IOH+J*IOH
     0113678     122*       H(J)=IH(J)
     0113738     123*       H(J)=H(J)/1000.
SEQ    123* CAUTION - RESULT - H TO LEFT OF = APPEARED TO LEFT OF PREVIOUS =    **********
     0113778     124*       IF(IH(J).GT.IHHI) GO TO 22
     0114068     125*       G=H(J)-HSTAR(I)
     0114178     126*       IF(A*A+G*G.GT.80.)GO TO 24
     0114228     127*       GDFH(J)=(2.*A*A*A*DNDH(I)*G)/(1.7725*2.7183**(A*A*G*G))*(-1.)
SEQ    127* CAUTION - MULTIPLY OR DIVIDE BY 1     **********************************************
     0114448     128*       GO TO 25
     0114468     129*    24 GDFH(J)=0
     0114548     130*    25 GFH(J)=GFH(J)+GDFH(J)
     0114648     131*    23 CONTINUE
                      C    ACCUMULATE HYPERFINE COMPONENTS
     0114718     132*       DO 26 J=1,IDELTA
     0114778     133*    26 TOTL(J)=TOTL(J)+GFH(J)
     0115238     134*    22 CONTINUE
                      C   WRITES FIELD VALUES AND INTENSITIES
     0115278     135*       WRITE(6,1006)
     0115358     136*  1006 FORMAT(1H0,60HMAGNETIC FIELD VALUES AND INTENSITIES FOR GAUSSIAN L
                         1INESHAPE/)
     0115358     137*       WRITE(6,1004)(H(I),TOTL(I),I=1,IDELTA)
                      C   RETAINS PRESENT IHZ IHX AND IDELTA
     0115668     138*    29 JHZ=IHZ
     0115708     139*       JHX=IHX
```

```
0115718      140*        IOLLM1=IDELTA
                C     ARE THERE ANY MORE HYPERFINE LINES
0115728      141*        GO TO 2
                C    ADDS EXTRA EXPERIMENTAL POINTS IF NECESSARY
0115748      142*     28 IDIFF=IDELTA-NDATA
0115778      143*        IF(IDIFF)33,33,31
0116018      144*     31 NDP1=NDATA+1
0116048      145*        DO 32 I=NDP1,IDELTA
0116168      146*     32 S(I)=0.
                C    PUTS FIELD VALUES IN IH AND H
0116338      147*     33 IDP1=IDELTA+1
0116368      148*        ID2=2*IDELTA
0116378      149*        DO 34 I=IDP1,ID2
                C   ALL INTEGRAL VALUES EXCEPT IHSTRT AND IHEND ARE IN MILLIGAUSS
0116518      150*        IH(I)=(IHSTRT*1000)+((I-IDP1)*IDH)
0116618      151*        H(I)=IH(I)
0116668      152*     34 H(I)=H(I)/1000.
                C    FINDS MINIMUM AND MAXIMUM CALCULATED AND EXPERIMENTAL INTENSITIES
SEQ   152* CAUTION - RESULT - H TO LEFT OF = APPEARED TO LEFT OF PREVIOUS =    **********
0116758      153*        CMIN=0.
0116758      154*        CMAX=0.
0116758      155*        EMIN=0.
0116768      156*        EMAX=0.
0116778      157*        DO 35 I=1,IDELTA
0117068      158*        IF(TOTL(I).GT.CMAX)CMAX=TOTL(I)
0117208      159*        IF(TOTL(I).LT.CMIN)CMIN=TOTL(I)
0117368      160*        IF(S(I).GT.EMAX)EMAX=S(I)
0117428      161*     35 IF(S(I).LT.EMIN)EMIN=S(I)
                C     NORMALISES EXPERIMENTAL SPECTRUM
0117558      162*        ECNORM=(CMAX-CMIN)/(EMAX-EMIN)
0117618      163*        DO 36 I=1,IDELTA
0117708      164*        IPL=I+IDELTA
0117768      165*     36 TOTL(IPL)=S(I)*ECNORM
                C    WRITES NORMALISED SPECTRUM
0120658      166*        WRITE(6,1009)
0120138      167*   1009 FORMAT(1H0,32HNORMALISED EXPERIMENTAL SPECTRUM/)
0120138      168*        WRITE(6,1004)(H(I),TOTL(I),I=IDP1,ID2)
0120478      169*        DO 1972 I=1,ID2
0120568      170*        O(1,I)=H(I)
0120668      171*        O(2,I)=TOTL(I)
0120778      172*   1972 CONTINUE
0121028      173*        CALL PINIST (0,ID2)
0121068      174*        NPLOT=2
                C    CALCOMP ROUTINES
0121068      175*        CALL SCALE(H,10.0,ID2,1)
0121148      176*        CALL SCALE(TOTL,8.0,ID2,1)
0121218      177*        YMIN=-TOTL(ID2+1)/TOTL(ID2+2)
0121318      178*        CALL AXIS(0.0,YMIN,5HFIELD,-5,10.0,0.0,H(ID2+1),H(ID2+2))
0121528      179*        CALL AXIS(0.0,0.0,15HSIGNAL STRENGTH,15,8.0,90.0,TOTL(ID2+1),TOTL(
                1ID2+2))
0121738      180*        X(IDELTA+1)=H(ID2+1)
0122038      181*        X(IDELTA+2)=H(ID2+2)
0122138      182*        Y(IDELTA+1)=TOTL(ID2+1)
0122238      183*        Y(IDELTA+2)=TOTL(ID2+2)
0122358      184*        DO 38 I=1,NPLOT
0122458      185*        DO 37 J=1,IDELTA
0122558      186*        JJ=J+IDELTA*(I-1)
0122678      187*        X(J)=H(JJ)
0122668      188*     37 Y(J)=TOTL(JJ)
```

```
                      C   FOR FIRST GRAPH K IS NOT ZERO, AND CENTRED SYMBOLS ARE PUT ON THE
                      C   GRAPH.  THE REPEAT CYCLE IS DETERMINED BY LPT.
     0123028     .    189*        K=2-I
     0123038          190*        KK=IPT*K
     0123048          191*     38 CALL LINE(X,Y,IDELTA,1,KK,K)
     0123178          192*        GO TO (39,39,40),IG
                      C   UNLESS LAST GRAPH, MOVES PLOT ORIGIN
     0123248          193*     39 CALL PLOT(0.0,9.0,-3)
     0123318          194*     40 CONTINUE
     0123358          195*        CALL ENPLOT(12.0)
     0123408          196*        STOP
     0123428          197*        END


     0127258          198*        SUBROUTINE H174(SQK,ELIP)
                      C             THIS SUBROUTINE CALCULATES THE ELLIPTIC INTEGRAL.   HASTINGS,
                      C    NUMERICAL APPROXIMATIONS FOR DIGITAL COMPUTERS P174
                      C -
     0127258          199*        ETA=1.-SQK
     0127268          200*        ELIP=(1.3862943611+0.0967361844259*ETA+0.0359009293*ETA*ETA+0.0374
                                  12563713*ETA*ETA*ETA+0.0145119621Z*ETA*ETA*ETA*ETA)+(0.5+0.12498593
                                  2597*ETA+0.0688024857*ETA*ETA+0.0332835346*ETA*ETA*ETA+0.0044178701
                                  312*ETA*ETA*ETA*ETA)*ALOG(1.0/ETA)
     0127558          201*        RETURN
     0127578          202*        END


     0130108          203*        SUBROUTINE ERROR(IDELTA,IDELM1)
     0130108          204*        WRITE(6,2001)IDELTA,IDELM1
     0130208          205*  2001 FORMAT(1H0,55HADJUSTMENT OF HILIM AND LOLIM HAS NOT WORKED CORRECT
                               1LY./1X,24HTHIS TIME FIELD RANGE IS,I7/1X,16HLAST TIME IT WAS,I7)
     0130208          206*        RETURN
     0130218          207*        END
SEQ    207* COMMENT - 6 WORDS USED IN SETUP OF SUBPROGRAM   ************************************
```

SPINGT½

```
      PROGRAM CALESR(INPUT,OUTPUT,TAPE7=INPUT,TAPE2=OUTPUT,TAPE62)      JOB    2
C                                                                        JOB    3
C     PROGRAM TO SET UP AND SOLVE MATRIX FOR ANY SPIN.                   JOB    4
C     S/R SETUP SETS UP THE MATRIX, TRANSFORMING THE FINE STRUCTURE TSPHJOB    5
C     FOR X AND Y AS GIVEN IN POWERS AND OWEN REPT PROGR PHYS P320 1955.JOB    6
C     THE EIGENVALUES ARE FOUND BY S/P EIGEN. TRANSITIONS ARE PREDICTED JOB    7
C     WHEN THE DIFFERENCE IN ENERGY BETWEEN ANY PAIR OF EIGENVALUES      JOB    8
C     IS EQUAL TO THE MICROWAVE QUANTUM HV. AT THESE VALUES OF FIELD     JOB    9
C     THE MATRIX IS SET UP AGAIN AND THE EIGENVECTORS FOR EACH           JOB   10
C     LEVEL AND THE TRANSITION PROBABILITY ARE FOUND AND PRINTED.        JOB   11
      INTEGER PLOTT,DHPLOT                                               JOB   12
      REAL MSPIN                                                         JOB   13
      INTEGER ANGVAR                                                     JOB   14
      COMPLEX AP(36,36),LAMBDA(36),HP(36,36),HQ(36,36)                   JOB   15
      DIMENSION OFF(72)                                                  JOB   16
      DIMENSION A(72,72),QUOT(3),E(72),G(3),H(36),EEV(1,10),DEV(1,1),    JOB   17
     1EJ(2,630),SE(2,630),AMBDA(10),V(72,72),STOPEE(1,1),EL(72),         JOB   18
     2STORET(100),FIELD(33),ADIA(5184),PDIA(5184),DMRES(1,1),DTP(1,1),   JOB   19
     3ND(1)                                                              JOB   20
      DIMENSION SN(3),QUOTN(3)                                           JOB   21
      DIMENSION SY(1)                                                    JOB   22
      DIMENSION STORLU(100),STOREL(100),STORER(100)                      JOB   23
      DIMENSION STA(19)                                                  JOB   24
      DIMENSION XAXIS(10),YAXIS(10)                                      JOB   25
      DIMENSION XAXIS2(1),YAXIS2(1),PLUS(1)                              JOB   26
      DIMENSION XX(6,6),YY(6,6),ZZ(6,6),PX(6,6),QX(6,6),RX(6,6),P(6,6),  JOB   27
     1Q(6,6),R(6,6),X(6,6),Y(6,6),W(6,6)                                 JOB   28
      DIMENSION TCN(6),THETA2(10),PHI2(10),PSI2(10)                      JOB   29
      DIMENSION IAXSYS(1)                                                JOB   30
      DIMENSION THETA1(10),PHI1(10),PSI1(10)                             JOB   31
      COMMON HL,GAU,IDH,DH,IHSTRT,IHEND,NDATA,NORM,HH(1004),TOTL(1004),  JOB   32
     1S(505),XXX(505),YYY(505)                                           JOB   33
      COMMON FH(501),IHH(501),DFH(501),GFH(501),SDFH(501)                JOB   34
      DIMENSION D(2,1002)                                                JOB   35
      REAL NORM                                                          JOB   36
      COMMON/TP/XX,YY,ZZ,X,Y,W,P,Q,R,PX,QX,RX                            JOB   37
      COMMON EJ                                                          JOB   38
      COMMON/DIAGYS/MAGS,ISINXL                                          JOB   39
      COMMON/DIFAX/ NDIFAX,THETA1,PHI1,PSI1,IAXSYS                       JOB   40
      COMMON/FOPT/ CHALLA,FTERM,OFF                                      JOB   41
      COMMON DEG,L,STOTHE(349),STOPHI(349)                               JOB   42
C  LABELS FOR SPIN STATES                                                JOB   43
      DATA TEN/8H       G,8H      GN,8H       D,8H      AN,8H      AL,   JOB   44
     1 8H       D/                                                       JOB   45
      DATA XAXIS2/6HFIELDS/                                              JOB   46
      DATA YAXIS2/6HANGLES/                                              JOB   47
      DATA PLUS /1H+/                                                    JOB   48
      DATA SY(1)/1H+/                                                    JOB   49
      DATA STA            /6H  9/2 ,6H   4  ,6H  7/2 ,6H   3  ,6H  5/2 ,JOB   50
     1 6H   2  ,6H  3/2 ,6H   1  ,6H  1/2 ,6H   0  ,6H -1/2 ,6H  -1  ,6HJOB   51
     2-3/2 ,6H  -2  ,6H -5/2 ,6H  -3  ,6H -7/2 ,6H  -4  ,6H -9/2 /      JOB   52
      EQUIVALENCE (A(1,1),ADIA(1),HP(1,1)),(V(1,1),ADIA(1),HQ(1,1))      JOB   53
      EQUIVALENCE (PDIA(2592),AR(1,1))                                   JOB   54
      DEG=180./3.14159265                                                JOB   55
C LABELS FOR X,Y AND Z                                                   JOB   56
      ASX=0                                                              JOB   57
      ASY=0                                                              JOB   58
      ASZ=0                                                              JOB   59
      DO 140 I=1,3                                                       JOB   60
  140 GN(I)=0.0                                                          JOB   61
C     PUT NEAT.EQ.1 FOR SAVING OF LINES PRINTED                          JOB   62
C     PUT NEAT.EQ.0 TO STOP ALL ANGLES AND ANGLE CAPTIONS BEING PRINTED  JOB   63
      READ(7,5020) NEAT                                                  JOB   64
 5020 FORMAT(I3)                                                         JOB   65
 5001 CONTINUE                                                           JOB   66
      NOANG=0.0                                                          JOB   67
      READ(7,1005) SPIN                                                  JOB   68
 1005 FORMAT(F10.4)                                                      JOB   69
      IF(SPIN.LT.0.01) GO TO 5000                                        JOB   70
      N=2.0*SPIN+1.2                                                     JOB   71
      CALL START(2)                                                      JOB   72
      CALL PLOT(1.0,1.0,-3)                                              JOB   73
      READ(7,901)IHSTRT,IHEND,NDATA,IDATA                                JOB   74
  901 FORMAT(4I5)                                                        JOB   75
      WRITE(2,100)IHSTRT,IHEND,NDATA,IDATA                               JOB   76
  100 FORMAT(1X,7HIHSTRT=,I5,6HIHEND=,I5,6HNDATA=,I5,6HIDATA=,I5)        JOB   77
      IF(IDATA.GT.0)GO TO 903                                            JOB   78
      READ(7,902)(S(I),I=1,NDATA)                                        JOB   79
  902 FORMAT(13F6.1)                                                     JOB   80
      WRITE(2,101)(S(I),I=1,NDATA)                                       JOB   81
  101 FORMAT(1X,17HEXPERIMENTAL DATA,/1X,13F6.1)                         JOB   82
      GO TO 9002                                                         JOB   83
  903 DO 9001 JJ=1,NDATA                                                 JOB   84
 9001 S(JJ)=0.0                                                          JOB   85
 9002 CONTINUE                                                           JOB   86
C   CALCULATES STEPLENGTH                                                JOB   87
      RR=IHEND-IHSTRT                                                    JOB   88
      DN=NDATA-1                                                         JOB   89
      DH=RR/DN                                                           JOB   90
C   ALL INTEGRAL FIELD VALUES EXCEPT IHSTRT AND IHEND ARE IN MILLIGAUSS  JOB   91
      IDH=1000.*DH+0.5                                                   JOB   92
      DH=IDH                                                             JOB   93
      DH=DH/1000.                                                        JOB   94
      READ(7,904) NORM,GAU,HL,LPT                                        JOB   95
  904 FORMAT(3F5.1,I3)                                                   JOB   96
      WRITE(2,102)DH,NORM,GAU,HL,LPT                                     JOB   97
  102 FORMAT(1X,3HDH=,F10.5,5HNORM=,F3.1,4HGAU=,F3.1,3HHL=,F5.1,4HLPT=,I JOB   98
     13)                                                                 JOB   99
      HH(1)=0.                                                           JOB  100
      TOTL(1)=0.                                                         JOB  101
      DO 900 I=2,1004                                                    JOB  102
      J=I-1                                                              JOB  103
      HH(I)=HH(J)+DH                                                     JOB  104
  900 TOTL(I)=0.                                                         JOB  105
      IHSTRT=1000*IHSTRT                                                 JOB  106
      IHEND=1000*IHEND                                                   JOB  107
      READ(7,1005) NSPIN                                                 JOB  108
      NI=2*NSPIN+1.2                                                     JOB  109
      NS=N                                                               JOB  110
C  CALCULATES WHICH LABELS ARE NEEDED FOR SPIN STATES                    JOB  111
      IFII=10.0+2.0*NSPIN                                                JOB  112
      ISTI=10.0-2.0*NSPIN                                                JOB  113
      IST=10.0-2.0*SPIN                                                  JOB  114
      IFI=10.0+2.0*SPIN                                                  JOB  115
      IF(NI.EQ.1) GO TO 152                                              JOB  116
      ISAVE=ISTI                                                         JOB  117
```

```
      IST1=IST                                                          JOB  118
      IST=ISAVE                                                         JOB  119
      ISAVE=IFI                                                         JOB  120
      IFI=IFII                                                          JOB  121
      IFII=ISAVE                                                        JOB  122
  152 CONTINUE                                                          JOB  123
      READ(7,1061)OHPLOT                                                JOB  124
 1061 FORMAT(I1)                                                        JOB  125
      READ(7,5017) MAGS,ISINXL                                          JOB  126
C  READS IN MICROWAVE FREQUENCY, G VALUES, D VALUE FOR Z DIRECTION,      JOB  127
C   AND INCREMENTAL STEP LENGTHS FOR CHANGING LAMBDA.                    JOB  128
C   NLAM IS THE NUMBER OF VALUES OF LAMBDA REQUIRED, STARTING FROM ZERO. JOB  129
C     DEV(1,1) IS THE D VALUE. AMSTEP IS THE STEPLENGTH FOR VARYING      JOB  130
C     LAMBDA. NLAM IS THE NUMBER OF VALUES OF LAMBDA TO BE COMPUTED IN   JOB  131
C     ADDITION TO AMSTT, WHICH IS THE STARTING VALUE OF LAMBDA.          JOB  132
C     THESE ARE USED IF (OHPLOT.EQ.0).                                   JOB  133
C     WHEN (OHPLOT.NE.0) THEN DEV(1,1) IS THE STARTING VALUE OF D, ADA   JOB  134
C     IS THE LAMBDA VALUE, NDEV IS THE NUMBER OF VALUES OF D TO BE       JOB  135
C     COMPUTED IN ADDITION TO DEV(1,1). DEVST IS THE STEPLENGTH FOR      JOB  136
C     VARYING D                                                          JOB  137
      IF(OHPLOT.NE.0) GO TO 23                                          JOB  138
      READ(7,1000)FRE,(G(I),I=1,3),DEV(1,1),AMSTEP,NLAM,AMSTT          JOB  139
 1000 FORMAT(F7.1,3F7.4,2F6.4,I3,F6.4)                                  PHC    1
      GO TO 24                                                          JOB  141
   23 READ(7,1061)FRE,(G(I),I=1,3),DEV(1,1),ADA,NDEV,DEVST             JOB  142
 1061 FORMAT(F7.1,3F7.4,F6.2,F6.4,I4,F6.4)                              JOB  143
      DEV(1,1)=DEV(1,1)-DEVST                                           JOB  144
C     NCH, STEPL AND HINIT ARE THE NO. OF FIELD VALUES, STEPLENGTH AND   JOB  145
C     INITIAL FIELD FOR THE RESONANCE FIELD SEARCH. THE RANGE HERE       JOB  146
C     SHOULD BE WIDER THAN IHCHO - IHSTPT                                JOB  147
   24 READ(7,3000) NCH,STEPL,HINIT                                      JOB  148
 3000 FORMAT(I3,2F10.4)                                                 JOB  149
      READ(7,3001) SMALLA,FTERM,DTERM,QR                                JOB  150
 3001 FORMAT(4F10.4)                                                    JOB  151
      READ(7,5010) AX,AY,AZ                                             JOB  152
 5010 FORMAT(3F10.5)                                                    JOB  153
      READ(7,1005) SISPIN                                               JOB  154
 1005 FORMAT(F3.1)                                                      JOB  155
      ISI=2*SISPIN+1.2                                                  JOB  156
      IF(ISI.EQ.1) GO TO 8000                                           JOB  157
      READ(7,5010) ASX,ASY,ASZ                                          JOB  158
 8000 CONTINUE                                                          JOB  159
      N=NCH*NI*ISI                                                      JOB  160
      IF(NI.EQ.1) GO TO 170                                             JOB  161
      READ(7,3003)(GN(I),I=1,3)                                         JOB  162
 3003 FORMAT(4F10.5)                                                    JOB  163
  170 CONTINUE                                                          JOB  164
      READ(7,1027) PLOTT                                                JOB  165
 1027 FORMAT(I1)                                                        JOB  166
      READ(7,3021) ANGVAR                                               JOB  167
 3021 FORMAT(I1)                                                        JOB  168
C     FOR THE ICOSAHEDRAL APPROXIMATION, L MUST BE AN INTEGER SUCH AS    JOB  169
C     1(9 ANGLES), 2(27 ANGLES), 3(93 ANGLES), 4(345 ANGLES).....       JOB  170
C     L MAY BE PUT EQUAL TO 0  FOR INCREMENTAL CHANGES OF ANGLE.         JOB  171
 4720 READ(7,1027) L                                                    JOB  172
      IF(L.EQ.0) GO TO 4722                                             JOB  173
      IF(L.EQ.1) NCYC = 9                                               JOB  174
      IF(L.EQ.2) NCYC = 27                                              JOB  175
      IF(L.EQ.3) NCYC = 93                                              JOB  176
      IF(L.EQ.4) NCYC = 345                                             JOB  177
      GO TO 4723                                                        JOB  178
 4722 READ(7,3021) NCYC                                                 JOB  179
 4723 READ(7,3000) NDIFAX                                               JOB  180
      NDIFAX=NDIFAX-1                                                   JOB  181
      DO 3333 I=1,19                                                    JOB  182
      IAXSYS(I)=0                                                       JOB  183
 3333 CONTINUE                                                          JOB  184
      IF(NDIFAX.EQ.0) GO TO 4719                                        JOB  185
      DO 4718 I=1,NDIFAX                                                JOB  186
 4718 READ(7,3001) THETA1(I),PHI1(I),PSI1(I)                            JOB  187
      DO 5018 I=1,NDIFAX                                                JOB  188
      THETA2(I)=THETA1(I)                                               JOB  189
      PHI2(I)=PHI1(I)                                                   JOB  190
      PSI2(I)=PSI1(I)                                                   JOB  191
      THETA1(I)=3.14159*THETA1(I)/180.0                                 JOB  192
      PHI1(I)=3.14159*PHI1(I)/180.0                                     JOB  193
 5018 PSI1(I)=3.14159*PSI1(I)/180.0                                     JOB  194
      READ(7,5017) IAXSYS                                               JOB  195
 5017 FORMAT(10I2)                                                      JOB  196
 4719 CONTINUE                                                          JOB  197
      READ(7,3002) TOL                                                  JOB  198
 3002 FORMAT(F10.4)                                                     JOB  199
      READ(7,1027) NOPRW                                                JOB  200
      ILST=10.0-2.0*SISPIN                                              JOB  201
C  CALCULATES SIZE OF QUANTUM                                           JOB  202
      HV=FRE*3.3363E-05                                                 JOB  203
      BETA=4.66975E-05                                                  JOB  204
      BETAN=2.54278E-08                                                 JOB  205
C  CYCLE FOR VALUES OF LAMBDA                                           JOB  206
      NLAM=NLAM+1                                                       JOB  207
      IF(OHPLOT.NE.0) GO TO 25                                          JOB  208
      NX1=NLAM                                                          JOB  209
      GO TO 309                                                         JOB  210
   25 NX1=NDEV+1                                                        JOB  211
  309 DO 71 IA=1,NX1                                                    JOB  212
      IF(OHPLOT.NE.0) GO TO 310                                         JOB  213
C  CALCULATES LAMBDA AND DEV                                            JOB  214
      AMBDA(IA)=(FLOAT(IA-1))*AMSTEP+AMSTT                              JOB  215
      EEV(1,1)=AMBDA(IA)*DEV(1,1)                                       JOB  216
      GO TO 26                                                          JOB  217
  310 CONTINUE                                                          JOB  218
      NX=0                                                              JOB  219
      DEV(1,1)=DEV(1,1)+DEVST                                           JOB  220
      EEV(1,IA)=ADA*DEV(1,1)                                            JOB  221
C  TRANSFORMS D AND E FOR X AN DY                                       JOB  222
   26 CONTINUE                                                          JOB  223
      IF(OHPLOT.NE.0) GO TO 27                                          JOB  224
      DEEV=DEV(1,1)*AMBDA(IA)                                           JOB  225
      WRITE(2,181)SPIN,NSPIN,SISPIN,HV                                  JOB  226
  181 FORMAT(1H1,10X,16HELECTRON SPIN = ,F3.1,5X,15HNUCLEAR SPIN = ,    JOB  227
     1F3.1,5X,22HLIGAND NUCLEAR SPIN = ,F3.1,5X,9HENERGY = ,F7.3,2X,    JOB  228
     2/4HOH=1//)                                                        JOB  229
      WRITE(2,182)(G(I),I=1,3),(GN(I),I=1,3),BETAN                      JOB  230
  182 FORMAT(50X,3HG VALUES/26X,8HELECTRON,52X,7HNUCLEAR/10X,5HGZ = ,   JOB  231
     1F6.4,2X,5HGY = ,F6.4,2X,5HGX = ,F6.4,22X,5HGZ = ,F6.4,2X,5HGY = , JOB  232
     2F6.4,2X,5HGX = ,F6.4,2X/60X,7HBETA = ,F10.8,2X,4HOH=1//)          JOB  233
      WRITE(2,184) DEV(1,1),DEEV,AMBDA(IA),SMALLA,FTERM                 JOB  234
```

```
  184 FORMAT(48X,23HZERO FIELD TERMS (CM-1)/7X,4HD = ,F10.6,7X,4HE = ,   JOB  234
     1F10.6,7X,3HLAMBDA = ,F10.6,7X,4HA = ,F10.6,7X,4HF = ,F10.6//)      JOB  235
       WRITE(2,193) AZ,AY,AX,ASZ,ASY,ASX                                 JOB  236
  193 FORMAT(49X,22HHYP_RFINE TERMS (CM-1)/24X,11HOWN NUCLEUS,47X,       JOB  237
     11HPLIGAND NUCLEUS/11X,5HAZ = ,F7.5,2X,5HAY = ,F7.5,2X,5HAX = ,     JOB  238
     2F7.5,20X,5HAZ = ,F7.5,2X,5HAY = ,F7.5,2X,5HAX = ,F7.5,2X//)        JOB  239
       WRITE(2,195) QTERM,QP                                             JOB  240
  195 FORMAT(49X,22HQUADRUPOLE TERM (CM-1)/21X,10HAXIAL Q = ,F10.6,39X,  JOB  241
     1124HPHOTON IC Q = ,F10.6//)                                        JOB  242
       WRITE(2,196)                                                      JOB  243
  196 FORMAT(34X,57HORIENTATION OF TENSORS (TO ZERO FIELD TENSOR) DEGREE JOB  244
     1S//22X,6HTENSOR,19X,5HTHETA,20X,3HPHI,21X,3HPSI)                   JOB  245
       DO 197 I=1,6                                                      JOB  246
       IF(I.EQ.3) GO TO 197                                              JOB  247
       WRITE(2,187) TEN(I)                                               JOB  248
  187 FORMAT(13X,A8)                                                     JOB  249
  188 WRITE(2,194)                                                       JOB  250
  194 FORMAT(1H+,45X,6H  0.00,18X,6H  0.00,18X,6H  0.00)                 JOB  251
  197 CONTINUE                                                           JOB  252
  197 CONTINUE                                                           JOB  253
       WRITE(2,199)                                                      JOB  254
  199 FORMAT(///)                                                        JOB  255
       WRITE(2,4721)PLOTT,ANGVAR,L,NCYC,NDIFAX,NOPPW,TOL                 JOB  256
 4721 FORMAT(1X,69H      PLOTT     ANGVAR      L       NCYC     NDIFAX   JOB  257
     1   NOPPW      TOL,//6I11,F10.1,//)                                JOB  258
C  X,Y AND Z CYCLE                                                       JOB  259
   27 CONTINUE                                                           JOB  260
       CALL THEPHI                                                       JOB  261
   28 DO 21 INT=1,NCYC                                                   JOB  262
       DTHETA = STOTH(INT)                                               JOB  263
       DPHI = STOPHI(INT)                                                JOB  264
       DPSI = 0.0                                                        JOB  265
       THETA=DTHETA*3.14159/180.0                                        JOB  266
       PHI=DPHI*3.14159/180.0                                            JOB  267
       PSI=DPSI*3.14159/180.0                                            JOB  268
       NI(=1                                                             JOB  269
 1062 STHETA=180.0*THETA/3.14159                                         JOB  270
       SPHI=180.0*PHI/3.14159                                            JOB  271
       SPSI=180.0*PSI/3.14159                                            JOB  272
       IF(NI.EQ.0) GO TO 11                                              JOB  273
       IF(NI.GT.1.OR.ISI.GT.1) GO TO 1090                                JOB  274
       WRITE(2,1092) STHETA,SPHI,SPSI,(STA(I),I=IST,IFI,2)               JOB  275
 1092 FORMAT(1X//1X,26HFIELD AT ANGLE OF THETA = ,F6.2,5X,10HAND PHI = ,JOB  276
     1F6.2,5X,10HAND PSI = ,                                             JOB  277
     1F6.2//1X,10HTRANSITION,10X,5HFIELD,10X,10HTRANSITION,31X,14HWAVE FJOB  278
     1UNCTIONS/1X,7HBETWEEN,13X,5HVALUE,10X,11HPROBABILITY,22X,          JOB  279
     2A6,2X,A6,2X,A6,2X,A6,2X,A6,2X,A6)                                  JOB  280
       GO TO 11                                                          JOB  281
 1090 WRITE(2,1092) STHETA,SPHI,SPSI                                     JOB  282
 1092 FORMAT(1X//1X,26HFIELD AT ANGLE OF THETA = ,F10.5,5X,10HAND PHI = JOB  283
     1,F10.5,5X,10HAND PSI = ,                                           JOB  284
     1F10.5//1X,10HTRANSITION,10X,5HFIELD,10X,10HTRANSITION/1X,7HBETWEENJOB  285
     2,13X,5HVALUE,10X,11HPROBABILITY)                                   JOB  286
   11 CONTINUE                                                           JOB  287
C  FIELD CYCLE                                                          JOB  288
       DO 6 IH=1,NOH                                                     JOB  289
       IF(IH.EQ.1) GO TO 150                                             JOB  290
       DO 151 NT=1,NTRAN                                                 JOB  291
          EJ(2,NT)=EJ(1,NT)                                              JOB  292
  151  SE(2,NT)=SE(1,NT)                                                 JOB  293
  150  CONTINUE                                                          JOB  294
C  CALCULATES FIELD VALUES                                               JOB  295
          H(IH)=HINIT+STEPL*(IH-1)                                       JOB  296
C  CALCULATES G2M TERMS                                                  JOB  297
          QUOTN(1)=BETAN*H(IH)*COS(THETA)                                JOB  298
          QUOTN(2)=BETAN*H(IH)*SIN(THETA)*SIN(PHI)                       JOB  299
          QUOTN(3)=BETAN*H(IH)*SIN(THETA)*COS(PHI)                       JOB  300
          QUOT(1)=BETA*H(IH)*COS(THETA)                                  JOB  301
          QUOT(2)=BETA*H(IH)*SIN(THETA)*SIN(PHI)                         JOB  302
          QUOT(3)=BETA*H(IH)*SIN(THETA)*COS(PHI)                         JOB  303
          CALL TENSYS(A,G,GN,CEV,DEV,NS,NI,ISI,AX,AY,AZ,ASX,ASY,ASZ,QTERM,JOB  304
         1QR,QUOT,QUOTN)                                                 JOB  305
          N=2*N                                                          JOB  306
          L=0                                                            JOB  307
          DO 57 IP=1,N                                                   JOB  308
          DO 57 IQ=1,IP                                                  JOB  309
          L=L+1                                                          JOB  310
   57  ADIA(L)=A(IP,IQ)                                                  JOB  311
          CALL EIGEN(ADIA,RDIA,N,1)                                      JOB  312
          DO 56 IP=1,N                                                   JOB  313
          L=IP+IP*(IP-1)/2                                               JOB  314
   56  EL(IP)=ADIA(L)                                                    JOB  315
          IYZ=1                                                          JOB  316
          DO 65 IP=2,N,2                                                 JOB  317
          EL(IYZ)=EL(IP)                                                 JOB  318
   65  IYZ=IYZ+1                                                         JOB  319
          N=1.5*N+0.1                                                    JOB  320
          IF(PLOTT.EQ.0)GO TO 60                                         JOB  321
          FIELD(IH)=H                                                    JOB  322
          DO 20 NL=1,N                                                   JOB  323
   20  STORE(IH,NL)=EL(NL)                                               JOB  324
   60  NTRAN=0                                                           JOB  325
          NMIN=N-1                                                       JOB  326
          DO 8 KMIN=1,NMIN                                               JOB  327
    8  NTRAN=NTRAN+KMIN                                                  JOB  328
          DO 6 NT=1,NTRAN                                                JOB  329
C  FINDS NUMBERS OF LEVELS INVOLVED                                      JOB  330
          CALL LEVELS(NT,IU,IL,N)                                        JOB  331
C  CALCULATES DIFFERENCE EJ                                              JOB  332
          EJ(1,NT)=HV-EL(IU)+EL(IL)                                      JOB  333
C  FINDS SIGN OF EJ                                                      JOB  334
          SE(1,NT)=SIGN(1.,EJ(1,NT))                                     JOB  335
C  AVOIDS TEST WITH PREVIOUS RESULT IF IH EQUALS ONE                     JOB  336
          IF(IH.EQ.1) GO TO 6                                            JOB  337
C  COMPARES SIGN WITH PREVIOUS RESULT                                    JOB  338
          IF(SE(1,NT).EQ.SE(2,NT)) GO TO 4                               JOB  339
C  ADDS ONE TO TRANSITION COUNT                                          JOB  340
C  CALCULATES RESONANT FIELD                                             JOB  341
          HRES=H(IH)-ABS(STEPL*EJ(1,NT))/ABS(EJ(2,NT)-EJ(1,NT))         JOB  342
C  ADJUSTS QUOT                                                          JOB  343
          QUOTN(1)=BETAN*H(IH)*COS(THETA)                                JOB  344
          QUOTN(2)=BETAN*H(IH)*SIN(THETA)*SIN(PHI)                       JOB  345
          QUOTN(3)=BETAN*H(IH)*SIN(THETA)*COS(PHI)                       JOB  346
          QUOT(1)=BETA*H(IH)*COS(THETA)                                  JOB  347
          QUOT(2)=BETA*H(IH)*SIN(THETA)*SIN(PHI)                         JOB  348
          QUOT(3)=BETA*H(IH)*SIN(THETA)*COS(PHI)                         JOB  349
```

```
      IYJ=1                                                              JOB  350
      EOUM2=EJ(1,NT)                                                     JOB  351
      DO 31 IZX=1,3                                                      JOB  352
      QUOTN(IZX)=QUOTN(IZX)*(HRES/H(IH))                                 JOB  353
   31 QUOT(IZX)=QUOT(IZX)*(HRES/H(IH))                                   JOB  354
      SETS UP MATRIX FOR HRES AND FIELD EIGENVALUES                      JOB  355
  517 CONTINUE                                                           JOB  356
      CALL TENSYS(A,G,GN,EEV,DEV,NS,NI,ISI,AX,AY,AZ,ASX,ASY,ASZ,QTERM,   JOB  357
     1103,QUOT,QUOTN)                                                    JOB  358
      N=2*N                                                              JOB  359
      L=1                                                                JOB  360
      DO 3041 IP=1,N                                                     JOB  361
      DO 3041 IQ=1,IP                                                    JOB  362
      L=L+1                                                              JOB  363
  041 ADIA(L)=A(IP,IQ)                                                   JOB  364
      CALL EIGEN(ADIA,ROIA,N,1)                                          JOB  365
      IYZ=1                                                              JOB  366
      DO 3040 IP=2,N,2                                                   JOB  367
      L=IP+IP*(IP-1)/2                                                   JOB  368
      E(IYZ)=ADIA(L)                                                     JOB  369
 1040 IYZ=IYZ+1                                                          JOB  370
      N=0.5*N+0.1                                                        JOB  371
      EDUMMY=HV-E(IU)+E(IL)                                              JOB  372
      IF(ABS(EOUM2-EDUMMY).LT.0.0001) GO TO 516                          JOB  373
      HDUMMY=H(IH)-ABS((H(IH)-HRES)*EOUM2)/ABS(EOUM2-EDUMMY)             JOB  374
      IF(ABS(HDUMMY-HRES).LT.TOL) GO TO 516                              JOB  375
      IF(ABS(HDUMMY-HRES).GT.5.0*TOL.AND.IYJ.EQ.10) HDUMMY=-HDUMMY       JOB  376
      IF(IYJ.GT.11) GO TO 516                                            JOB  377
      EJ(1,NT)=EDUMMY                                                    JOB  378
      DO 3043 IZX=1,3                                                    JOB  379
      QUOTN(IZX)=QUOTN(IZX)*(HDUMMY/HRES)                                JOB  380
 3043 QUOT(IZX)=QUOT(IZX)*(HDUMMY/HRES)                                  JOB  381
      HRES=HDUMMY                                                        JOB  382
      IYJ=IYJ+1                                                          JOB  383
      GO TO 517                                                          JOB  384
  516 IF(IYJ.EQ.1) GO TO 519                                             JOB  385
      HRES=HDUMMY                                                        JOB  386
  519 EJ(1,NT)=EOUM2                                                     JOB  387
      IF(MAGS.EQ.1) GO TO 1967                                           JOB  388
      QUOTN(1)=BETAN*HRES*COS(THETA)                                     JOB  389
      QUOTN(2)=BETAN*HRES*SIN(THETA)*SIN(PHI)                            JOB  390
      QUOTN(3)=BETAN*HRES*SIN(THETA)*COS(PHI)                            JOB  391
      QUOT(1)=BETA*HRES*COS(THETA)                                       JOB  392
      QUOT(2)=BETA*HRES*SIN(THETA)*SIN(PHI)                              JOB  393
      QUOT(3)=BETA*HRES*SIN(THETA)*COS(PHI)                              JOB  394
      CALL TENSYS(A,G,GN,EEV,DEV,NS,NI,ISI,AX,AY,AZ,ASX,ASY,ASZ,QTERM,   JOB  395
     1103,QUOT,QUOTN)                                                    JOB  396
      GO TO 1968                                                         JOB  397
 1967 CONTINUE                                                           JOB  398
      CALL MAGSYS(A,G,GN,EEV,DEV,NS,NI,ISI,AX,AY,AZ,ASX,ASY,ASZ,QTERM,   JOB  399
     1104,THETA,PHI,PSI,HRES)                                            JOB  400
 1968 CONTINUE                                                           JOB  401
      N=N+N                                                              JOB  402
      L=0                                                                JOB  403
      DO 58 IP=1,N                                                       JOB  404
      DO 58 IQ=1,IP                                                      JOB  405
      L=L+1                                                              JOB  406
   58 ADIA(L)=A(IP,IQ)                                                   JOB  407
      CALL EIGEN(ADIA,ROIA,N,0)                                          JOB  408
      L=0                                                                JOB  409
      DO 59 IP=1,N                                                       JOB  410
      DO 59 IQ=1,N                                                       JOB  411
      L=L+1                                                              JOB  412
   59 V(IP,IQ)=ROIA(L)                                                   JOB  413
      N=0.5*N+0.1                                                        JOB  414
      IU1=2*IU-0.9                                                       JOB  415
      IL1=2*IL-0.9                                                       JOB  416
      CALL TPROJ(V,NS,NI,NT,T,SPIN,THETA,PHI,TA,ISI)                     JOB  417
      CALL SIMP(NS,THETA,PHI,PSI,T,TA)                                   JOB  418
      TP=T                                                               JOB  419
      IF(PLOTT.EQ.0)GO TO 61                                             JOB  420
      IF(TP.LT.0.01) GO TO 61                                            JOB  421
      STOREU(NIX)=E(IU)                                                  JOB  422
      STOREL(NIX)=E(IL)                                                  JOB  423
      STORER(NIX)=HRES                                                   JOB  424
      NIX=NIX+1                                                          JOB  425
   61 CONTINUE                                                           JOB  426
      IF(ANGVAR.EQ.0) GO TO 4090                                         JOB  427
      IF(TP.LT.0.1) GO TO 4090                                           JOB  428
      NOANG=NOANG+1                                                      JOB  429
      WRITE(5) NT,NOANG,INT,HRES                                         JOB  430
 4090 CONTINUE                                                           JOB  431
      NX=NX+1                                                            JOB  432
            IF(OHPLOT.EQ.0) GO TO 188                                    JOB  433
      OHRES(IA,NX)=HRES                                                  JOB  434
      OTP(IA,NX)=TP                                                      JOB  435
      NOH(IA)=NX                                                         JOB  436
  188 CONTINUE                                                           JOB  437
      IF(NI.GT.1) GO TO 4000                                             JOB  438
      IF(ISI.GT.1) GO TO 4000                                            JOB  439
      IF(TP.LT.0.005) GO TO 2225                                         JOB  440
      IF(NEAT.EQ.0) GO TO 2226                                           JOB  441
      WRITE(2,1004) IU,IL,HRES,TP,(V(IU1,IK),IK=1,N)                     JOB  442
 1004 FORMAT(1X,I2,5H AND ,I2,10X,F8.1,10X,F6.2,10X,11HUPPER LEVEL,3X,18JOB  443
     1(F7.4,1X))                                                         JOB  444
 2226 CALL GAULOR(HRES,TP,STHETA,SPHI)                                   JOB  445
 2225 CONTINUE                                                           JOB  446
      IJ=N+1                                                             JOB  447
      IJ1=2*N                                                            JOB  448
      IF(TP.LT.0.005) GO TO 7                                            JOB  449
      IF(NEAT.EQ.0.OR.NEAT.LQ.1) GO TO 7                                 JOB  450
      WRITE(2,1006)(V(IU1,IK),IK=IJ,IJ1)                                 JOB  451
 1006 FORMAT(54X,11H       IMAG,3X,18(F7.4,1X))                          JOB  452
      WRITE(2,1007)(V(IL1,IK),IK=1,N)                                    JOB  453
 1007 FORMAT(54X,11HLOWER LEVEL,3X,18(F7.4,1X))                          JOB  454
      WRITE(2,1008)(V(IL1,IK),IK=IJ,IJ1)                                 JOB  455
 1008 FORMAT(54X,11H       IMAG,3X,18(F7.4,1X))                          JOB  456
    7 CONTINUE                                                           JOB  457
      GO TO 4                                                            JOB  458
 4000 N8=NI                                                              JOB  459
      IF(NOPRW.GT.0) GO TO 4020                                          JOB  460
      DO 4002 KJ=1,ISI                                                   JOB  461
      ILS=ILST+2*(KJ-1)                                                  JOB  462
      WRITE(2,160)STA(ILS)                                               JOB  463
      WRITE(2,1091) STA(ISTI)                                            JOB  464
 1091 FORMAT(9X,A6)                                                      JOB  465
```

```
      WRITE(2,1093)(STA(IW),IW=IST,IFI,2)                                JOB  466
 1093 FORMAT(69X,A6,2X,A6,2X,A6,2X,A6,2X,A6,2X,A6)                       JOB  467
      JY=NS*NI*(KJ-1)+1                                                  JOB  468
      JY=JX-1+NI                                                         JOB  469
      IF(KJ.NE.1) GO TO 162                                              JOB  470
      WRITE(2,1004) IU,IL,HRES,TP,(V(IU1,JZ),JZ=1,NI)                    JOB  471
      GO TO 161                                                          JOB  472
  162 WRITE(2,4004)(V(IU1,JZ),JZ=JX,JY)                                  JOB  473
  161 CONTINUE                                                           JOB  474
      DO 4002 JK=2,NS                                                    JOB  475
      JX=(JK-1)*NI+1                                                     JOB  476
      JY=JK*NI                                                           JOB  477
      IWI=ISTI+2*JK-2                                                    JOB  478
      WRITE(2,160)STA(ILS)                                               JOB  479
  160 FORMAT(65X,2HLI,2X,A6)                                             JOB  480
      JY=JY+NS*NI*(KJ-1)                                                 JOB  481
      JX=JX+NS*NI*(KJ-1)                                                 JOB  482
      WRITE(2,1091) STA(IWI)                                             JOB  483
      WRITE(2,1093)(STA(IW),IW=IST,IFI,2)                                JOB  484
      WRITE(2,4004)(V(IU1,JZ),JZ=JX,JY)                                  JOB  485
 4004 FORMAT(69X,18(F7.4,1X))                                            JOB  486
 4002 CONTINUE                                                           JOB  487
      DO 4005 KJ=1,ISI                                                   JOB  488
      JX=NS*NI+1                                                         JOB  489
      JY=NI*(NS+1)                                                       JOB  490
      WRITE(2,160)STA(ILS)                                               JOB  491
      WRITE(2,1091) STA(ISTI)                                            JOB  492
      WRITE(2,1093)(STA(IW),IW=IST,IFI,2)                                JOB  493
      JX=JX+NS*NI*(KJ-1)                                                 JOB  494
      JY=JY+NS*NI*(KJ-1)                                                 JOB  495
      IF(KJ.NE.1) GO TO 163                                              JOB  496
      WRITE(2,4003)(V(IU1,JZ),JZ=JX,JY)                                  JOB  497
      GO TO 164                                                          JOB  498
  163 WRITE(2,4004)(V(IU1,JZ),JZ=JX,JY)                                  JOB  499
  164 CONTINUE                                                           JOB  500
 4003 FORMAT(61X,4HIMPG,3X,18(F7.4,1X))                                  JOB  501
      NS2=2*NS                                                           JOB  502
      NS1=NS+2                                                           JOB  503
      JIZ=1                                                              JOB  504
      DO 4005 JK=NS1,NS2                                                 JOB  505
      JX=(JK-1)*NI+1                                                     JOB  506
      JY=JK*NI                                                           JOB  507
      IWI=ISTI+2*JIZ                                                     JOB  508
      WRITE(2,160)STA(ILS)                                               JOB  509
      WRITE(2,1091) STA(IWI)                                             JOB  510
      WRITE(2,1093)(STA(IW),IW=IST,IFI,2)                                JOB  511
      JIZ=JIZ+1                                                          JOB  512
      JX=JX+NS*NI*(KJ-1)                                                 JOB  513
      JY=JY+NS*NI*(KJ-1)                                                 JOB  514
 4005 WRITE(2,4004)(V(IU1,JZ),JZ=JX,JY)                                  JOB  515
      WRITE(2,4009)                                                      JOB  516
 4009 FORMAT(1H )                                                        JOB  517
      DO 4007 KJ=1,ISI                                                   JOB  518
      JX=1                                                               JOB  519
      JY=NI                                                              JOB  520
      JX=JX+NS*NI*(KJ-1)                                                 JOB  521
      JY=JY+NS*NI*(KJ-1)                                                 JOB  522
      WRITE(2,160)STA(ILS)                                               JOB  523
      WRITE(2,1091) STA(ISTI)                                            JOB  524
      WRITE(2,1093)(STA(IW),IW=IST,IFI,2)                                JOB  525
      IF(KJ.NE.1) GO TO 165                                              JOB  526
      WRITE(2,4006)(V(IL1,JZ),JZ=JX,JY)                                  JOB  527
      GO TO 166                                                          JOB  528
  165 WRITE(2,4004)(V(IL1,JZ),JZ=JX,JY)                                  JOB  529
  166 CONTINUE                                                           JOB  530
 4006 FORMAT(54X,11HLOWER LEVEL,3X,18(F7.4,1X))                          JOB  531
      DO 4007 JK=2,NS                                                    JOB  532
      JX=(JK-1)*NI+1                                                     JOB  533
      JY=JK*NI                                                           JOB  534
      JX=JX+NS*NI*(KJ-1)                                                 JOB  535
      JY=JY+NS*NI*(KJ-1)                                                 JOB  536
      IWI=ISTI+2*JK-2                                                    JOB  537
      WRITE(2,160)STA(ILS)                                               JOB  538
      WRITE(2,1091) STA(IWI)                                             JOB  539
      WRITE(2,1093)(STA(IW),IW=IST,IFI,2)                                JOB  540
 4007 WRITE(2,4004)(V(IL1,JZ),JZ=JX,JY)                                  JOB  541
      DO 4008 KJ=1,ISI                                                   JOB  542
      JX=NS*NI+1                                                         JOB  543
      JY=NI*(NS+1)                                                       JOB  544
      JX=JX+NS*NI*(KJ-1)                                                 JOB  545
      JY=JY+NS*NI*(KJ-1)                                                 JOB  546
      WRITE(2,160)STA(ILS)                                               JOB  547
      WRITE(2,1091) STA(ISTI)                                            JOB  548
      WRITE(2,1093)(STA(IW),IW=IST,IFI,2)                                JOB  549
      IF(KJ.NE.1) GO TO 167                                              JOB  550
      WRITE(2,4003)(V(IL1,JZ),JZ=JX,JY)                                  JOB  551
      GO TO 168                                                          JOB  552
  167 WRITE(2,4004)(V(IL1,JZ),JZ=JX,JY)                                  JOB  553
  168 CONTINUE                                                           JOB  554
      JIZ=1                                                              JOB  555
      DO 4008 JK=NS1,NS2                                                 JOB  556
      JX=(JK-1)*NI+1                                                     JOB  557
      JY=JK*NI                                                           JOB  558
      JX=JX+NS*NI*(KJ-1)                                                 JOB  559
      JY=JY+NS*NI*(KJ-1)                                                 JOB  560
      IWI=ISTI+2*JIZ                                                     JOB  561
      WRITE(2,160)STA(ILS)                                               JOB  562
      WRITE(2,1091) STA(IWI)                                             JOB  563
      WRITE(2,1093)(STA(IW),IW=IST,IFI,2)                                JOB  564
      JIZ=JIZ+1                                                          JOB  565
 4008 WRITE(2,4004)(V(IL1,JZ),JZ=JX,JY)                                  JOB  566
      WRITE(2,4009)                                                      JOB  567
      WRITE(2,4009)                                                      JOB  568
 4001 CONTINUE                                                           JOB  569
      GO TO 4                                                            JOB  570
 4020 CONTINUE                                                           JOB  571
      WRITE(2,4024) IU,IL,HRES,TP                                        JOB  572
 4024 FORMAT(1X,I2,5H AND ,I2,10X,F8.1,10X,F6.2)                         JOB  573
C  IF LAST FIELD VALUE PRINTS DETAILS OF TRANSITIONS                     JOB  574
    4 IF(IH.LT.NGH) GO TO 6                                             JOB  575
    6 CONTINUE                                                          JOB  576
      IF(PLOTT.EQ.0)GO TO 21                                            JOB  577
   21 CONTINUE                                                          JOB  578
      IF(ANGVAR.EQ.0) GO TO 2046                                        JOB  579
 2046 CONTINUE                                                          JOB  580
      IF(OHPLOT.EQ.0) GO TO 32                                          JOB  581
```

```
   32 CONTINUE                                                          J08  582
      CMIN=0.                                                           J08  583
      CMAX=0.                                                           J08  584
      EMIN=0.                                                           J08  585
      EMAX=0.                                                           J08  586
      IF(IDATA.GT.0) EMIN=-1.0                                          J08  587
      IF(IDATA.GT.0) CMAX=1.0                                           J08  588
      DO 932 I=1,NDATA                                                  J08  589
      IF(TOTL(I).GT.CMAX)CMAX=TOTL(I)                                   J08  590
      IF(TOTL(I).LT.CMIN)CMIN=TOTL(I)                                   J08  591
      IF(IDATA.GT.0) GO TO 932                                          J08  592
      IF(S(I).GT.EMAX)EMAX=S(I)                                         J08  593
      IF(S(I).LT.EMIN)EMIN=S(I)                                         J08  594
  932 CONTINUE                                                          J08  595
      WRITE(2,103)CMAX,CMIN,EMAX,EMIN                                   J08  596
  103 FORMAT(1X,23HCMAX, CMIN, EMAX, EMIN=,4E13.7)                      J08  597
      ECNORM=(EMAX-EMIN)/(CMAX-CMIN)                                    J08  598
      DO933 I=1,NDATA                                                   J08  599
  933 TOTL(I)=TOTL(I)*ECNORM                                            J08  600
      DO 1973 I=1,1004                                                  RHC    2
      IF(1000.*HH(I).LT.FLOAT(IHSTRT))  HH(I)=FLOAT(IHSTRT)/1000.       RHC    3
 1973 CONTINUE                                                          RHC    4
      IF(GAU.LT.1.) GO TO 911                                           J08  601
C   WRITES FIELD VALUES AND INTENSITIES                                 J08  602
      WRITE(2,920)                                                      J08  603
  920 FORMAT(1H0, 71HMAGNETIC FIELD VALUES AND NORMALISED INTENSITIES FOJ08  604
     1R GAUSSIAN LINESHAPE/)                                            J08  605
      WRITE(2,921)(HH(I),TOTL(I),I=1,NDATA)                             J08  606
  921 FORMAT(1X,F8.1,F12.7,F9.1,F12.7,F9.1,F12.7,F9.1,F12.7,F9.1,F12.7, J08  607
     1F8.1,F12.7)                                                       J08  608
      GO TO 930                                                         J08  609
  911 WRITE(2,922)                                                      J08  610
  922 FORMAT(1H0, 73HMAGNETIC FIELD VALUES AND NORMALISED INTENSITIES FOJ08  611
     1R LORENTZIAN LINESHAPE/)                                          J08  612
      WRITE(2,921)(HH(I),TOTL(I),I=1,NDATA)                             J08  613
C PUTS FIELD VALUES IN HH AND IN IH                                     J08  614
  930 IOP1=NDATA+1                                                      J08  615
      IO2=2*NDATA                                                       J08  616
      DO 931 I=IOP1,IO2                                                 J08  617
      J=(I-IOP1)+1                                                      J08  618
      TOTL(I)=S(J)                                                      J08  619
      IHH(I)=(IHSTRT)+((I-IOP1)*IOH)                                    J08  620
      HH(I)=IHH(I)                                                      J08  621
  931 HH(I)=HH(I)/1000.                                                 J08  622
      IF(IDATA.GT.0) GO TO 960                                          J08  623
      WRITE(2,934)                                                      J08  624
  934 FORMAT(1H0,21HEXPERIMENTAL SPECTRUM/)                             J08  625
      WRITE(2,921)(HH(I),TOTL(I),I=IOP1,IO2)                           J08  626
  960 CONTINUE                                                          J08  627
      DO 950 I=1,IO2                                                    J08  628
      D(1,I)=HH(I)                                                      J08  629
      D(2,I)=TOTL(I)                                                    J08  630
  950 CONTINUE                                                          J08  631
      CALL PINIST(0,IO2)                                                J08  632
      NPLOT=2                                                           J08  633
C   CALCOMP ROUTINES                                                    J08  634
      CALL SCALE(HH,10.0,IO2,1)                                         J08  635
      CALL SCALE(TOTL,8.0,IO2,1)                                        J08  636
      YMIN=-TOTL(IO2+1)/TOTL(IO2+2)                                     J08  637
      CALL AXIS(0.0,YMIN,5HFIELD,-5,10.0,0.0,HH(IO2+1),HH(IO2+2))       J08  638
      CALL AXIS(0.0,0.0,15HSIGNAL STRENGTH,15,8.0,90.0,TOTL(IO2+1),TOTL(J08  639
     1IO2+2))                                                           J08  640
      XXX(NDATA+1)=HH(IO2+1)                                            J08  641
      XXX(NDATA+2)=HH(IO2+2)                                            J08  642
      YYY(NDATA+1)=TOTL(IO2+1)                                          J08  643
      YYY(NDATA+2)=TOTL(IO2+2)                                          J08  644
      DO 935 I=1,NPLOT                                                  J08  645
      DO 936 J=1,NDATA                                                  J08  646
      JJ=J+NDATA*(I-1)                                                  J08  647
      XXX(J)=HH(JJ)                                                     J08  648
  936 YYY(J)=TOTL(JJ)                                                   J08  649
      K=2-I                                                             J08  650
      KK=LPT*K                                                          J08  651
  935 CALL LINE(XXX,YYY,NDATA,1,KK,K)                                   J08  652
      GO TO 5001                                                        J08  653
 5000 CONTINUE                                                          J08  654
      CALL ENPLOT(30.0)                                                 J08  655
      STOP                                                              J08  656
      END                                                               J08  657
```

```
      SUBROUTINE GAULOR(HSTAR,DNOH,DTHETA,DPHI)                          JOB  658
      COMMON WL,GAU,IDH,D1,IHSTRT,IHEND,NDATA,NORM,HH(1004),TOTL(1004),  JOB  659
     1S(505),XXX(505),YYY(505)                                           JOB  660
      COMMON FH(501),IHH(501),DFH(501),GFH(501),GDFH(501)                JOB  661
      COMMON EJ(2,639)                                                   JOB  662
      COMMON DEG,L,STOTHI(349),STOPHI(349)                               JOB  663
      REAL NORM                                                          JOB  664
      HSTAR=ABS(HSTAR)                                                   JOB  665
      DNOH=NORM*DNOH                                                     JOB  666
      ITHETA=DTHETA+0.5                                                  JOB  667
      IPHI=DPHI+0.5                                                      JOB  668
      IF(ITHETA.EQ.90 .OR.IPHI.EQ.90 .OR.IPHI.EQ.0 )DNOH=DNOH/2.         JOB  669
      IF(ITHETA.EQ.0 .AND.IPHI.EQ.0 ) DNOH=DNOH/2.                       JOB  670
      IF(ITHETA.EQ.90 .AND.IPHI.EQ.0 )DNOH=DNOH/2.                       JOB  671
      IF(ITHETA.EQ.90 .AND.IPHI.EQ.90 ) DNOH=DNOH/2.                     JOB  672
      IA=1000.*WL+0.5                                                    JOB  673
      IHSTAR=HSTAR*1000.+0.5                                             JOB  674
      GA=GAU                                                             JOB  675
      IF(GA.GT.1.) GO TO 400                                             JOB  676
      IF(GA.LT.1.) GO TO 401                                             JOB  677
400   IF((IHSTAR+2*IA).LT.IHSTRT.OR.(IHSTAR-2*IA).GT.IHEND)GO TO 600     JOB  678
      IHHI=IHSTAR+2*IA                                                   JOB  679
      IHLO=IHSTAR-2*IA                                                   JOB  680
      GO TO 402                                                          JOB  681
401   IF((IHSTAR+4*IA).LT.IHSTRT.OR.(IHSTAR-4*IA).GT.IHEND)GO TO 600     JOB  682
      IHHI=IHSTAR+4*IA                                                   JOB  683
      IHLO=IHSTAR-4*IA                                                   JOB  684
402   CONTINUE                                                           JOB  685
      DO 123 I=1,NDATA                                                   JOB  686
      IFIELD=IHSTRT-IDH+I*IDH                                            JOB  687
      IF((IHLO-IFIELD).GT.IDH) GO TO 123                                 JOB  688
      M1=I-1                                                             JOB  689
      IF(I.EQ.1) M1=1                                                    JOB  690
      IHLO=IFIELD-IDH                                                    JOB  691
      IF(I.EQ.1) IHLO=IFIELD                                             JOB  692
      IF(GA.LT.1.)GO TO 403                                              JOB  693
      IHHI=IHLO+4*IA                                                     JOB  694
      GO TO 404                                                          JOB  695
403   IHHI=IHLO+8*IA                                                     JOB  696
404   CONTINUE                                                           JOB  697
      GO TO 124                                                          JOB  698
123   CONTINUE                                                           JOB  699
124   IDELTA=(IHHI-IHLO)/IDH+1                                           JOB  700
      AL=1./WL                                                           JOB  701
      M2=M1+IDELTA                                                       JOB  702
      IF(GA.GT.1.) GO TO 905                                             JOB  703
      DO 906 J=1,NDATA                                                   JOB  704
      DFH(J)=0                                                           JOB  705
906   FH(J)=0                                                            JOB  706
      DO 907 J=M1,M2                                                     JOB  707
      IF(J.GT.NDATA) GO TO 908                                           JOB  708
      IHH(J)=IHLO+(J-M1)*IDH                                             JOB  709
      HH(J)=IHH(J)                                                       JOB  710
      HH(J)=HH(J)/1000.                                                  JOB  711
      IF(IHH(J).GT.IHHI)GO TO 908                                        JOB  712
      D=HH(J)-HSTAR                                                      JOB  713
      DFH(J)=((4*AL**3)/(3.1416))*(DNOH*D)/((1.+AL*AL*D*D)**2)*DH*(-1.)  JOB  714
909   FH(J)=FH(J)+DFH(J)                                                 JOB  715
907   CONTINUE                                                           JOB  716
908   CONTINUE                                                           JOB  717
      DO 910 I=M1,M2                                                     JOB  718
      IF(I.GT.NDATA) GO TO 600                                           JOB  719
910   TOTL(I)=TOTL(I)+FH(I)                                              JOB  720
      IF(GA.LT.1.) GO TO 600                                             JOB  721
905   DO 13 J=1,NDATA                                                    JOB  722
      GDFH(J)=0                                                          JOB  723
 13   GFH(J)=0                                                           JOB  724
      DO 23 J=M1,M2                                                      JOB  725
      IF(J.GT.NDATA) GO TO 22                                            JOB  726
      IHH(J)=IHLO+(J-M1)*IDH                                             JOB  727
      HH(J)=IHH(J)                                                       JOB  728
      HH(J)=HH(J)/1000.                                                  JOB  729
      IF(IHH(J).GT.IHHI)GO TO 22                                         JOB  730
      G=HH(J)-HSTAR                                                      JOB  731
      GDFH(J)=(2.*AL*AL*AL*DNOH*G)/(1.7725*2.7183**(AL*AL*G*G))*(-1.)    JOB  732
      GO TO 25                                                           JOB  733
 25   GFH(J)=GFH(J)+GDFH(J)                                              JOB  734
 23   CONTINUE                                                           JOB  735
 22   CONTINUE                                                           JOB  736
      DO 26 J=M1,M2                                                      JOB  737
      IF(J.GT.NDATA) GO TO 600                                           JOB  738
 26   TOTL(J)=TOTL(J)+GFH(J)                                             JOB  739
600   CONTINUE                                                           JOB  740
912   RETURN                                                             JOB  741
      END                                                                JOB  742
```

Errata

P-101 L-14

The gyromagnetic ratio $g = \mu/p$ is the factor for converting angular momentum to magnetic moment. The Bohr magneton β is the unit of quantization of electron magnetic moment.

P-189 L-10 to foot of page

Oxygen activity cannot be taken as $10^{-5}/N$, but consider the ½ reaction 5.4 as being an equilibrium. Initially no 0 will be present. Under the hydrothermal conditions the equilibrium oxygen activity (for $\Delta G = 0$, $E = 0$) is 4.4×10^{-17}. The corresponding oxygen concentration will be formed and could be removed from the system by two routes:

1 formation of 0_2 molecules which can then go into the crystal, or

2 direct induction of 0 atoms into the crystal lattice, where they would be stabilized.

The reaction 5.4 will then maintain the equilibrium concentration of 0 in the growth medium.